The Design, Development, and Validation of a Residual Limb Evaluation System for the Real-Time Data Mapping of the Trans-Tibial Amputee Socket-Limb Interface for Prosthetic Fitment.

By: Scott Bruton

BRTSCO001

SUBMITTED TO THE UNIVERSITY OF CAPE TOWN

In fulfilment of the requirements for the degree of

MSc (Biomedical Engineering)

Supervisor: Assoc. Prof. George Vicatos

Co-supervisor: Assoc. Prof. Sudesh Sivarasu

Date of Submission: 01/07/2018

Declaration of Authorship

I, *Scott Bruton*, hereby declare that the work on which this dissertation/thesis is based is my original work (except where acknowledgements indicate otherwise) and that neither the whole work nor any part of it has been, is being, or is to be submitted for another degree in this or any other university.

I empower the university to reproduce for the purpose of research either the whole or any portion of the contents in any manner whatsoever.

Signature: Signed by candidate

Date: 29/01/2018

Abstract

Introduction: Skin problems are known to occur on the residual limb (RL) of trans-tibial amputees (TTAs). These are induced by an improper prosthetic socket fitment, alignment or component selection. It was identified that there is a lack of RL evaluation systems (RLESs) that are tailored for the prosthetic fitting procedure that analyse the pressures and temperatures on the RL, as well as the gait phases of stance. This observation established the hypothesis that a tactile RL evaluation device and recording software system can provide reliable socket-limb interface (SLI) information which can be used to identify vulnerable areas on the RL induced by the socket during the gait movements of TTAs.

Methods: A prototype RLES was designed and developed. It was comprised of tactile pressure and temperature transducers, gait ground reaction force (GRF) transducers and device-specific software tailored for the evaluation of the RL within the SLI. A pilot study was designed to evaluate the capabilities of the RLES which entailed the evaluation of its skin temperature tracking ability, pressure measurement repeatability within the SLI, and ability to interpret the pressures during (natural) walking movements. Study participants were recruited through the private practice of prosthetist Eugene Russouw, as well as Vincent Palloti Hospital (South Africa, Cape Town) and consisted of two bilateral and three unilateral TTAs, who were enrolled in the pilot study. Each participant performed three experimental procedures: a static stand (SS); a straight-line walk (SLW); and a figure-of-8 walk (F8W). Skin temperature change due to loading and unloading was monitored during the SS procedure. Peak pressure results from the SLW and F8W procedures were gathered to evaluate the coefficient of variance (COV) between strides. This was used to evaluate the repeatability of the pressure measurements and allowed for a comparison between the SLW and F8W methods. GRF data collected from the SLW dataset was used to evaluate the RLES's ability to track gait phases.

Results: The developed RLES software provided a tailored prosthetic fitting analysis platform (in the form of a graphical user interface) which allowed the user to perform a real-time, in-depth analysis of different RL areas, as well as provided an overview of all areas simultaneously. It provided functions for the recording, playback, and export of testing data which was used to evaluate the RLES capabilities. The RLES produced an average COV of 7.16%, which fell within the 6.94% ± 1.7% range in literature. The SS procedure produced an average temperature increase of 0.45 °C, found over all RL areas, which corresponds to similar studies in literature. This validated its ability to track RL skin temperature by producing the expected skin temperature change trend. Additionally, the RLES produced an expected TTA gait GRF curve (similar to literature) in which different gait phases could be identified. The comparison between the SLW and F8W methods found that pressure sore areas endured large pressures without relief from other movements (when compared to healthier areas), and suggests that the SLW and F8W comparison may be an important additional evaluation method during the prosthetic fitting procedure. The RLES identified all of the pressure sores presented within the 24 RL areas over all the TTA participants and suggested that a safe pressure threshold of 100 kPa is an appropriate guideline to be used during the prosthetic fitting procedure.

Conclusions: The RLES proved to work efficiently and successfully within the study, and was capable of identifying vulnerable areas of pressure sores. With the high prevalence of skin problems on the RLs of TTAs, the implementation of a RLES during the fitting procedure, which can tailor the prosthesis design and fitment to the amputee, may potentially identify vulnerable areas of future skin problems and allow preventative actions to be performed.

Acknowledgements

This research was supported by the National Research Fund (NRF) and the RC&I Pre-Seed Explorer Fund. Any opinion, findings, recommendations or conclusions expressed within this dissertation are solely that of the author, and therefore the NRF does not accept any accountability in regard thereto.

I would like to acknowledge and express my gratitude to the following people and organisations:

The University of Cape Town, for providing me with office space, computational hardware, manufacturing, and the means to complete this dissertation efficiently and effectively;

Associate Professor George Vicatos and Associate Professor Sudesh Sivarasu for all the guidance, supervision and support throughout the duration of the Master's program. Your guidance and support has been invaluable;

Mr Theodorus Kriel, Mr Justin Rix, and Mr Jayson Chin, from Jayson Chin & Associates at Vincent Pallotti Hospital (Cape Town, South Africa), for providing participant details and knowledge of which residual limb areas to analysis within the study;

Eugene Rossouw (Orthotist and Prosthetist) for helping me recruit participants for the study, providing a venue to perform the study procedure, helping me will all the questions I had about prosthetics, and providing me recommendations for my system from a prosthetists point of view. This helped immensely in the design of the RLES;

To all participants who took part in the study. Without your participation, my study would not have been possible;

Miss Elizabeth Kruse, Mr Edmund Wessels, Mr Giancarlo Beukes, and Mr Gokul Nair, from the Division of Biomedical Engineering at the University of Cape Town, for proofreading and editing my dissertation;

Mr Alastair During for assisting and helping me with every aspect of my project;

Mr Jerry Sam who supported, pushed and encouraged me throughout the entire duration of the project.

To my parents, Dr Neal Bruton and Mrs Lyn Bruton for all of your love and support, proofreading my dissertation, and the long phone calls to help me cope with the stress;

Most importantly, thank you to my best friend, my rock and the best support structure I could ask for, Miss Kershia Naidoo, for helping me through all the stressful days and nights, being a shoulder for me to lean on when things became tough, and for being the biggest role model to me. Your love and support has been invaluable and I deeply thank you.

Table of Contents

List of Figures

List of Tables

List of Abbreviations

COV	Coefficient Of Variance
DMC	Distal Medial Calf
DT	Distal Tibial
FH	Fibula Head
FSR	Force Sensitive Resistor
GRF	Ground Reaction Force
NTC	Negative Temperature Coefficient
PF	Popliteal Fossa
PT	Patella Tendon
PTB	Patella Tendon Bearing
PTC	Positive Temperature Coefficient
ProxTib	Proximal Tibia
QOL	Quality Of Life
RL	Residual Limb
RLES	Residual Limb Evaluation System
SD	Standard Deviation
SLI	Socket-Limb Interface
SLT	Socket Load Transfer
TR	Total Range
TSB	Total Surface Bearing
TTA	Trans-tibial Amputee
VP	Vincent Pallotti

List of Units

cm	centimetre
g	gram
Hz	Hertz
kg	kilogram
kPa	kilopascals
mA	milliamps
mm	millimetre
ms	milliseconds
mV	millivolts
N	Newton
V	Voltage

1 Introduction

The following project investigates a common problem experienced by below-knee amputees, commonly referred to as trans-tibial amputees (TTAs). This problem relates to soft tissue problems experienced on the residual limb (RL), that occur while wearing a prosthesis. These occur due to the RL experiencing intolerable pressures and temperatures induced by an improper socket design, fitment, prosthesis alignment, or liner type. It is assumed that these problems arise due to human error in the prosthetic fitting procedure, since the current process is empirical which increases the probability of missing problematic pressure and temperature exposures to the RL. To address this problem, the project involves: research into the effect that these variables have on the RL; the related skin issue and their prevalence in the TTA population; the current commercially available systems for RL evaluation; and the design and development of a new RL evaluation system (RLES) to analyse these variables within the socket-limb interface (SLI). The capabilities of the prototype RLES are evaluated by a pilot study performed on TTAs to determine its efficiency and practicality. A RLES could potentially grant a prosthetist the increased ability to identify vulnerable RL areas within the SLI during the fitment procedure to improve prosthetic fitment and component selection. This chapter entails background information related to the project, the identification and significance of the problem, and the definition of the aims and objectives of the study.

1.1 Background to the Study

Lower limb amputation commonly occurs as a result of tumours, severe trauma, disease, severe infection or nerve damage and can leave the amputee mostly immobile for the duration of the rehabilitation process (Dudek, Marks, & Marshall, 2006). This circumstance has a significant effect on the patient's social, psychological and physical state and can cause severe depression. The first solution that most amputees turn to is prosthetics which give the amputees another chance at mobility and not only improves their movement but has shown to improve their psychosocial state to within general population norms in approximately two years' post-amputation (Horgan & MacLachlan, 2004). Therefore, the design, function, and feel of a prosthesis are essential elements in the rehabilitation and well-being of an amputee.

Below knee prostheses entail the use of a prosthetic socket which needs to support the amputee's body weight during ambulation (walking). During the gait cycle, high peak ground reaction forces (GRFs) of approximately 90 – 110% body weight, are transferred from the prosthetic foot onto the RL. This induces high compression and shearing forces onto the RL soft tissue (Su, Gard, Lipschutz, & Kuiken, 2010). The RL soft tissue is generally not adapted for the repetitive application of these large dynamic forces, and therefore, if not distributed correctly over the RL, can cause soft tissue breakdown. This can lead to several types of skin issues such as ulcers, inclusion cysts, blisters, fungal infections, calluses, oedema, etc. (Dudek et al., 2006).

Prosthetic sockets are generally designed and fitted to minimise large pressure magnitudes on the sensitive soft tissue areas by distributing pressure loads equally over the RL, or placing larger loads on tolerant areas (such as the patella tendon and popliteal fossa). However, if an incorrect load distribution subjects the bony prominences and subcutaneous areas (such as the fibula head and distal tibia) to intolerable loads, several skin problems can arise, as mentioned previously. These skin problems can become extremely uncomfortable and painful for the wearer. This may decrease their prosthesis use time, movement, and consequently impact their quality of life (QOL).

This load transfer can be defined as the socket load transfer (SLT) which defines the contact relationship and fitment between the RL and socket within the SLI. An incorrect SLT can be induced by either an incorrect socket design, socket and prosthesis alignment, socket fitment, and other prosthetic components (liner types, sock types, liner thickness, etc.), as well as a change in weight or RL volume of the amputee.

The SLT is generally assessed by the prosthetist on a visual basis during the prosthetic socket fitment process in an attempt to find the correct fit for the amputee and minimise the risk of future complications. However, studies show that approximately 30 - 70%, of the lower limb amputee populations studied, suffer from skin issues which are directly related to the SLT and health of their RL while wearing their prosthesis socket (Koc et al., 2008; Meulenbelt, Geertzen, & Jonkman, 2009). The health of the RL soft tissue is governed by the physical variables within the SLI such as direct (orthogonal) stress (referred to as pressure within this study), shear stress, temperature and humidity (Swain & Bader, 2002). The type, design, alignment, and fitment of the prosthetic components used, determine the magnitude of these factors.

Due to this high prevalence of recorded skin issues, research has been conducted over the past 70 years measuring these variables in an attempt to understand the SLT and assess/validate socket design types (Ferreira et al., 2017; Mueller & Hettinger, 1954). The advancement of tactile sensor technology has given rise to new ways of measuring these variables from using regular strain gauge technology implanted into sockets, to the use of devices such as micro-electro-mechanical systems (MEMS), optic fibre and piezoresistive carbon nanotubes. The result of years of SLI pressure measurement research shows a dramatic improvement in socket design and SLT efficiency with the majority of maximum pressure loads for studies published before year 2000 generally ranging from 200 – 400 kPa (Convery & Buis, 1998; Rae & Cockrell, 1971; J Sanders, Daly, & Burgess, 1993; Zhang, Turner-Smith, Roberts, & Tanner, 1996; Zhang, Turner-Smith, Tanner, & Roberts, 1998) to 50 – 200 kPa in the years after 2000 (Ali et al., 2013; Dumbleton et al., 2009; Pirouzi et al., 2014; Rajtukova et al., 2014). However, even with these improved socket designs and decreased pressures, a 2011 clinical study by Meulenbelt et al. (2011), who researched the prevalence of skin problems in 124 amputees, found that of the amputees studied, 36% showed signs of skin issues, with pressure ulcers (39%) being the most common, caused by an incorrect SLT. These statistics indicate that merely analysing the prosthetic socket design, fitment and SLT may not be the only variables to consider when performing a prosthetic fitting procedure.

Researchers found that by changing the prosthesis alignment, the pressure distribution and loading areas on the RL could be changed, therefore, highlighting that gait assessment is critical for efficient prosthetic fitment (J Sanders, Bell, Okumura, & Dralle, 1998; Seelen, Anemaat, Janssen, & Deckers, 2003). Additionally, researchers have also started analysing RL skin temperature as a method of vulnerable RL area identification. Cutti et al. (2014) found that thermography (thermal imaging) of the RL can identify RL areas of inflammation, thrombosis and painful/sensitive areas. Kokate et al. (1995) found that skin temperature is directly related to the soft tissue's susceptibility to external interface pressure, whereby an increase in skin temperature decreases the safe interface pressure threshold. Therefore, it can be stated that there is a definite link between overall RL health, the gait cycle motion and GRFs, the SLT, and the temperature of the RL skin under interface pressures. However, current commercially available RL analysis tools only measure the direct pressure on the RL without including the source of these pressures (gait GRFs and motion) or the RL health and soft tissue reaction to these pressures (the temperature of the skin).

Therefore, the current study will involve designing and developing a prototype RLES which will allow the combined analysis of skin temperatures and direct interface pressures experienced by the RL, as well as illustrate the timing and phases of gait GRFs throughout the prosthetic fitting process. This knowledge would potentially allow the prosthetist to perform the following functions efficiently:

- Fitment analysis of the prosthetic socket design.
- Prosthesis alignment analysis.
- Identification of high loading areas.
- RL skin temperature tracking throughout the procedure.
- The temperature retention of different liner/socks or prosthetic garments.
- Gait cycle GRFs and related RL pressures analysis.

These functions would assist the prosthetist in making a more informed selection of the prosthetic components (liners, socket design, ankles, feet, etc.) for each specific amputee to minimise future skin complications.

1.2 Clinical Problem Description

The clinical problem identified is centred around the lack of SLI variable knowledge provided to the prosthetist during the fitment procedure and the resulting skin problems that are induced in the RL soft tissue.

During ambulation, the SLI environment is not ideal for the RL's soft tissue due to the following factors:

- Dynamic and repetitive orthogonal and shear forces are applied to the RL soft tissue, which it is not necessarily suited for.
- Friction is created within the SLI which can cause irritation and abrasions, increasing the risk of infection as well as increasing the RL skin temperature.
- Elevated skin temperatures within the SLI increases perspiration and sweat damming around the RL. This can increase the risk of skin infection and decrease the soft tissues resilience to interface pressure.
- Intimate contact between the socket/liner/sock and skin, increases the potential for allergic reactions and mechanical/chemical irritations.

These factors, coupled with the specific individual's human variability, can make the prosthetic socket design, component selection, fitting, and alignment procedure a long iterative process to find the best combination for the specific amputee. This process will be referred to as the prosthetic fitting procedure and is usually performed over 1-6 months for new amputees. Generally this procedure takes place in five stages: 1) Evaluation of the RL and amputee's activities; 2) measurement and casting of the socket; 3) fitting and alignment of the socket and prosthesis; 4) delivery of the final prosthetic socket; 5) and follow-ups and socket repairs (Biometrics, 2017; James, 1991). The first three stages are the most critical as they determine the success of the prosthesis post-fitting. These stages entail the evaluation of the RL capabilities, the RL measurements, the casting of a prosthetic socket mould, the creation of a test socket, and the fitting and alignment of the prosthetic test socket onto the RL. The latter is a crucial stage, because if not performed correctly, there exists the potential for an incorrect SLT from the final prosthesis.

The test socket is made of transparent thermoplastic and created to initially diagnose the socket fitment before the final socket is created by granting an unobstructed view of the RL skin beneath the socket walls. The health of the skin is visually inspected while the TTA is standing and areas of concern are

identified by the absence or presence of skin blanching which represent inadequate or excessive pressure areas respectively. To relieve or shift pressures, the prosthetist will often make volume adjustments by either splitting the socket or heat-modifying and trimming away portions of the socket (Quigley, 2010). However, the prosthetist has no quantitative knowledge regarding the actual SLT or other SLI environment variables, and the process is purely empirical. Therefore, the quality and performance of the final prosthetic socket, the suggested prosthetic components, and their alignment on the amputee, is solely the product of the expertise and experience of the prosthetist who performs a visual inspection without the aid of SLI variable knowledge (pressure and temperature). This leaves significant room for human error, and if the fitment, alignment, or selected components are incorrect, it can create an SLI environment that may experience intolerable pressure spots or problematic temperatures which will potentially cause RL discomfort and skin problems.

A vast number of studies have been performed on the prevalence of skin problems on the RL of lower limb amputees. Meulenbelt et al. (2011) conducted a clinical study which entailed the collection of previous research surveys, questionnaires and studies performed on skin problem prevalence. The combined population size was 2199 lower limb amputees of which, 1037 (47.2%) presented skin problems on their RL with the vast majority being caused by the socket fitment and prosthetic components used. These issues cause much discomfort for the amputee and studies by Hagberg & Brånemark (2001) and Meulenbelt et al. (2009) stated that 33% of a 97 size study population and 57% of a 463 size study population respectively, had been forced to remove their prosthesis temporarily due to this discomfort. These statistics clearly indicate that there is scope for further investigations into the SLI and even the most skilled prosthetist has difficulty gauging the actual SLT, health, and RL's susceptibility to future problems within the socket by visual inspection alone. The source of these problems originates from the physical variables (pressure, shear force, temperature, and humidity) experienced by the RL skin, which cannot be determined without the use of additional measurement tools to assist in the analysis of the RL health.

To improve the fitment of the prosthetic socket, many researchers have developed transducer (sensor) based devices to investigate the stresses experienced by the RL, as discussed in Section 1.1. However, these are all used for the data collection for the specific research study and are not tailored systems for the prosthetic fitment procedure. Commercially there are a limited amount of prosthetic socket fitment systems that have been developed, which will be discussed in Section 2.6, with the most popular being the F-Scan™ or F-Socket™ from Tekscan® (South Boston, United States). However, these systems solely measure the direct pressure and neglect the temperatures of the RL. Additionally, they do not provide prosthetic fitment tailored software and rely on generic pressure output software which is used for all of their pressure interface products. There does not exist a RLES which comprises a device to measure gait information and the SLI variables (such as RL pressure and temperature), with a tailored prosthetic socket fitment software, to allow an overall and in-depth analysis into specific RL areas.

The lack of SLI knowledge and systems to obtain this knowledge efficiently, is the problem that needs to be addressed and highlights the need for a RLES to be developed that can analyse these variables and help identify vulnerable areas to decrease the risk of future skin complications.

1.3 Problem Significance

Currently, there are no accurate statistics that quantify the number of lower limb amputees within South Africa, however, the World Health Organisation (2005) estimated that in Asia, Latin America and Africa there were approximately 30 million people who required prosthetic limbs during 2004. Additionally, the Amputee Coalition of America (2016) approximated that there are 185,000 new American amputees each

year and, as stated by Ziegler-Graham (2008), “Over the next 45 years, the number of persons living with the loss of a limb is expected to more than double from 1.6 million in 2005 to 3.6 million in 2050”. (Amputee Coalition, 2016; Ziegler-Graham, MacKenzie, Ephraim, Travison, & Brookmeyer, 2008). With this fast-growing population of amputees, and the high statistical prevalence of RL skin issues, the importance of finding improved and more efficient prosthetic fitment procedures and systems is increasing.

The lack of prosthetic fitment systems forces prosthetists to perform the prosthetic fitment procedure visually. There exists a considerable degree of human error within the procedure without additional assistive systems to evaluate the fitment and inform the prosthetist of the quality of fit. The results of human error can be seen from the statistics found in studies which research the prevalence of skin problems in lower limb amputees. The clinical study by Meulenbelt et al. (2011), tabulated previous studies researching the prevalence of skin issues in lower limb amputees. The results gathered from this study, with the addition of previous studies on TTA RL skin issue prevalence, have been recreated and are presented in Table 1.1. It was found that out of a total of 2298 participants, 1137 (49.5%) exhibited skin issues on their RL. These statistics indicate that approximately 50% of amputees will experience a skin problem from their prosthesis. In addition to this statistic, Dudek et al. (2005) performed a six-year review of skin lesions diagnosed in patients examined in an outpatient clinic at a rehabilitation hospital (Ottawa, Canada) in which 337 (63.8%) of 528 skin problems found were on amputee lower RLs, and 68.5% of these were mechanically induced by the socket. The high percentage found in skin issue prevalence studies suggests that many amputees still suffer from a decreased QOL induced by skin problems in addition to the consequential QOL decrease that stems from limb loss. QOL is the top priority in prosthetic design and fitment, and although there has been considerable global research, little has been performed in South Africa.

Table 1.1: Collection of previous studies on the prevalence of lower residual limb skin issues (Meulenbelt et al., 2011).

FIRST AUTHOR, YEAR	STUDY TYPE	NUMBER OF PARTICIPANTS	AGE MEAN ± SD	GENDER (M/F)	SKIN ISSUES PREVALENCE
Lyon et al. (2000)	Q	210	52.6 ± 19.8	52/19	71 (34%)
Meulenbelt et al. (2011)	Q	124	58 ± 17	88/36	44 (35%)
Hagberg et al. (2001)	S	97	48	60/37	23 (24%)
Koc et al. (2008)	PE	142	29.2 ± 9.7	139/3	105 (74%)
Dudek et al. (2005)	CR	745	57.3 ± 16.7	634/111	337 (40.7%)
Chan et al. (1990)	Q/PE	47	75.4	21/26	14 (30%)
Meulenbelt et al. (2009)	Q	805	60 ± 15	498/307	507 (63%)
DesGroseilliers et al. (1978)	PE	50	39 ± 15.5	NA	17 (34%)
Dillingham et al. (2001)	CR/I	78	NA	68/10	19 (24%)
Total		2298			1137 (49.5%)

NA - Not available in publication, CR - Chart Review, I - Interview, PE - Physical Examination, Q - Questionnaire, S - Survey, SD - Standard Deviation, M - Male, F - Female.

Hagberg and Brånemark et al. (2001) performed QOL surveys on 90 TTAs, and found that in the categories of heat/sweating, sores/chaffing and stump pressure pain, 72%, 62% and 51% respectively reported a moderate decrease in QOL and 40%, 39% and 20% respectively reported a considerable to worse decrease in QOL. An efficient RLES which measures the pressures and temperature on the RL within the socket would have the potential to evaluate these categories before they develop into problems that decrease the QOL of the amputee.

The goal of a prosthesis is to give the amputee a certain degree of mobility to increase their QOL to normal standards. The fact that studies, referenced in Section 1.2 and 1.3, have shown that

approximately half of all amputees studied suffer from skin problems, that the majority suffer a decrease in QOL due to these as a result, and that some are physically forced to stop wearing their prosthesis, is of great concern. Consequently, the need for an assistive RLES to improve the socket fitment analysis is extremely relevant.

1.4 Project Aim

This project aims to design and develop a prototype RLES which could be used as an assistive system during the prosthetic fitting procedure. The system is required to provide the user (prosthetist) with relevant quality SLI data and gait knowledge during all natural movements of a TTA, as well as to identify any vulnerable areas at risk of future potential skin issues.

1.5 Project Objectives

The project objective is to design, develop and clinically validate a prototype RLES capable of producing a graphical representation of the pressures and temperatures of a TTA's RL areas within the SLI, as well as the timing and phases of the amputee's gait GRFs in real-time. The system should provide the means to perform a full analysis of each area during the prosthetic fitting procedure of any TTA. To achieve this goal the following design and research objectives need to be met to satisfy the aim.

1.5.1 Design Objectives

The design objectives comprise of two sections: the device objectives and the software objectives.

Device Objectives

- The device must feature four transducer sets, each of which comprise of one temperature sensor and one pressure sensor which can fit in-between the TTA's socket/liner and RL without causing pain or injury, and be attached to any area of a TTA's RL of any diameter or length.
- The direct pressure and temperature transducers must be calibrated to have an accuracy error of less than 10%.
- The device must feature two load sensors capable of being attached underneath the TTA's shoe, positioned on the heel and toe, to indicate the start and end of significant gait phases.
- The device must entail a control box which holds the circuitry, connects to the transducer sets, attaches to the TTA with no obstruction, and provides a connection port for the transfer of data to the software.

Software Objectives

- Device specific software must be developed and tailored for use in the prosthetic fitting procedure which must provide the following appropriate functions:
    - The registration and loading of the TTA information onto the system.
    - The selection of the RL side, areas to be analysed, and pressure and temperature thresholds to alert the user if magnitudes on the RL are too large.
    - The display of the RL and associated areas on the GUI with pressure and temperature magnitude indicators.
    - An option to analysis all areas simultaneously or an in-depth analysis of a specific area.
    - The provision of statistical information on the maximum, minimum and standard deviation of the pressures and temperatures in an area.
    - The real-time recording and display of all pressure, temperature and gait data in an appropriate manner to be used to evaluate the research objectives in the study.

1.5.2 Research Objectives

- To perform a pilot study on the reliability, efficiency and patient comfort of the RLES in a real-world setting by attaching the device to the RL of at least five TTAs and validating the following system functions by means of a literature comparison:
    - The repeatability of the pressure measurements by comparing the coefficient of variance (COV) of the mean peak pressure results, obtained during a straight line walk, with COV values found in literature for the same procedural type. COV is the percentage ratio of the standard deviation (SD) from the mean and is explained in Appendix E, Section 15.1.
    - The skin temperature tracking ability, by measuring the temperature of the RL areas under loading and unloading, and comparing the trend of the skin temperature change to the trend found in literature.
    - The reliability of the pressure and temperature measurements by comparing the pressure and temperature results, obtained during a straight line walk, to expected trends found in literature
    - The comfort of the attached transducer sets within the SLI during the experimental procedures by performing a survey among the TTA participants.
- Perform an original comparison study between the results obtained from a straight line walk and a figure-of-8 walk configuration to validate assumptions of expected results and evaluate the system's ability to track the figure of eight's more natural movement.
- Evaluate all results obtained and analyse the RLES's ability to identify vulnerable areas on the RL.

1.6 Project Deliverables

Figure 1.1 illustrates a basic example of the proposed system. The deliverables of this project are comprised of three sections: the RL transducer sets and gait sensors; the control box encapsulating the circuitry; and the software for the real-time display of the measurement data.

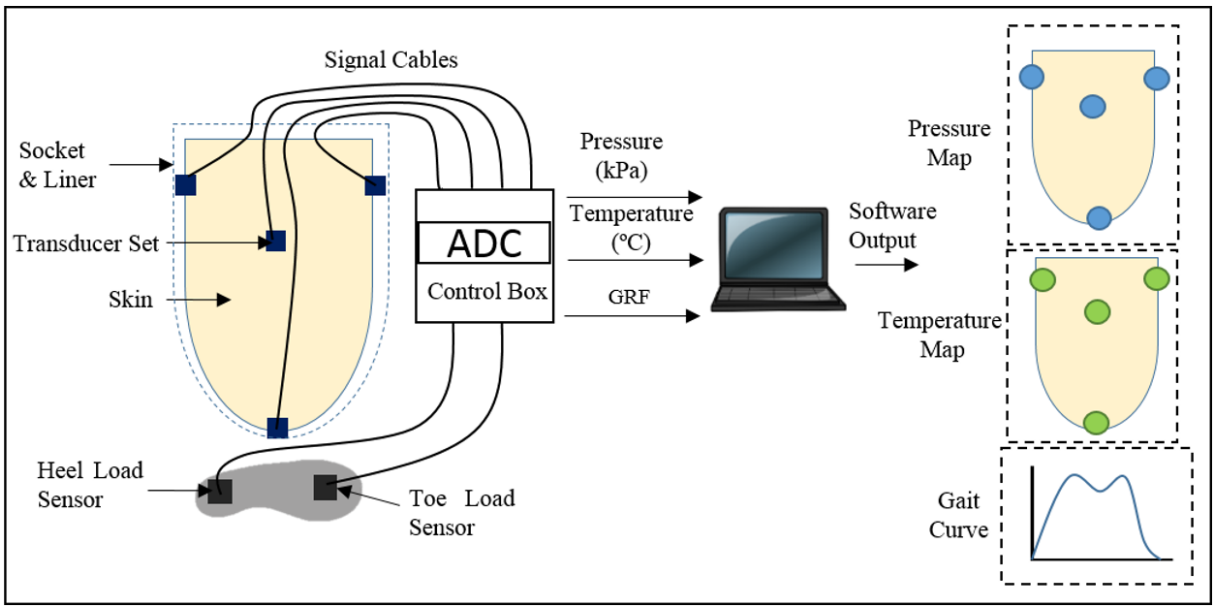

Figure 1.1: Basic Illustration of Proposed System: A system which entails a device comprised of pressure and temperature sensors (transducer set) that can be attached to the RL skin, two load sensors that can be attached to the base of the prosthetic foot, and software that displays the sensor results in a visually appropriate manner.

1.7 Research Approach

The study is comprised of two sections: the design and development of the prototype RLES, and a pilot study on TTAs to evaluate the system in a real-world setting. The pilot study will evaluate the efficiency and reliability of the system, as well as its ability to evaluate the RL during natural movements (figure-of-8 walking) and identify potentially vulnerable areas. This study will attempt to answer the following research question, "Can the real-time pressure, temperature, and gait information, obtained from a tactile measurement device and recording software system, efficiently evaluate the residual limb within the socket during different walking patterns and determine vulnerable stump areas of discomfort or injury?"

1.8 Scope of the Study

The study is focused on and limited to, the design and development of a prototype assistive RLES capable of determining the direct pressures and temperatures at selected RL areas, the timing and phases of gait GRFs, and software that illustrates the obtained information and presents it to the user. This is the investigation of a proof of concept to gauge the function of such a system in obtaining the magnitude of pressure and temperature found on the RL and identifying areas of concern. Therefore, for the proof of concept the study is limited to determining direct pressure and temperature at four selected RL areas which provide the highest probability of returning significant pressures for device validation.

1.9 Dissertation Overview

Figure 1.2 illustrates the dissertation process taken to complete the project.

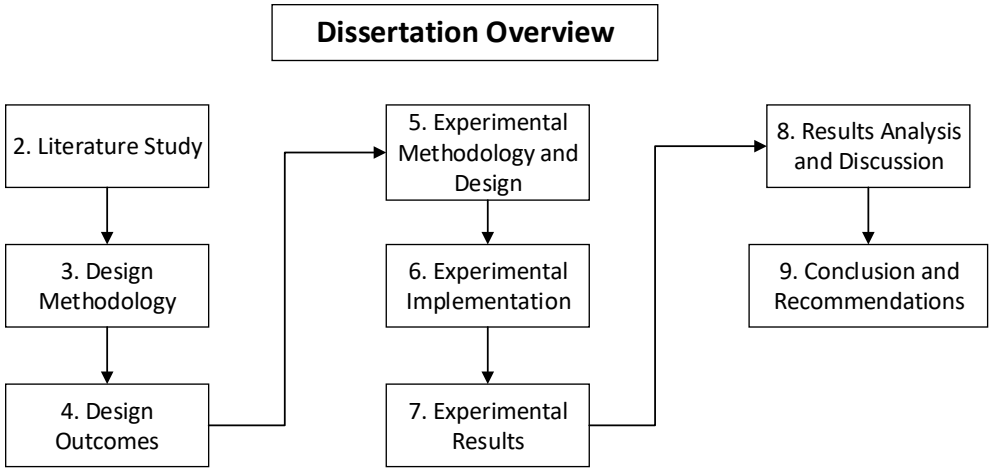

Figure 1.2: Dissertation Overview.

1.10 Conclusions

Chapter 1 identified that there is a high prevalence of skin problems found the RL of TTAs which are induced by improper prosthetic fitment, alignment and/or component selection. It highlighted that there is a lack of prosthetic fitting evaluation systems to be used within the fitting procedure and that the currently available products do not measure all parameters needed to perform an efficient analysis. Therefore, the aim and objectives of the study focus on developing a prototype device and software capable of measuring RL pressures and temperatures within the SLI, as well as identifying the timing and phases of gait GRFs of a TTA. Chapter 2 reviews the literature surrounding the development of skin complications and the research needed to develop and evaluate a system to potentially solve the problem.

2 Literature Study

Figure 2.1 illustrates the process of the literature study within this chapter.

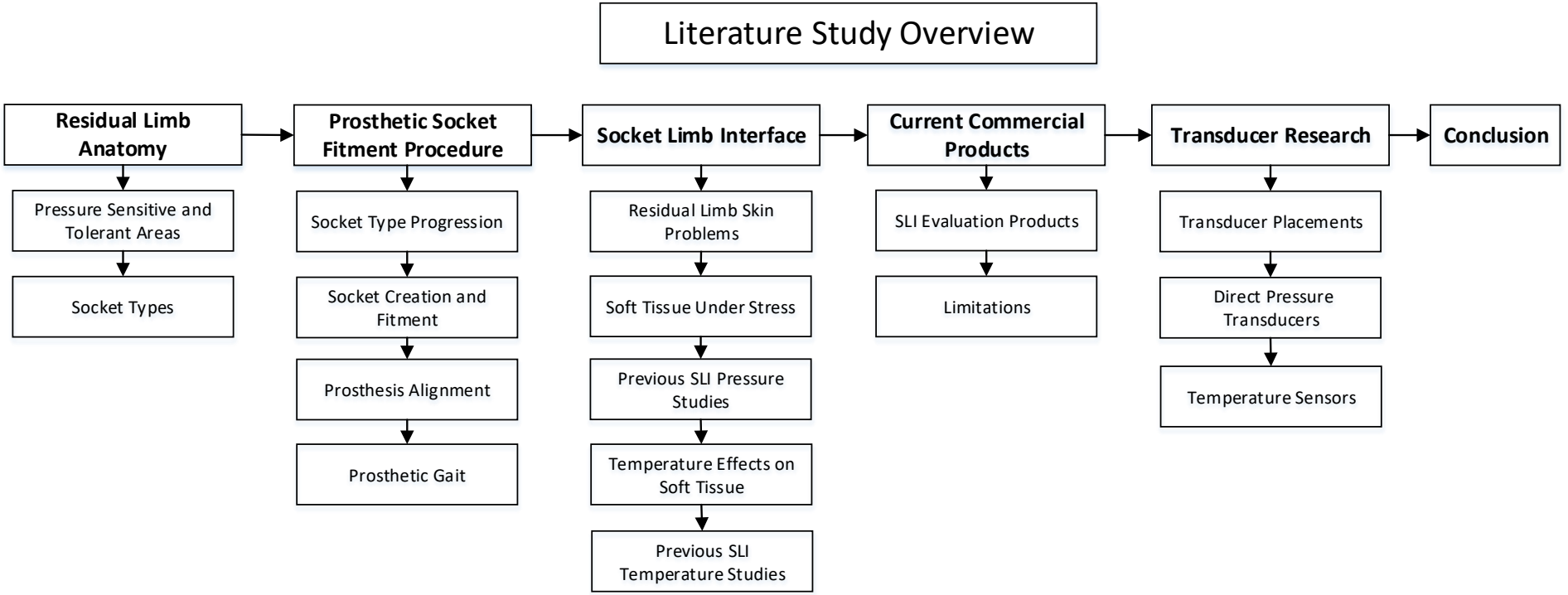

Figure 2.1: Literature Study Overview: The process of literature research to obtain the necessary knowledge to create the proposed device.

2.1 Introduction

The development of an efficient trans-tibial RLES requires the following knowledge: the anatomy and characteristics of a TTA RL; knowledge of how the prosthetic socket creation, fitment, and alignment is performed; how changes in these procedures affect the SLT distribution; what skin problems arise due to these errors; what variables need to be measured to detect these errors; and what types of products can potentially be used to measure these variables and identify the errors. The following chapter entails research into the relevant areas to obtain this information.

2.2 Trans-Tibial Amputee Residual Limb Anatomy

Figure 2.2 illustrates the anatomy of a male lower limb. A trans-tibial amputation is defined by the amputation line falling on the shaft of the tibia bone, within the shaded area.

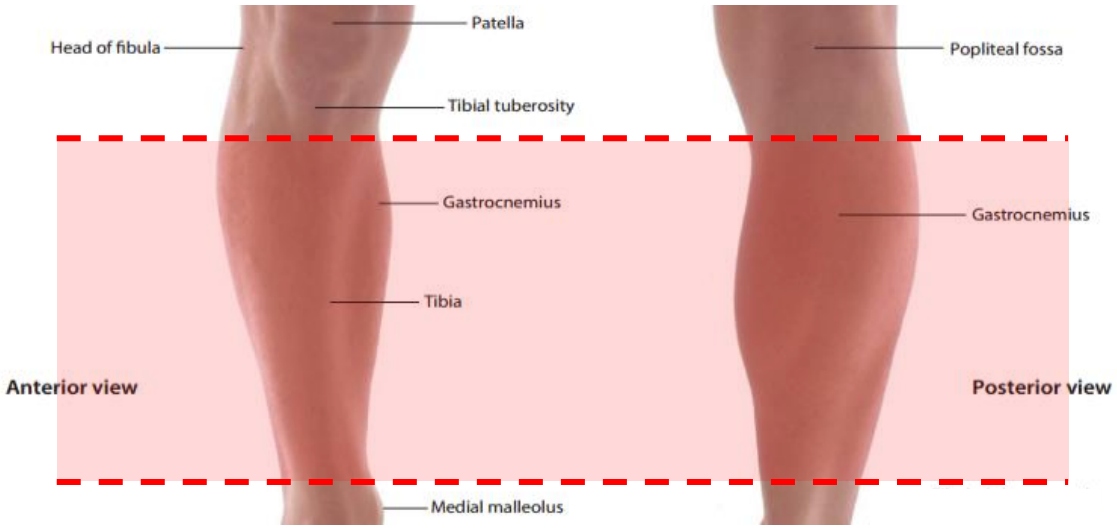

Figure 2.2: Lower limb anatomy and the region of a trans-tibial amputation line (Drake, Vogl, Mitchell, Tibbitts, & Richardson, 2008).

Once amputated, the limb is clinically termed the residual limb (RL). To regain mobility, the RL is inserted into a prosthetic socket which is connected to a prosthetic leg and foot. A basic illustration of the RL and prosthesis is shown in Figure 2.3.

Figure 2.3: Basic illustration of a (a) TTA residual limb and (b) TTA prosthesis.

This makes the RL soft tissue the interface between the body weight and the prosthetic socket, which consequently has to endure large dynamic loads during walking. These loads need to be distributed over the RL areas correctly for a prosthesis to function efficiently. These areas vary in load vulnerability, since some areas entail subcutaneous bony areas, such as the fibula head, anterior tibia, or the tibial tuberosity, while others consist of denser soft tissue, such as the popliteal area and calf muscle, which need to be taken into consideration when designing the prosthetic socket. These anatomically significant sites have been categorised into pressure sensitive and pressure tolerant areas and are provided in Table 2.1.

Table 2.1: Anatomical pressure sensitive and tolerant areas (Friedel & Tarakhchyan, 2017).

PRESSURE SENSITIVE AREAS

ANTERIOR VIEW	LATERAL VIEW	AREA NUMBER	AREA NAME
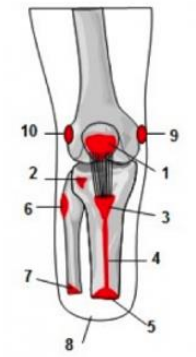	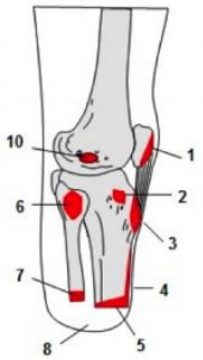	1	Patella
		2	Lateral Tibial Condyle
		3	Tibial Tuberosity
		4	Tibial Crest
		5	Anterior-Distal End of Tibia
		6	Fibular Head
		7	Distal End of Fibula
		8	Distal End of Stump
		9	Medial Femoral Condyle
		10	Lateral Femoral Condyle

PRESSURE TOLERANT AREAS

ANTERIOR VIEW	LATERAL VIEW	AREA NUMBER	AREA NAME
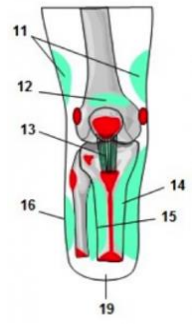	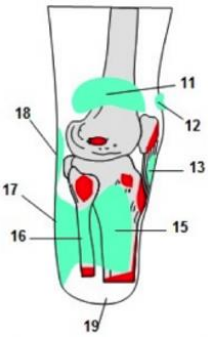	11	Supracondylar Areas
		12	Suprapatellar Area
		13	Patella Tendon
		14	Medial Flare of Tibia
		15	Lateral Flare of Tibia
		16	Lateral Flare of Fibula
		17	Posterior Area of the RL
		18	Popliteal Area
		19	Distal End of Stump

Red Areas – Areas that are vulnerable to pressures, Green Areas - Areas that can tolerate larger pressures without damage.

Every TTA has a unique RL with regards to its load sensitivity, volume, length, skin characteristics and area pressure threshold. Prosthetists consider these variables when deciding on the type of prosthetic socket to create for the amputee. The two most common types of prosthetic sockets that prosthetists can create for their patients are the Patella Tendon Bearing socket (PTB) and the Total Surface Bearing (TSB) socket, which are illustrated in Figure 2.4. The PTB socket (Figure 2.4.a) was introduced in 1959 and was the first socket design to be created by using an intimate mould of the RL (Laing, Lee, & Goh, 2011). The socket is hand cast around the RL mould which the prosthetist can modify to include build-ups or removal of material in specific areas to control the load distribution. For example, the removal of the horizontal section of mould material at the patella tendon area, casts the patella tendon bar protrusion on the inner surface of the created socket (seen in Figure 2.4.a). This concentrates higher pressures onto the patella tendon area (a high load tolerant area) shifting pressures off intolerant areas (Fleer & Bennett, 1962). This socket is generally used for primary amputees (less than 12-18 months post-amputation), with sensitive RL areas that need pressure relief.

Figure 2.4: Socket Types: (a) Patella Tendon Bearing (PTB) socket, which contains features for concentrating large pressures onto pressure tolerant areas (Patella Tendon Bar). (b) Total Surface Bearing (TSB) socket, which distributes the load equally over the residual limb (Barnard, 2017).

Approximately 30 years later the TSB socket (Figure 2.4.b) was introduced, which is cast using a mould created around the RL within an air bladder or vacuum system (Laing et al., 2011). These systems use uniform water pressure to cast the exact mould of the RL. Therefore, the cast socket will produce an equal distribution of load over the RL (Shikh, Abu Osman, & Latif, 2007). TSB is a term used to describe the equal load distribution principle which is implemented in socket designs such as the hydrostatic or pressure cast socket. TSB sockets are generally used by more active amputees whose RL volume has set and has adapted to the loads (Friedel & Tarakhchyan, 2017).

2.3 Prosthetic Socket Fitment Procedure

A brief description of the testing procedure will be discussed to identify when and where a RLES can potentially be used. The knowledge provided, on the prosthetic fitting process, has been referenced from the *Atlas of Limb Prosthetics: Surgical, Prosthetic, and Rehabilitation Principles* (Quigley, 2010).

2.3.1 Post-Amputation Prosthesis Progression

From the postoperative prosthetic socket (received 24-hours post amputation) to the final (definitive) prosthetic socket (received once the RL has stabilised), the amputee is fitted with numerous types of prosthetic socket designs. This is an iterative process, and the socket type progression is shown in Figure 2.5.

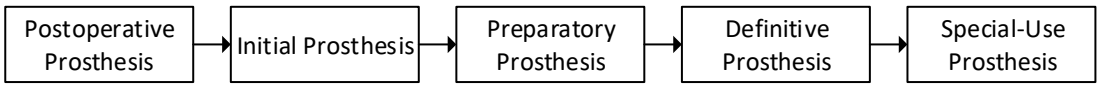

Figure 2.5: Prosthesis type progression. The progression that each prosthesis has to go through before the final prosthesis is prescribed to the amputee.

The postoperative prosthesis is provided within 24 hours of amputation. This prosthesis is to supply the RL soft tissue with pressure to keep a constant and correct RL volume and shape. Once the sutures are removed from the amputation line, the initial prosthesis is provided during the acute phase of healing (one to four weeks after amputation) until the soft tissue adapts to tolerate stress and the suture lines are stable. During the next few months, a preparatory prosthesis is provided which is a prototype prosthesis for the final definitive prosthesis. Its role is to allow ambulation before the RL has fully stabilised and helps the prosthetist to clarify the final details of the future prosthesis. The preparatory prosthesis is generally used for three to six months, however, this duration is determined by factors such

as health problems, weight loss and gain, and speed of RL stabilisation. Once the RL has stabilised and fully matured, the definitive prosthesis is prescribed, which is based on the information and knowledge accumulated during the previous phases. This is the final prosthesis provided to the amputee, and its average lifespan is three to five years. A special-use prosthesis is prescribed to an amputee who wishes to get involved in specific activities such as swimming, golf, sprinting etc. The prosthetic socket of each prosthesis needs to be created and fitted according to the amputee's RL characteristics. This process is discussed in Section 2.3.2.

2.3.2 Prosthetic Socket Creation and Fitment

The prosthetic socket creation and fitting procedure can be described in five steps: 1) Patient and RL evaluation; 2) impression procedure; 3) prosthetic design and creation; 4) test socket creation evaluation 5) and prosthesis alignment. A flow diagram of these steps is displayed in Figure 2.6.

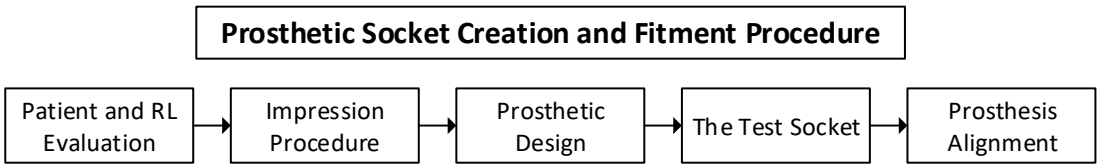

Figure 2.6: Prosthetic Socket Creation and Fitment Procedure.

2.3.2.1 Patient and RL Evaluation

The prosthetic fitting procedure starts with the amputee evaluation which includes two phases, a physical examination and a medical examination. The physical examination includes recording details such as range of motion, muscular development, oedema, scar tissue, and RL measurements. Measurements are taken of both the RL and sound limb.

2.3.2.2 Impression Procedure

On the RL, the length and circumference are measured, after which a negative cast (hollow cast) is created. For PTB sockets, this cast is produced by intimately wrapping the RL with fibreglass, hollow plaster, or plaster impregnated bandage and allowing it to dry (Fleer & Bennett, 1962). In TSB sockets, the cast is created by the vacuum within a water or air bladder chamber (Laing et al., 2011). Bony prominences and important landmarks are marked on the cast to identify load sensitive areas.

2.3.2.3 Prosthetic Socket Design

The negative cast acts as a mould to create a model which accurately represents the TTA's RL which the prosthetist can hand modify by building up or removing material from load sensitive and tolerate areas. The socket is then cast around the model using a resin-based material which moulds the inner surface of the socket to the modified RL model. This produces the required SLT needed for appropriate load distribution. The first socket cast is generally a test socket made from a transparent thermoplastic (Artificial Limb, 2006).

2.3.2.4 The Test Socket

The transparency of the test socket allows for an unobstructed view of the RL within the socket and allows for evaluation to be performed during weight bearing tests. These tests entail the fitment of the test socket onto the RL and for the amputee to bear weight equally over both limbs (generally by standing). The fitment of the test socket is evaluated by drilling holes through the socket wall in strategical areas (over bony prominences, etc.) and probing the underlying skin with a small, blunt rod to determine local

skin pressures (Quigley, 2010). Areas of inadequate or excessive pressures can be identified by the absence or presence of skin blanching or the compression of the prosthetic sock against the inner test socket wall. The thermoplastic property of the test socket allows the prosthetist to heat and modify the socket shape until the fitment is satisfactory (Artificial Limb, 2006). This process is performed visually, which leaves a high probability of human error and if any of the vulnerable areas are missed, the potential for future complications is created. A RLES would potentially mitigate the need to drill holes into the test socket as well as provide the prosthetist with quantitative data of the pressures and temperatures that the RL is exposed to, for a quality assessment of the test socket fitment.

2.3.2.5 Prosthesis Alignment

Once the test socket fitment is complete, it must be aligned correctly with respect to the remainder of the prosthesis, the RL and the biomechanical structure of the body for sufficient movement and gait. The alignment procedure entails the initial, static and dynamic alignment of the socket (Friedel & Tarakhchyan, 2017). The initial alignment is performed without the amputee and is performed solely on the socket and the rest of the prosthetic leg components. The prosthesis is then fitted and aligned on the RL during static sitting and standing positions to ensure that the necessary translation, inclination, and height corrections are made to fit the specific biomechanical profile of the amputee. The dynamic alignment is then assessed visually while the amputee is walking with the attached prosthesis and is a trial and error process (Fleer & Bennett, 1962).

Correct alignment of the prosthesis is crucial, since it determines the way in which the amputee walks which directly contributes to the SLI pressure magnitudes experienced by the RL. Kobayashi et al. (2013) and Boone et al. (2013) found that the coronal and sagittal plane socket reaction moments and occurrences within the gait cycle can be manipulated through alignment changes. These moments induce the SLI pressures and determine their magnitude which highlights the effect that alignment has on the RL load distribution. Malalignment has been seen to induce a change in interface pressures ranging from 40 kPa (Frank Appoldt, Bennet, & Renato, 1968) to 266 kPa (Pearson, Holmgren, March, & Oberg, 1973) in certain RL areas. In addition to prosthesis alignment, the type of shoe an amputee wears also contributes to the type of SLT. Seelen et al. (2003) studied how RL pressures shifted when the interface between the prosthetic foot and the ground changed. It was found that when adding a 0.5 cm thick wedge under the heel, the pressures at the patella tendon decreased by 30.4%, but consequently increased the pressure at the distal tibia by 40% (a pressure sensitive area). Additionally, by adding a 0.5 cm wedge under the forefoot, the pressures at the distal tibia were decreased by 30%.

This research suggests that the socket design and fitment, prosthesis alignment and selection of prosthetic components are all equally important when controlling the load distribution on the RL. A RLES which can measure the SLI pressures while monitoring the gait GRF pattern of the prosthesis can potentially provide a more efficient evaluation of these critical components, improve the quality of the final prosthesis, and improve the QOL of the amputee. Additionally, this system would have the potential to analyse the socket fitment data while the amputee performs normal daily activities, such as incline/decline/straight-line walking, sitting, standing, running, specific sport movements, etc. This would expand the RL evaluation of the test socket design and allow the prosthetist to modify and tailor the design the prosthetic socket. This would reduce the risk of incorrect load distribution as well as future mechanically induced skin problems.

2.3.3 Prosthetic Gait

The term gait defines the walking pattern of an individual. A complete gait cycle begins at the heel strike of one limb and ends at the next heel strike of the same limb. This cycle comprises of two main phases:

stance and swing. The stance phase is determined by the duration of foot contact with the ground (60% of the cycle), and the swing phase is the period between the foot lifting off the ground (toe off) and its next contact with the ground (heel strike). An example of the vertical GRFs found during an amputee gait cycle can be seen in Figure 2.7, which is an extract from a study by Su et al. (2007) who investigated the gait differences between abled body and bi-lateral TTA participants.

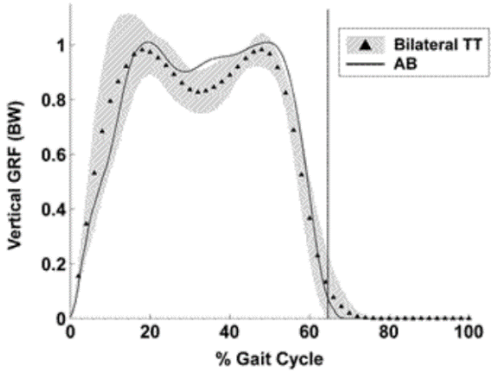

Figure 2.7: Mean pattern of the GRF for subjects with bilateral trans-tibial amputations vs abled body walking. GRFs were normalized by body weight (BW). The shaded area on either side of Bilateral TTA mean represents 1 standard deviation. The vertical line represents toe-off (Su et al., 2007).

The GRF curve of the TTA stance phase comprises of five stages: heel strike, foot flat, mid stance, terminal stance, and toe off. The stance phase starts with initial contact of the prosthetic foot (heel strike). Plantar flexion of the prosthetic foot then starts increasing until foot flat which takes place within 5 - 15% gait. The body weight then starts to transfer from the heel to the forefoot as the body moves over the foot during mid-stance. During this phase the RL supports the entire body weight. Terminal stance begins as the body weight vector passes the forefoot until the contralateral heel strikes the ground. The second peak defines the end of terminal stance after which the weight starts to transfer to the contralateral leg (40 – 55%). Toe off defines the end of the stance phase as the foot leaves the ground. The stance phase is approximately 60 - 66% of the entire gait cycle (J Sanders et al., 1993; Su et al., 2010). The SLT, during walking, only takes places during the stance phases. Therefore, a RLES that can produce the GRF gait curve can help the prosthetist identify and correlate the specific phase in gait at which RL pressures occur. This function can help assess the fitment and alignment of the prosthesis.

The reaction forces between the body weight and the prosthetic socket determine the magnitude of the SLI pressures which change between standing and walking movements. Zhang et al. (1998) found that during straight line walking, the direct pressure and shear stress of RL areas increased relative to standing pressures by 3.1 ± 1.5 times and 3.1 ± 0.9 times respectively. Researchers found that this increase was variable between TTAs and could not be predicted from standing RL pressures (Seelen et al., 2003; Zachariah & Sanders, 2001; Zhang et al., 1998). This suggests that the pressures found during the standing weight-bearing tests (Section 2.3.2.4), while evaluating the test socket, cannot predict the pressures that occur on the RL while walking. Although the comfort of the socket on the RL is evaluated during the dynamic alignment phase, it is difficult to visually gauge the magnitude of the SLI pressures while the amputee is walking.

TTA gait differs from abled body gait (Figure 2.7) since, depending on the prostheses type, it generally lacks the medial-lateral rotation and ankle rotational movement, therefore, learning to walk correctly again is difficult. During the fitting and alignment procedure, the prosthetist looks for deviations in gait (incorrect walking habits) and corrects them before the amputee adopts them. Gait deviations are usually identified by insufficient gait symmetry between both limbs (Berger, 2010). If not identified, the deviation

may be adopted by the TTA which is then hard to correct and can lead to injury, muscle strain, or pain. RL discomfort or pressure pain while walking, due to an improper fitted or aligned prosthesis, is common in TTAs and is a primary cause of gait deviations. For example, RL discomfort may cause the amputee to have an uneven step length between limbs whereby a longer step is taken on the healthy leg than with the prosthesis to relieve the RL from pain. Gait analysis can be performed using force-plates, however, these are expensive and only provide data on a single step, and therefore most prosthetists perform the procedure empirically. A RLES which can obtain the gait GRF curves and step lengths between both TTA limbs, as well as the SLI pressures, would potentially assist in the identification of gait deviations, and assess the RL during the correction process to obtain the most efficient solution.

2.4 Common Residual Limb Skin Problems and Causes

Incorrect socket fitment, prosthesis alignment or prosthetic component selection can lead to the SLI environment becoming susceptible to many different forms of skin problems. The most prevalent of such, which are found on the TTA's RL, are presented in Table 2.2 which briefly describes the issues, their causes, treatments and which variable would need to be measured to analyse the susceptibility of the tissue to this skin problem.

Table 2.2: Skin problems of the TTA residual limb, their causes, solutions and variables involved (Levy, 1980).

RESIDUAL LIMB SKIN PROBLEM	BRIEF DESCRIPTION	CAUSES	SOLUTIONS	SLI VARIABLE
Oedema	Soft tissue swelling	Incorrect socket fitment or alignment	Socket fitment and prostheses alignment corrections.	Direct Pressure Shear Stress
Contact Dermatitis	Acute or chronic skin inflammation	Allergic reaction or irritation to the prosthetic component material. Humidity, heat and friction intensities the reaction.	Increased RL hygiene. Prosthetic liner or socket material selection.	Shear Pressure Moisture Temperature
Nonspecific Eczematisation	Dermatitis over the distal portion of the residual limb	Incorrect socket fitment that causes oedema and congestion at the end of the stump.	Socket fitment or prosthesis alignment corrections.	Shear Pressure Direct Pressure Moisture Temperature
Epidermoid Cysts	A benign cyst that develops under the skin.	Trapped keratin build-up induced by skin trauma.	Socket fitment or prosthesis alignment corrections.	Direct Pressure Shear Pressure
Bacterial and fungal infections	Bacterial folliculitis or boils on the skin.	Bacteria invasion into the hair follicle. Warm and moist skin increases invasion ability.	Increased RL hygiene. A decrease in heat retention within the SLI.	Moisture Temperature
Ulcers	A crater-like wound found on the skin	Bacterial infection in the soft tissue, pressure induced blood supply interruptions or vascular disorders.	Increased RL hygiene, Socket fitment or prosthesis alignment corrections.	Direct Pressure Moisture Temperature
Verrucose Hyperplasia	A warty condition at the distal end of the RL	Invasion of a common wart virus into the skin.	Sufficient compression of the distal RL soft tissue.	Direct Pressure

Dudek et al. (2006, 2005) conducted studies (discussed in Section 1.3) investigating the type, frequency and cause of lower limb amputee skin problems. These skin problems and their causes found in these studies were extracted, categorised and illustrated as a percentage as shown in Figure 2.8

Skin Problem Types and Etiologies

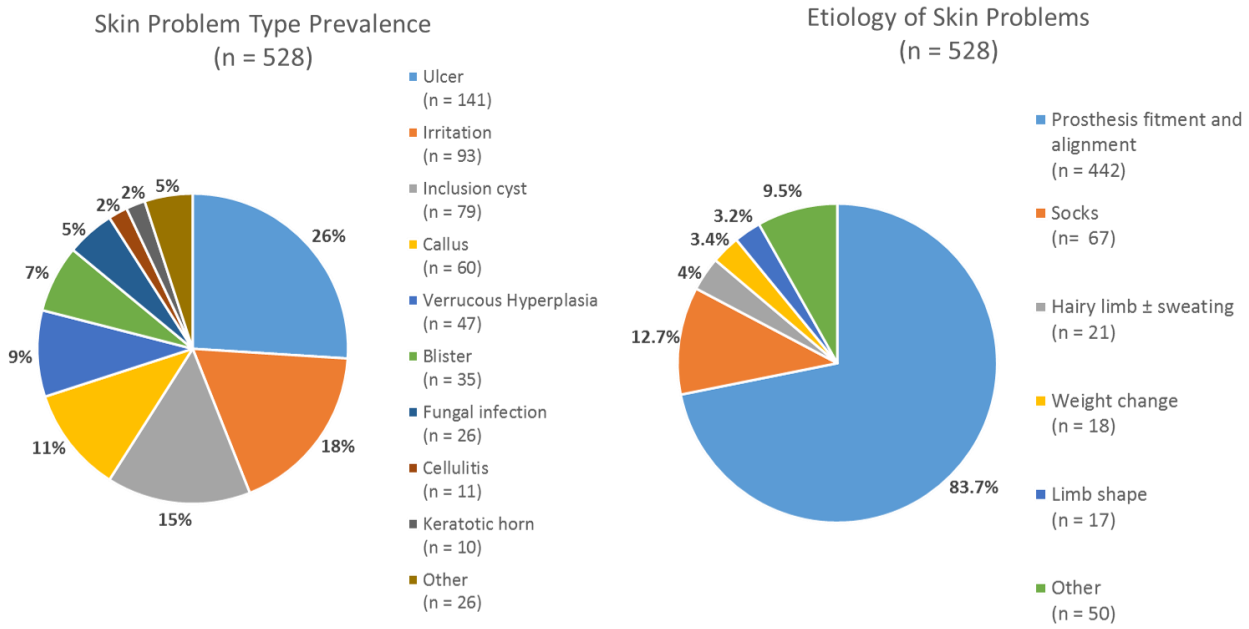

Figure 2.8: Skin problem prevalence and major contributors (Dudek et al., 2006, 2005).

The results presented in Figure 2.8 suggest that the top three contributors to lower limb amputee skin problems are the prosthetic fitment and alignment, prosthetic components (socks/liners), and RL hair and perspiration. Table 2.2 shows that the SLI variables produced by these contributors are direct pressure, shear stress, temperature and moisture. This suggests that measuring all of these variables within the SLI during the prosthetic fitting procedure could potentially provide a thorough analysis of the RL health within the socket, and allow for appropriate corrections to be made. This may potentially decrease the risk of these common skin problems. The scope of this study is limited to developing a RLES that measures only the direct pressure and skin temperature on RL areas. However, future studies should incorporate additional means of measuring shear stress and moisture within the SLI.

2.5 Socket Limb Interface

2.5.1 Soft Tissue Under Stress

Every object that is subjected to a force undergoes a variety of stresses depending on the type of material, the shape of the object, the point of force application, and the angle of the force. Stress is a term to describe the magnitude of force per unit area which is measured in Pascals (Pa). Stress consists of two main stresses acting on an element, these are normal stresses, σ, which acts perpendicular to the element surface and shear stresses, τ, which is the frictional force between the material elements under force and act parallel to the surface of the element. The scope of the study is limited to the measurement of normal stress which will be referred to as pressure.

2.5.1.1 Pressure

Pressure is always directed perpendicular to the area or plane on which the force is acting upon and is calculated by the equation 1:

$$\sigma = \frac{F}{A} \qquad [1]$$

Where F is the force load, A is the area over which the load is acting, and σ is the unit of pressure felt over the area (measured in Pascal which will be presented in kilopascal (kPa) within this study).

2.5.1.2 The Effect of Pressure and Shear Stress on The Residual Limb Soft tissue

While walking, the SLT onto the RL induces shear stress and pressure on the soft-tissues which can cause structural damage to the cells that can lead to the development of skin problems. The soft tissue layers between the bones and the skin surface are composed of the epidermis, dermis, subcutaneous fat and muscle (Figure 2.9). Each layer consists of different thicknesses, location and nutrition supply.

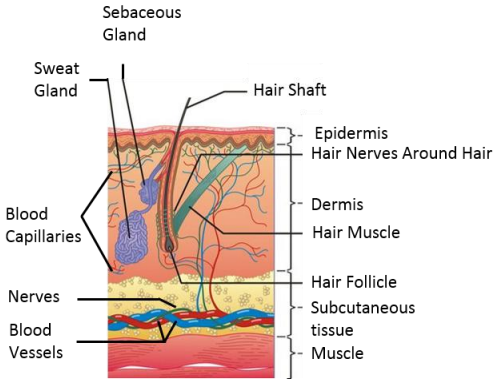

Figure 2.9: Soft tissue layers between bone and skin surface (Geoface, 2017).

These layers serve many functions such as body temperature regulation, as well as fat and water excretion, but their two primary functions are the protection of the inner organs and sensory feedback to the central nervous system. For the smooth function of critical metabolic activities, the skin cells rely on blood vessels to provide oxygen through blood as well as the removal of toxic metabolic by-products (Shea, 1975). Cell compression and tension from mechanical loads can interrupt this function which can cause many problems and can lead to cell death.

The TTA's RL comprises of bony prominences (fibula head, tibia crest, etc.) and subcutaneous bone which are vulnerable to mechanical loads since they create pressure points between the RL and the socket. These areas are common sites for pressure sores (ulcers), which are the most common skin problems found within the TTA population (Dudek et al., 2006). Potential reasons for this is that when a pressure is exerted to the soft tissue over a bony prominence, a pressure gradient is formed between the skin surface and the bone as illustrated in Figure 2.10 (Collier & Moore, 2006). This is known as the McClement Cone Effect which describes how the pressure increases in a cone-like shape from the surface of the skin (at load contact), through the soft tissue layers, to the surface of the bone. Pressure increases along this gradient (represented by the green arrows) reaching three to five times the initial skin contact pressure magnitude (P_0) which is felt within the muscle layer (P_1) (Butcher & Thompson, 2009; Collier & Moore, 2006; Dunk & Gardner, 2015).

The subcutaneous fat layer comprises of loose connective tissue consisting primarily of adipocytes (fat cells). Adipocytes can compress or stretch when subject to mechanical stresses. This offers shock absorption to protect deeper layers, however, this also applies pressure to the blood vessels that flow through this layer. Pressure from large mechanical stresses can cause the adipocytes to compress the blood vessel which can compromise or occlude blood flow. Occlusion of a blood vessel stops the blood flow within an area which is known as ischemia. During ischemia, cells cannot retrieve oxygen from the blood or discard of their metabolic waste by-products, which becomes increasing harmful to the cell and can lead to apoptosis (cellular death). The magnitude of cell damage is dependent on the duration of ischemia and the magnitude of mechanical stresses (Shea, 1975; Stekelenburg, Gawlitta, Bader, & Oomens, 2008). If the damage to the soft tissue is irreversible, a pressure sore will form in the area.

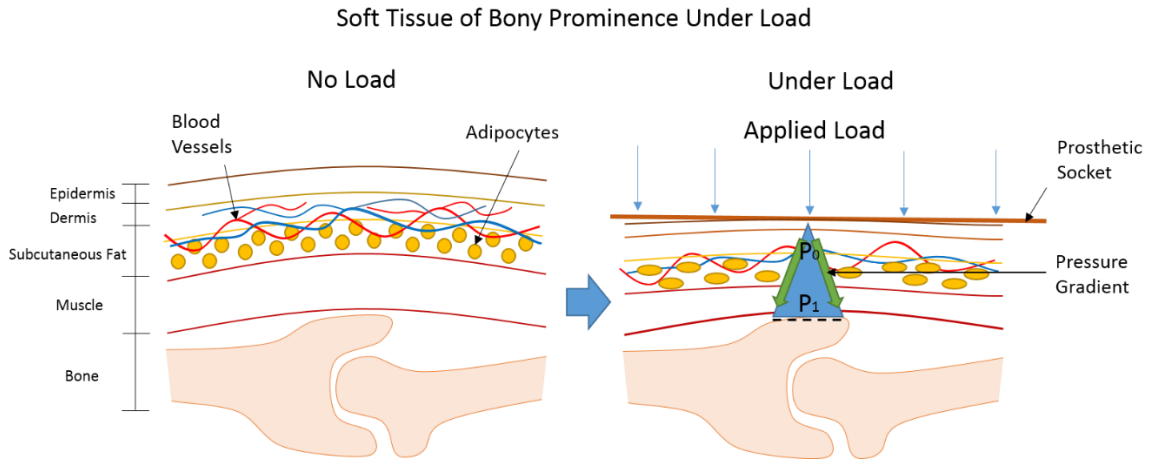

Figure 2.10: A pressure gradient is formed between the bone and the skin surface when an external load is applied to over a bony prominence. The pressure increases from the skin, through the soft tissue layers (P_0), to the bone surface (P_1).

The pressure-resistant threshold of blood capillaries has been found to be within 1.6 – 10 kPa (Chang & Seireg, 1999; Goossens, Zegers, Vandijke, & Snijders, 1994; Patterson & Fisher, 1986; Shea, 1975). Interface pressures exceeding this threshold begin to compress the blood vessel and compromise the blood flow which can lead to ischemia. Pressure related skin problems are commonly found in bedridden patients due to long durations of interface pressure being applied to soft tissue without relief. This common problem caused researchers to investigate the development of these pressure sores to form preventative methods and solutions.

Animal studies found that there is an inversely proportional relationship between the magnitude of pressure applied to the skin and the application duration required to induce irreversible skin damage (Bar, 1991; Linder-Ganz, Engelberg, Scheinowitz, & Gefen, 2006; Sacks, 1989). Reswick and Rodgers (1976) were the first to perform a human study on the pressure-time relationship and developed a pressure-time curve which indicates acceptable and unacceptable durations of applied pressure magnitudes. This curve is known as the Reswick & Rogers Pressure-Time Curve (Figure 2.11) and has been used as a guideline in pressure sore management studies ever since (Sacks, 1989; Stekelenburg et al., 2008). During TTA ambulation, the RL experiences pressures during each stance phase and relief during the swing phase. The stance phase duration is variable between individuals but can be approximated to 0.6 – 1 seconds (J Sanders et al., 1998). The threshold in Figure 2.11 suggests that pressures above approximately 100 kPa are dangerous to the soft tissue over this duration. A RLES with a function that alerts the prosthetist if a RL area is experiencing a pressure exceeding 100 kPa, could potentially help to minimise the risk of pressure sore development.

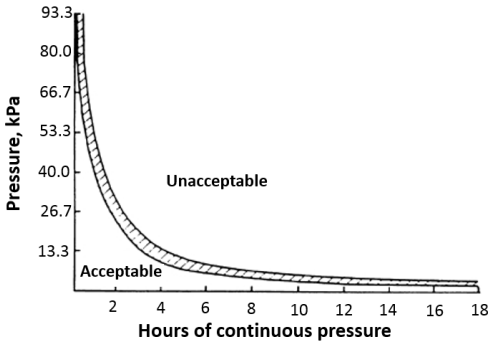

Figure 2.11: Reswick and Rodgers Pressure-Time Curve (Reswick & Rogers, 1976): Defines the threshold of acceptable pressures and their durations that can be applied to soft tissue before damage is caused.

This value can only be used as a guideline as soft tissue characteristics vary significantly between different individuals as well as RL areas.

2.5.1.3 Socket-Limb Interface Pressures

Evaluation of socket fitment, quality, design and alignment can be performed through the measurement of SLI pressures during ambulation. Studies during the past 50 years have utilised many different methods of measuring these pressures such as:

- Embedding strain gauges or load cells within the prosthetic socket wall (Goh, Lee, & Chong, 2003b; J Sanders et al., 1993; Joan Sanders & Daly, 1993; Zachariah & Sanders, 2001; Zhang et al., 1998).
- Embedding Force Sensitive Resistors (FSRs) within liners which are fitted on the RL underneath the socket (Beil, Street, & Covey, 2002; Boutwell, Stine, Hansen, Tucker, & Gard, 2012).
- Embedding Fibre Bragg Grating (FBG) optic sensors within liners which are fitted on the RL underneath the socket (E. Al-Fakih, Abu Osman, Mahamd Adikan, Eshraghi, & Jahanshahi, 2016)
- Inserting prototype capacitive sensors within the SLI (Laszczak et al., 2016).
- Commercially available piezoresistive interface pressure measurement systems placed within the SLI (Ali et al., 2013; Convery & Buis, 1998; Dumbleton et al., 2009; Eshraghi, Abu Osman, Gholizadeh, Ali, & Abas, 2014; Rajtukova et al., 2014; Shikh et al., 2007; Zhang et al., 1996).

The literature on SLI pressure measurements present a large range of pressures over different RL areas. For example, Al-Fakih et al. (2016) and Goh et al. (2003b) both used a commercially available product (Tekscan's® F-Socket™) to measure the SLI pressures on the RL anterior within a TSB socket and Al-Fakih found an average of 83.3 kPa whereas Goh found 28.4 kPa. Interestingly the subject within Goh's study weighed 76.2 kg whereas the participant in Al-Fakih's study weighed 58 kg. Additionally, Boutwell et al. (2012) found pressures ranging from 72 – 496 kPa on the patella tendon area (within the RL anterior) between 10 subjects, using TSB sockets, and that this range changed to 125 – 252 kPa when the same subjects wore a thicker liner. It was suggested by Boutwell et al. (2012), that this change was due to the shock-absorption capabilities of the thicker liner. A change in pressure due to liner type was also found by Ali et al. (2012) who found a significant pressure difference (p-value < 0.05) between the same subjects wearing two common liner types. Studies performed on PTB sockets present similar variations in SLI pressures, for example, Shikh et al. (2007) found an average of 12.5 kPa over the RL anterior whereas Zhang et al. (1996) found 215 kPa, and both studies utilised the same commercial sensor (Tekscan's® F-Scan™). These studies show that results vary significantly between studies which suggest that SLI pressures are governed by socket type, liner type, alignment settings, sensor types, sensor placements, gait GRF and human variation factors (Goh et al., 2003b). Therefore, this suggests that evaluating the reliability objective of the RLES (Section 1.5.2) cannot be performed by comparing the pressure results to a defined range approximated from literature. However, Radcliffe (1962) investigated the biomechanics of a below-knee prosthesis (PTB socket on a unilateral TTA) and presented the expected large pressure areas during walking. These areas comprise the patella tendon, anterodistal tibia, and in the popliteal. Additionally, literature states that bony prominences cause pressure points within the SLI, and therefore prosthetists design sockets to reduce the pressure within a range tolerable by the area. However, larger pressures are still to be expected within these areas than other areas due to their bony subcutaneous structure (Boutwell et al., 2012; Dudek et al., 2005; Highsmith & Jason, 2011; Joan Sanders & Daly, 1993). Lesser pressures tend to fall on the distal medial, posterior and lateral RL areas since the socket suspension area is more proximal on the RL which misses these areas. Furthermore, these areas generally contain more soft tissue volume which distributes the load. Therefore, this suggests that evaluating the

reliability objective (Section 1.5.2) should be performed by analysing the SLI pressures obtained on each participants RL and comparing the results with expected assumptions made in relation to each specific amputee's characteristics, RL features, socket type, etc.

2.5.2 Temperature Effects on Soft Tissue

Thermoregulation in humans is a process governed by the hypothalamus that controls and stabilises the core temperature of the body. In cold ambient temperatures, the arterioles that carry warm blood to the superficial capillaries constrict, thereby rerouting blood away from the skin towards the core of the body to prevent it from losing heat to the atmosphere and dropping the body's core temperature. In hot ambient temperature, eccrine sweat glands start to perspire (water with some dissolved ions) onto the surface of the skin, which leads to evaporation and the skin temperature to cool via convection. This is the only bodily function that humans have to lower their skin and core temperature and this important thermoregulatory function is interrupted within a prosthesis, which leads to an increase in temperature and perspiration build-up (Charkoudian, 2013).

The majority of prosthetic socket designs and component selections revolve around minimising the pressures between the prosthetic socket and limb. A usual prosthetic component selection is a socket liner, generally made from a silicone-based material, which is fitted over the RL underneath the socket to decrease the SLI shear and direct pressures. However, this creates an insulated silicone housing around RL which retains the heat, increases the RL skin temperature, and traps the perspiration. During ambulation, the RL skin temperature increases further due to muscle energy expenditure, friction between the RL skin and liner, and the soft tissue reaction to loading. Hagberg and Brånemark (2001) conducted a study on the QOL of lower limb amputees which reported that 72% of the 90 participants suffer from discomfort due to perspiration and heat within the SLI. An increase in skin temperature within an airtight and intimately fitted liner, causes an increase in perspiration which consequentially increases the moisture of the skin (Thiele & Senden, 1986).

Moisture has been seen to increase the risk of skin breakdown with theories stemming from the biomechanics of skin literature that suggest that moisture decreases the stiffness of the dermis and stratum corneum (the outer most layer of skin), which causes the skin to undergo greater elongation under stress (Papira, Hsu, & Wildnauer, 1975). This increases the strain from both pressure and shear stress and puts the cells at risk of trauma (Joan Sanders & Goldstein, 1995). Additionally, Highley et al. (1977) conducted a study investigating how moisture changes the frictional coefficient of skin and found that an application of distilled water dramatically increased this coefficient value from an average value of 0.19 - 0.28, for dry untreated skin, to approximately 1.5 before slowing decreasing as the skin became wetter. The consequence of this within the TTA SLI can be investigated by calculating the increase in frictional force that this has on the RL skin. The frictional force (F_f) between two objects is calculated using the equation 2:

$$F_f = \mu F_n \qquad [2]$$

Where μ is the frictional coefficient, and F_n is the normal (orthogonal) force between the two objects. Therefore, moist skin can increase the frictional force between the RL skin and liner/socket by five to seven times more than dry skin. Consequently, this may decrease slippage between the liner and the RL, but will subject the soft tissue of the RL to continual shear whilst walking. The increase in frictional force combined with the large increase in shear stresses found while walking, as well as the raised elastic properties of skin dermis, places a higher strain on the RL soft tissue when exposed to shear stresses by the liner/socket. This has been shown to promote the formation of friction blisters (Akers & Sulzberger, 1972; Naylor, 1955). Therefore, the combination of the skin moisture and mechanical stresses creates a

vulnerable environment for the RL soft tissue within the SLI. Additionally, a damming of perspiration around the limb creates an ideal environment for bacteria to enter and inflame the hair follicle causing folliculitis which is a common skin issue for amputees (Levy, 1980). Thiele and Senden (1986) investigated the skin water loss from the human forearm when subjected to a range of temperatures and found a proportional relationship between the two parameters. This emphasises the need to monitor the temperature of the RL when selecting a liner, sock, or socket material to decrease the amount of perspiration from the RL skin and decrease the vulnerability of the RL soft tissue to mechanical loads.

In addition to the increase in vulnerability of soft tissue by moisture, an increase in the temperature of soft tissue was found to decrease its resilience to pressure (Kokate et al., 1995). Kokate et al. (1995) performed an animal research study on the soft tissue of a swine to determine the effects of temperature on soft tissue degradation under pressure. A pressure of 13.33 kPa was applied to four different areas of the swine for a five-hour period using four temperature-controlled pressure discs at 25 °C, 35 °C, 40 °C and 45 °C respectively. They found that all tissue layers appeared normal at temperatures of 25 °C, however, at temperatures of 35 °C, 40 °C and 45 °C muscle damage and cell necrosis were clearly visible in which the severity of damage increased proportionally to the temperature increase of the area. This study indicates that soft tissue becomes increasingly more vulnerable with a temperature rise, and therefore highlights the importance of skin temperature analysis of the RL within the SLI.

2.5.2.1 Socket-Limb Interface Temperature Research

The literature on TTA RL temperature measurements is scarce and has only been performed over the last 15 years. The focus of the studies was merely to investigate the temperatures on the RL of amputees during activity. The most common temperature measurement method used in the studies is the attachment of thermistors to the RL skin while others use thermography or create predictive computer models. Huff et al. (2008) conducted a study investigating if activity increased the RL skin temperature of nine participants during a 30-minute treadmill walk (Figure 2.12).

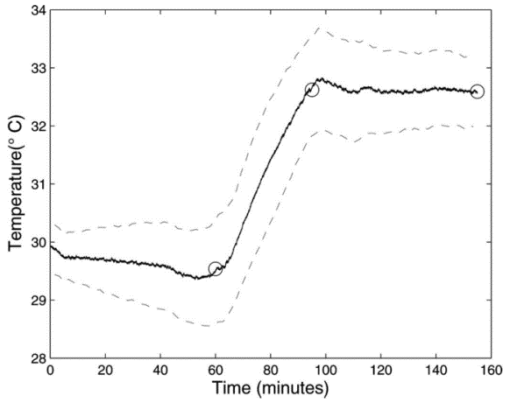

Figure 2.12: Average residual limb temperature results (16 temperature sensors) performed by Huff (2008). Testing procedure entailed participants to 1. Sit for 1 hour, 2. Treadmill walk for 30 minutes, 3. Sit for 1 hour. These sections are broken up by the plotted circles (Huff et al., 2008).

It was found that the RL temperature increased by 3.1 °C during the walk and after a 60-minute rest period the temperature had only decreased by 0.9 °C. This suggests that heat produced during walking is retained within the SLI for several hours after activity which can induce an increase in perspiration and moisture putting the RL at risk. Peery et al. (2005) conducted a similar study involving five TTAs and found that there was a difference in skin temperature increase between different socket and liner material as well as locations on the RL. It was also suggested that larger temperature increases are found over areas of more muscle mass due to metabolic energy expenditure (Peery et al., 2005).

These two studies involved a slight limitation which was that the ambient temperature of the testing environment was not recorded before performing tests. This variable has been shown to be an important parameter in determining the RL skin temperatures (Mathur, Glesk, & Buis, 2016). A study conducted by Mathur et al. (2016) found that RL skin temperature is a function of ambient temperature whereby, an increase in ambient temperature increased the RL skin temperatures of the same subject. The ambient temperature investigated in the study ranged from 10 °C to 25 °C which resulted in maximum RL skin temperatures of 26 °C and 31 °C respectively. An increase in temperature has been directly related to an increase in skin perspiration (Thiele & Senden, 1986). Therefore, these studies highlight the importance of analysing external parameters such as prosthetic component material and ambient temperatures during the prosthetic component selection.

RL skin temperature measurements have also been used to analyse the fit of a prosthetic socket. Cutti et al. (2014) used infrared thermography to track TTA RL skin temperature change during walking. The results suggested that RL skin temperature measurement can be used for identifying incorrect load distribution within the socket, areas of skin inflammation, and areas of thrombosis. This is due to how the blood capillaries below the skin react to large loads. If an external load applied to the skin surface constricts blood flow in a soft tissue area, there will be a lack of oxygen to the tissues and toxic metabolic by-products will begin to accumulate. Once pressure is relieved, blood flow will significantly increase to make up for oxygen lost as well as relieve the cells from toxins. This phenomenon is known as reactive hyperaemia and is illustrated in Figure 2.13.

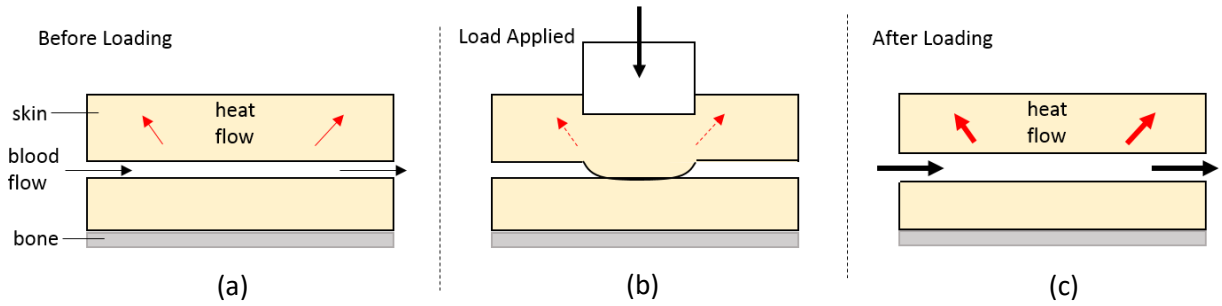

Figure 2.13: Reactive Hyperaemia. (a) Normal blood flow and heat transfer to the skin. (b) Occluded blood flow by load and decreased heat transfer to the skin. (c) Reactive hyperaemia increases blood flow and heat transfer to skin represented by the thicker arrows. Picture recreated from (Pye & Bowker, 1976).

The lack of oxygen and blood flow caused by the occlusion of blood is a primary contributor to the development of pressure ulcers which are frequently found on the bony prominences of bedridden patients. Therefore, this skin temperature reaction to loading has been studied by numerous researchers to investigate potential pressure sore indicators. However, all studies provide no hard conclusions that this temperature increase is related (Sae-Sia, Wipke-Tevis, & Williams, 2005; Sprigle, Linden, McKenna, Davis, & Riordan, 2001). They do, however, indicate that it is potentially possible to identify if an external pressure is causing ischemia in an area by analysing the initial temperature drop (Barnett & Ablarde, 1995; Meijer et al., 1989).

From the literature, it is evident that RL skin temperature changes are variable between individuals and is due to differences in soft tissue mass, muscle activity, prosthetic component material, induced load, and ambient temperature. Therefore, it can be assumed that the only cause of temperature change on the RL that can be controlled in the prosthetic fitting process, is the type of prosthetic component material and the SLT.

A RLES that has the ability to measure the RL skin temperature as well as the load acting on the soft tissue, could potentially allow the prosthetist to analyse the socket fitment and SLT, as well as determine which prosthetic component material is best suited for the amputee to reduce perspiration and keep the SLI environment as healthy as possible.

2.6 Commercial SLI Pressure Measurement Systems

The most commercially common in vivo pressure systems used have been found to be Xsensor® (Calgary, Canada), Tekscan® (F-Socket™, Boston, MA) Vista Medical (FSA In-socket Mat, Winnipeg, Canada), and the Rincoe Socket Fitting System (RSFS) (Munich, Germany). The latter three being the only SLI pressure mapping systems, and therefore will be investigated (Figure 2.14).

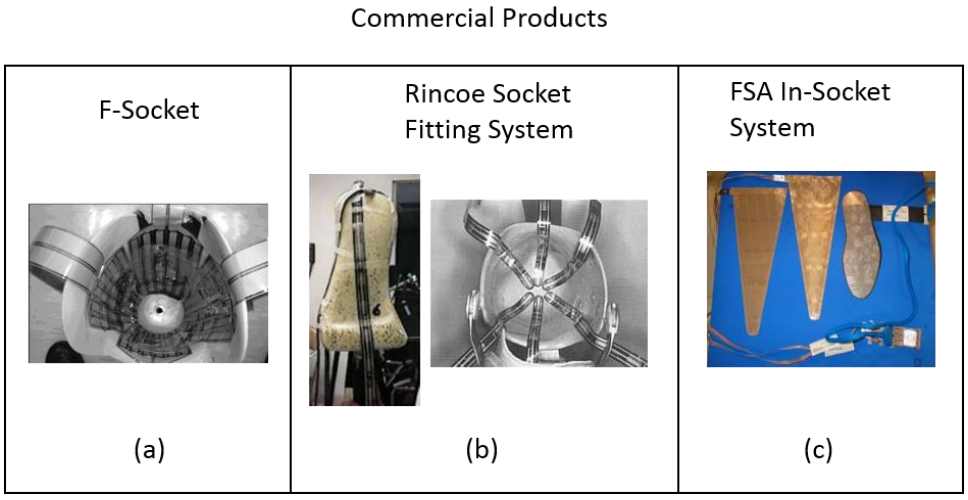

Figure 2.14: Commercial Prosthetic Fitting Products (a) Tekscan's® F-Socket™ (Dumbleton et al., 2009) *(b) Rincoe Socket Fitting System* (Lara, 2007) *(c) Vista Medical's FSA In-Socket System* (Vista Medical, 2017).

The F-Socket™, RSFS and the FSA pressure measurement systems all entail a matrix of piezoresistive force sensitive resistors that relate the change in resistance to the amount of applied force over the active sensing area. These are generally chosen for their ease of use, flexibility, small size, high sensitivity, availability and low cost, however, they have been shown to produce hysteresis and drift in their results. Piezoresistive sensors are very thin which makes them ideal to be placed within a prosthetic socket without concern of socket/limb interface change.

The most common device used in studies is the F-Socket™ also referred to as F-Scan™. The F-Socket™ comprises two sets of 96 individual sensors arranged in a matrix of 16 rows and 6 columns. Each sensing area is approximately 0.55 $cm^{2,}$ and the length of the total sensing areas is approximately 20 cm. The RSFS consists of 60 FSRs embedded into six 0.36 mm strips of polyvinylidene fluoride. Each strip allows for ten points of pressure measurements, and calibration steps are provided by the manufacturer (Shem, Breakey, & Werner, 1998). The FSR mat, from Vista Medical, comprises a piezoresistive socket insert along with an insole insert to collaborate socket pressures with gait characteristics. All systems allow for only the direct pressure measurement between the socket and the RL, however, out of all three systems, the Tekscan® F-Socket™ system is used in most SLI pressure measurement studies.

2.6.1 Commercial Product Limitations

The presented commercial SLI measurement systems (Figure 2.14) are limited to the measurement of direct pressure only. Even though pressure is one of the primary contributors to skin problems, it is not the only evaluation parameter of the RL to measure. Therefore, the current commercial products are mainly for the analysis of the SLT by specific socket designs, fits and alignments, which cannot give a full

analysis of how the RL fairs within the new socket-limb environment. Evaluations between the two most commonly used systems (RSFS and F-Socket™) have been performed by researchers to investigate the accuracy, hysteresis and drift errors (Polliack et al., 2000). Each system was evaluated on their performance by measuring pressure on a flat surface and a curved surface (RL mould) within a controlled environment. The results are presented in Table 2.3.

Table 2.3: RSFS and F-Socket™ system capability evaluation between a flat surface and curved surface (Polliack et al., 2000).

RSFS VERSUS F-SOCKET™ STUDY RESULTS

System Type:	RSFS		F- SOCKET™	
	Flat Bed	Mould	Flat Bed	Mould
Accuracy error	24.7 ± 19.02%	32.9 ± 31.2%	8.49 ± 7.21%	11.2 ± 9.58%
Hysteresis error	15.1 ± 7.98%	23.1 ± 15.1%	41.88 ± 14.9%	24 ± 19.2%
Drift error	7.43 ± 7.16%	11.3 ± 6.07%	11.9 ± 6.05%	33.2 ± 26.5%

The study also evaluated how each system performed against RL areas of different curvatures and it was found that the F-Socket™ and RSFS had an average accuracy error of 10% and 35% respectively (Polliack et al., 2000). The results show that the accuracy of the F-Socket™ is far more superior to the RSFS, however, prosthesis walking involves subjecting the RL to dynamic loading and unloading throughout the gait cycle which induces hysteresis. This is a limitation of the F-Socket™, since its average hysteresis value is 33% over the flatbed or mould. F-Socket™ is the most commonly used system within SLI pressure investigations, however, the limitations of the system suggest that the results obtained may be inaccurate due to hysteresis. Therefore, the design and development of the RLES system within this study, attempts to minimise this error to improve the quality of the evaluation capabilities.

2.7 Transducer Research

The following section evaluates current transducers and placement methods for SLI pressure and temperature measurements to be used in the RLES system.

2.7.1 Placement Techniques

There are four common categories of placement techniques for SLI transducers (Figure 2.15) namely: (a) mounted on socket wall with liner penetration; (b) mounted on socket wall without liner penetration; (c) in the skin-liner interface or liner-socket interface; (d) embedded within the socket. SLI pressure and temperature investigations (presented in Sections 2.5.1.3 and 2.5.2.1) have seen to utilise all placements method used in Figure 2.15. Configuration (a) and (b) has been used to measure both pressure and shear stress and involved manufacturing a test socket with embedded sensing mechanisms in the socket wall (F Appoldt, Bennett, & Contini, 1969; Goh, Lee, & Chong, 2003a; Goh et al., 2003b; J Sanders et al., 1993; Joan Sanders & Daly, 1993; Zachariah & Sanders, 2001). The piston which is flush with the skin or liner, transfers the pressure and shear stress experienced at the interface (induced by the socket) to a strain gauge system within the sensing mechanism. Strain gauge systems produce highly accurate results, however, entail manufacturing a new socket for testing. A RLES, to be used in the prosthetic fitting procedure, requires a method that can evaluate the SLT of a test socket or existing socket, and therefore renders this method inadequate to be used in this study. Configuration (d) entails the creation of a socket with embedded transducers within the resin of the socket wall which allows for the measurement of stresses experienced by the socket material (E. A. Al-Fakih, Abu Osman, & Mahmad Adikan, 2016). This method also entails manufacturing a new socket for testing, and therefore will not be considered for this study. Configuration (c) requires no modification to the socket and the method requires either inserting

transducers within the SLI or embedding them into a liner/sock to be placed within the SLI. This configuration was made possible by the introduction of tactile pressure measurement systems and has been seen to be the most commonly used method within SLI pressure measurement studies.

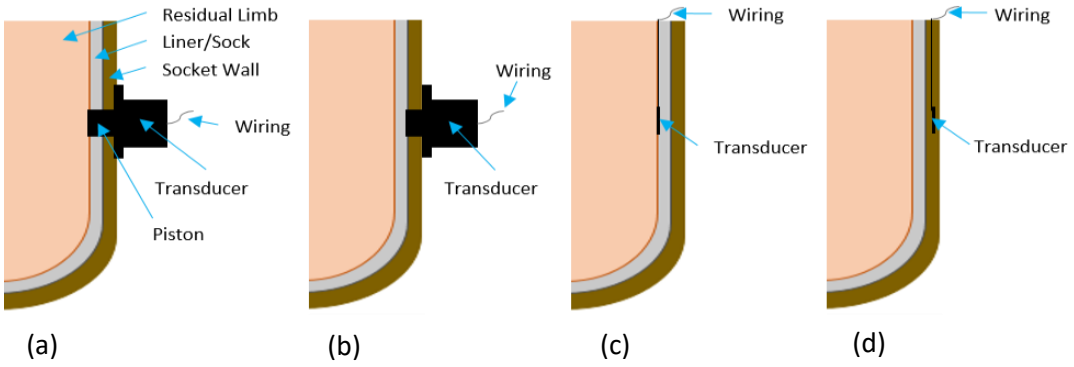

Figure 2.15: Transducer placement that have been found in literature: (a) mounted on socket wall with liner penetration; (b) mounted on socket wall without liner penetration; (c) in the skin-liner interface or liner-socket interface; (d) embedded within the socket (E. A. Al-Fakih et al., 2016).

The majority of transducers used in these placements are piezoresistive, FSRs, capacitive and optical-based transducers (discussed in Section 2.5.1.3). This placement method allows the amputees to wear their personal liner and socket, and therefore provides a more practical use in the prosthetic fitting process than the other placement methods. A RLES system needs to be able to evaluate any socket fitment, and therefore configuration (c) is the most appropriate method to be used in this study.

2.7.2 Direct Pressure Transducers

2.7.2.1 Strain gauges

Strain gauges have been used in the measurement of SLI pressures since the 1960s and have since been used on numerous research projects due to their high sensitivity and accuracy (Frank Appoldt et al., 1968). Diaphragm and rosette strain gauges have been used to measure the direct pressure and shear in all directions by Sanders et al. (1993), however, this required the development of a specific testing socket with embedded transducers. The general use of a strain gauge is to measure the strain (percentage change in length) induced by an external load on the object on which it is bound. The gauge is bound to the surface of the object by an adhesive, and when an external load is applied to the object, the gauge deforms proportionally with the object which changes its resistance. This change in resistance causes a change in voltage drop over the gauge which is proportional to the amount of strain in the object. The majority of studies utilising strain gauges investigate the shear stress induced at the SLI by creating a modified socket with embedded strain gauges to be used by all participants (J Sanders, Lam, Dralle, & Okumura, 1997; Zachariah & Sanders, 2001). This is because, in order for a strain gauge to measure the actual shear stress that the RL skin is experiencing, it would need to be either bonded onto the skin, which would cause injury, or embedded into a material with the same elastic properties as skin (approximately 100 kPa). The elastic properties of skin vary over areas of the RL and between each individual. Therefore, the material used would need to have a Young's modulus of less than that of the skin, to deform proportionally to the skin. Additionally, no strain gauge found has these elongation or elastic properties, and therefore the material would tear away from the gauge under shear stress. Metal strain gauges (diaphragm and rosettes) output strain results due to the deformation of its structure, therefore, compressive loads from the socket would cause inaccurate shear results in the rosettes and shear stress would cause inaccurate compressive load results in diaphragm strain gauges. This is a problem that faces all strain-based transducers, and therefore will be excluded from consideration within this study.

2.7.2.2 Fibre Bragg Grating Transducers

Fibre Bragg Grating (FBG) transducer setups for SLI pressure measurements have only been seen over the past ten years, and therefore are still experimental and are not commercially available. FBG transducers analyse light waves through thin optic tubes to determine the strain on the material in which they are embedded. Studies have obtained very accurate pressure results using them within the SLI and have shown that they can measure pressure, shear and temperature (Kanellos et al., 2010; Tsiokos, Kanellos, Papaioannou, & Pissadakis, 2012). These measure the strain of the material in which they are embedded, and therefore face similar limitation to that of strain gauges, however, FBGs have proven to provide similar pressure measurements to that of the F-Socket™ (E. Al-Fakih, Osman, Eshraghi, & Adikan, 2013). The results obtained from FBGs within the SLI pressure measurement field have been extremely successful in recent years, however, to obtain the measurement data from the sensors requires complex circuitry and expensive equipment to provide and analyse the light waves.

2.7.2.3 Capacitive Transducers

The use of capacitance-based pressure transducers within the field is relatively new, but recent studies have shown very encouraging results which promotes future use. The transducer measures pressure and shear stress by calculating the change in capacitance over the change in distance or area between two conductive pads. Results obtained from a study performed on a commercially available capacitive pressure transducer, the Pliance X System, by Novel Electronics Inc, showed accuracies to within ±150 Pa of the full-scale range. Commercial capacitive pressure transducers are limited to direct pressures only (Lai & Li-Tsang, 2009). Due to this limitation, Laszczak et al. (2015) designed, developed and validated a 3D printable capacitance transducer with the ability of accurately measuring direct and shear stresses up to 350 kPa and 80 kPa respectively with high repeatability, however, this has yet to be commercialised. These encouraging results validate the potential use of capacitive transducers in the future of SLI pressure measurements within prosthetics.

2.7.2.4 Force Sensitive Resistors

Many researchers have used FSRs for measuring SLI pressures because of their high sensitivity, small size, thin structure, flexibility, and ease of use. FSRs comprise of two conductive areas separated by an air gap, and when subject to a load the conductive areas close this air gap closing the circuit, thereby creating a resistance proportional to the amount of contact made (induced by the magnitude of load). Their downfall is their accuracy, drift and hysteresis error. Commercially there are three common FSRs namely Interlink FSR, Tekscan's® FlexiForce™, and the Lusense PS3. It was found that all sensors produced hysteresis as well as an average drift of 12% when subject to a load over 240 seconds (Hollinger & Wanderley, 2006). In the categories of accuracy, precision, hysteresis and drift the FlexiForce™ sensor was found to be the most efficient of the three (Hollinger & Wanderley, 2006; Vecchi et al., 2000).

2.7.3 Temperature Sensors

The three most common temperature sensors used to date, are the thermistor, thermocouple and resistive temperature detector (RTD). These temperature sensors measure the voltage drop of a physical change in their material resistance when exposed to a temperature. All SLI skin temperature research found, has utilised thermistors within their studies, and therefore have proven their worth within the field (Huff et al., 2008; Klute, Huff, & Ledoux, 2014; Mathur et al., 2016; Peery et al., 2005). This is due to the thermistors being inexpensive, easy to use, having small dimensions that can fit within the SLI, accurate within the required temperature range, and portray the most attractive qualities for the

application out of the three types. For selection within the RLES proposed in this study, a comparison between each temperature will be performed in the Design Chapter (Chapter 3).

2.8 Conclusions

Chapter 2 discusses the inefficiencies within the prosthetic fitting procedure due to the purely empirical process and highlights that current commercially available fitting systems only focus on pressure measurement and neglect important variables such as shear, temperature and moisture. Transducer devices and placements were also investigated for the use in the design of the RLES in Chapter 3.

3 Design Methodology

3.1 Introduction

Chapter 2 identified what is required for a RLES to provide an efficient analysis of the RL during the prosthetic fitting procedure. Chapter 3 involves the design considerations, the selection of sensors and electrical components, the electrical schematics, and the mechanical and software system designs to produce a RLES which meets the objectives presented in Section 1.5.

3.2 Design Considerations

The device of the system is to be used within the SLI which would place electronics in close vicinity to the skin. This places many constraints on the design. Therefore, this section discusses the considerations that were taken into account for each system component, to ensure safety to the user and efficient functioning of the system.

3.2.1 Sensor Selection Considerations

Prosthetic sockets are designed to have intimate contact with the RL, which creates a warm and humid environment. This places constraints on the size of the sensors that can be used. Therefore, the sensors used for SLI data measurement would need to avoid inducing pressure points (which could cause injury or pain) and operate efficiently within the SLI environment.

Transducer Set Dimensions

The proposed RLES would potentially be used for a brief period for RL analysis during the fitting procedure. However, the transducer set (comprising of one pressure and one temperature sensor) should not cause pain or injury during this process. The majority of TTAs wear a liner or sock underneath their socket. These are provided in several thicknesses ranging from 0.7 to 1.5 mm (Joan Sanders, Cagle, Harrison, & Karchin, 2012). Therefore, it can be assumed that if the transducer set thickness falls within this range, it will not cause any injury during the brief period.

Sensor Sensing Characteristics

Dynamic and static direct pressures and temperature changes are found within the SLI. Therefore, in order for the RLES to function efficiently as a diagnostic and evaluation tool, it must feature pressure sensors, capable of measuring dynamic and static loads, and temperature sensors, which are able to accurately measure skin temperature over the range of 25 – 40 °C.

3.2.2 Electronic System Considerations

The device will entail multiple sensors pressed up against the skin. The National Institute for Occupational Safety and Health (1998) stated that the lowest resistance for human skin is approximately 1000 Ω when wet and that the electrical current range which is tolerable by a human is between 1 – 16 mA. Therefore, the RLES should utilise a power supply within the range of 0 – 9 V (which could supply a max of 9 mA), all connection points must be insulated, and amplification of the signals should be performed outside of the socket to ensure wearer safety.

3.2.3 Mechanical System Considerations

The device is required to attach onto any amputee's RL. Therefore, it needs to accommodate for RLs of different dimensions and people of different heights. Additionally, the transducer sets need to be easily attached and removed without any risk of injury or pain to the amputee.

3.2.4 Software System Considerations

The software must be developed for the ease of use of a user with no prior knowledge of how the software functions.

3.3 RLES System Design Overview

The RLES prototype comprises of hardware and software to perform three essential tasks, the SLI analysis, the gait analysis, and the acquisition and display of data. A basic overview of what was needed to create the RLES prototype is presented in Figure 3.1.

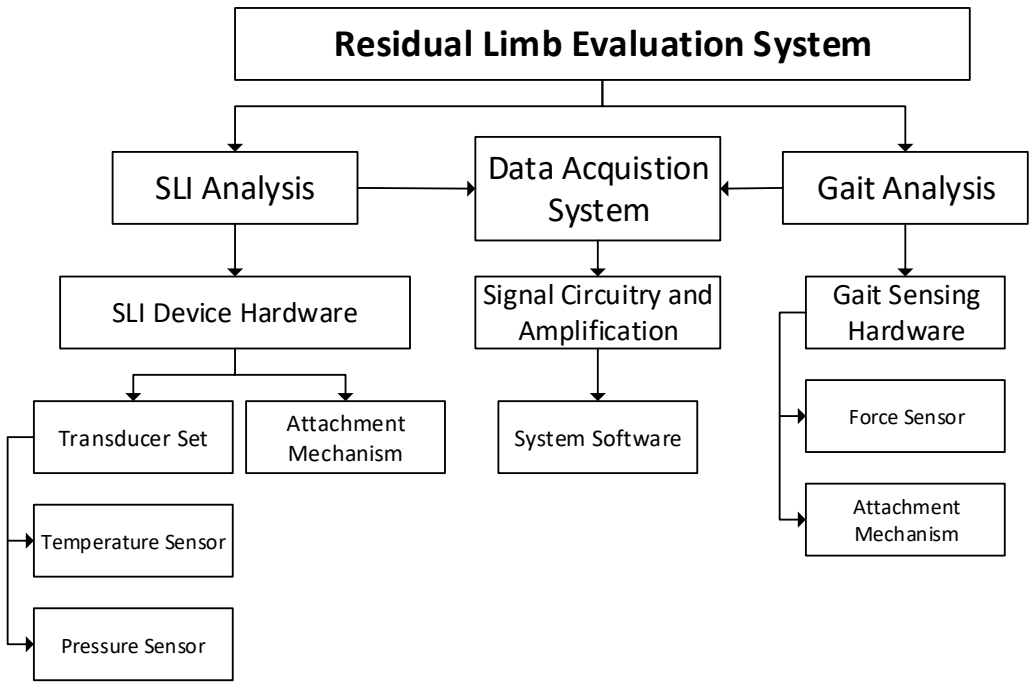

Figure 3.1: Basic overview of essential RLES components.

3.4 Design Methodology Flow Chart

The design flow to ensure efficient development of the RLES is presented in Figure 3.2.

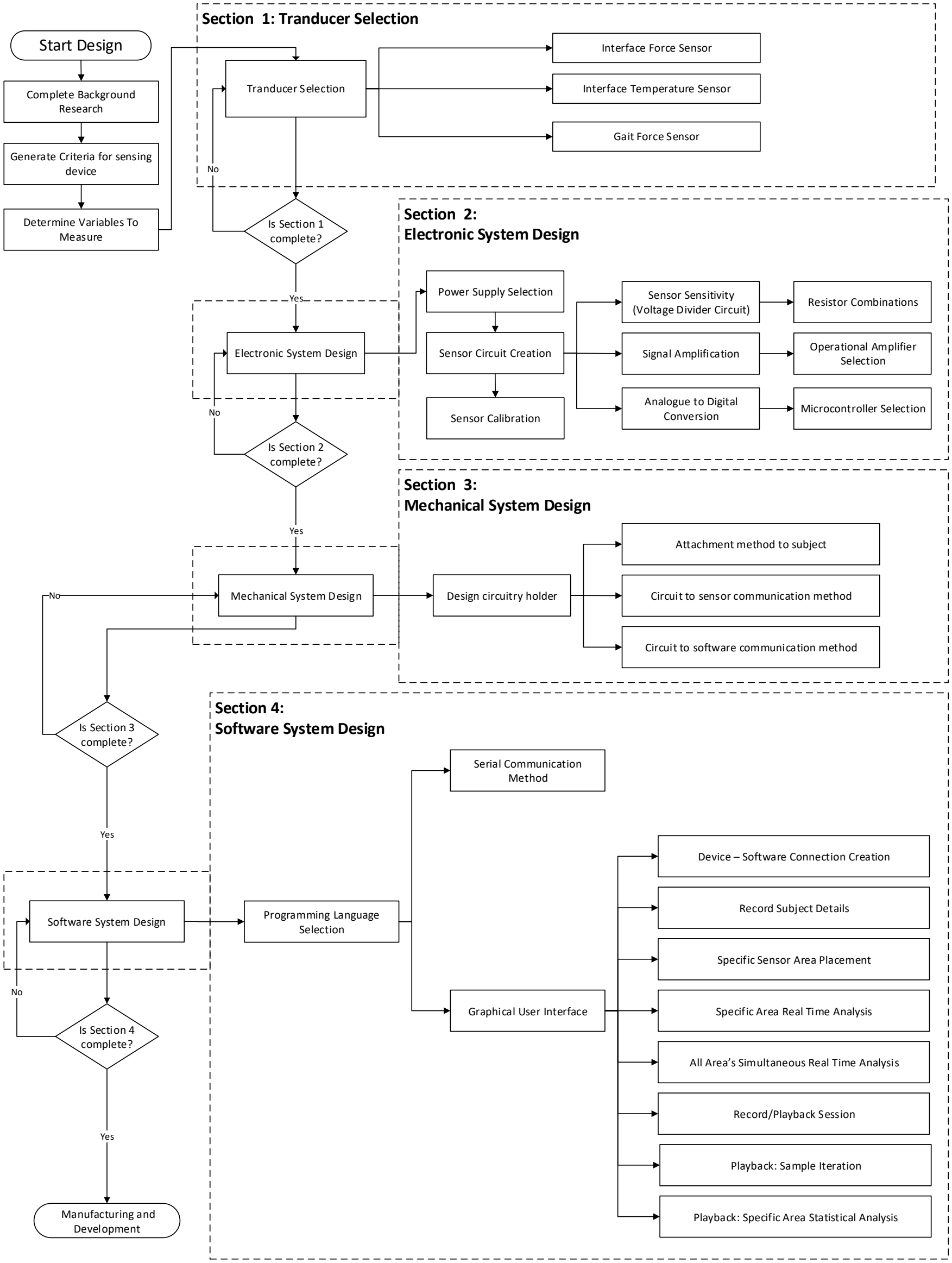

Figure 3.2: Design Methodology Flow Chart.

3.5 Sensor Selection

The following section evaluates the pressure and temperature sensors found in Section 2.7 and details the selection of the most appropriate for use in the development of the RLES

3.5.1 Pressure Sensor Selection

The accuracy, sensitivity and reliability of the proposed RLES relies on the type and quality of the sensors. Section 2.7.2 identified known transducer-based measurement devices used in SLI pressure measurement studies. A literature review of commercial pressure sensors, which comply with the design considerations (Section 3.2) was performed, and the properties of these sensors are presented in Table 3.1. The component properties were sourced from manufacturer data sheets (Interlink Electronics™, 2016; Tekscan®, 2016; Welltech Instrument Company, 2016).

Table 3.1: Commercial Pressure Sensor Properties.

PRESSURE SENSOR COMPARISON TABLE

EVALUATION CATEGORY	EVALUATION CRITERIA	FORCE SENSITIVE RESISTOR (INTERLINK FSR)	PIEZORESISTIVE SENSOR (FLEXIFORCE™ A201)	CAPACITIVE SENSOR (SINGLE TACT)	FBG OPTIC SENSOR
Performance	Load Range (Newton)	0 – 20	0 – 445	0 – 445	Material Dependant
	Accuracy Error	±5.9%	±3%	±2%	< 0.1%
	Hysteresis Error	±10%	±3.6%	±4%	±0.1%
	Drift Error	±5%	±3.3%	<2%	±0%
	Repeatability Error	±2%	<±3.5%	<1%	±0.5%
	Operating Temperature	-40 – 85 °C	-40 – 204 °C	-40 – 85 °C	-30 – 70 °C
	Dynamic Loading Capability	High/Medium	High/Medium	High/Medium	High
Sensor Dimensions	Embedding Required	No	No	No	Yes
	Width(mm)	0.3	0.2	0.35	0.5
Capabilities	Shear Stress	No	No	No	Yes
	Perpendicular Stress	Yes	Yes	Yes	Yes
Practicality	Commercially Available	Yes	Yes	Yes	Yes
	Manufacturing Complexity	-	-	-	High
	Circuit Complexity	Low	Low	Low	High
	Embedding	No	No	Yes	Yes
	Available in South Africa	Yes	Yes	No	No
	Cost per Sensor (R)	±140	±150	±800	±2400

The SLI is a unique environment with large dynamic forces and very limited space for the sensors to be inserted. Therefore, each evaluation category has been assigned a weight relative to its importance within the application[1]. These weights, relative compliance and weighted values are presented (Table 3.2) to select the best overall pressure sensor for the application.

[1] Literature has shown that the SLI provides limited space for the placement of sensors and experiences variable and dynamic forces. Therefore, the dimensions and performance of each sensor are important and were assigned a weight of 4. Practicality defines the availability of the sensor for purchase and the complexity of gathering data from the sensor and therefore, is the most important category with a weight of 5. The scope of the project was constrained to sensing direct pressure only and therefore, sensor capability was assigned a weight of 2.

Table 3.2: Pressure Sensor Selection Table.

PRESSURE SENSOR CATEGORY EVALUATION

Sensor Type:		INTERLINK FSR		FLEXIFORCE™		SINGLE TACT		FBG	
Category	Weight	RC	WV	RC	WV	RC	WV	RC	WV
Performance	4	3	12	4	16	4	16	5	20
Dimensions	4	4	16	5	20	3	12	2	8
Capabilities	2	4	8	4	8	4	8	5	10
Practicality	5	5	25	5	25	2	10	1	5
Total (Max:75)			61		69		46		43

RC – Relative Compliance, WV – Weighted Value, WV = Weight × RC

RC Values and Meaning: 0 – No Compliance, 1 – Low Compliance, 2 – Moderate Compliance, 3 – High Compliance, 4 – Full Compliance, 5 – Exceeds Compliance.

The results indicate that Interlink FSR and FlexiForce™ (A201) force sensors scored above 80% and are the most practical sensor types to evaluate for the use in the study. These sensors are relatively inexpensive, therefore, both were purchased and evaluated against each other.

The following sensor types were purchased:

- FSR Model 400 Short Tail (20 N), Active area of diameter: 5.62 mm
- FlexiForce™ Standard Model A201 100 lb (11 kg), Active area of diameter: 9.53 mm
- FlexiForce™ Standard Model A201 1 lb (0.45 kg), Active area of diameter: 9.53 mm

Each sensor has similar characteristics in structure illustrated in Figure 3.3.

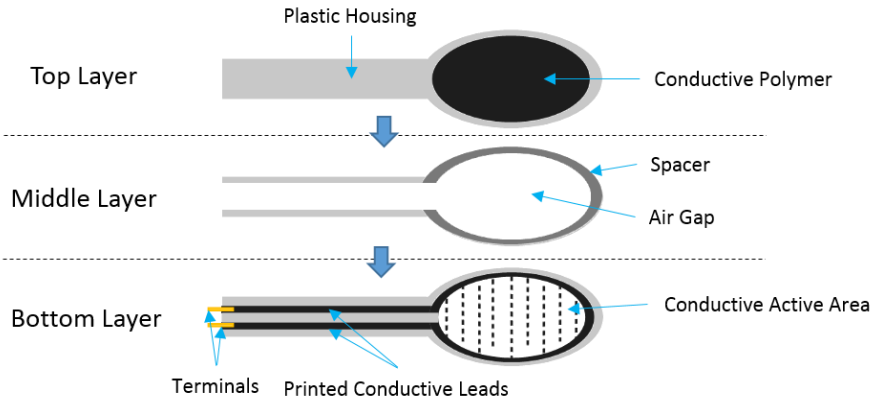

Figure 3.3: Force Sensitive Resistor (FSR) structure.

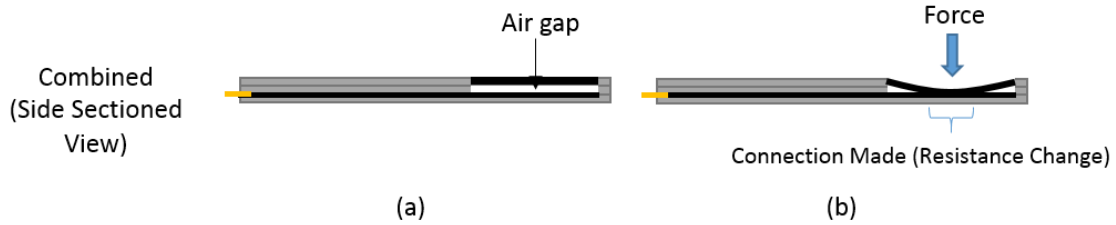

Figure 3.4: Force sensitive resistor function. (a) unloaded FSR (b) loaded FSR.

Figure 3.4 illustrates how a FSR/FlexiForce™ sensor interprets a force. In configuration (a) the sensor is unloaded and an air gap exists between the two conductive layers creating an open circuit. An applied load of sufficient magnitude, would close the air gap between the conductive layers, thereby creating a closed circuit (b). The amount of contact between these layers determines the amount conductivity between the terminals. Therefore, more contact offers less resistance and allows a greater flow of

current. The change in resistance induces a voltage drop over the sensor terminals, which is proportional to the force magnitude. As a result, the FSR/FlexiForce™ sensor can be calibrated to calculate the force magnitude by relating it to the voltage drop induced.

To compare the FSR and FlexiForce™ sensors, a circular acrylonitrile butadiene styrene (ABS) plastic plate (force plate) was designed and manufactured according to the diameter of each sensor's active area. Thereafter, the plates were attached over the active area to direct the load. A basic analogue-to-digital (ADC) circuit configuration was set up to compare the results of each sensor. An Arduino Uno was used as the ADC, which interpreted and saved the signal. Precision weights were used to incrementally load and unload each sensor force plate to 2 kg by increments of 0.1 kg. During a pre-calibration trial of the FSR sensor, it was found that the resistance changed depending on the location of the weight on the force plate which caused sporadic results (Figure 3.5).

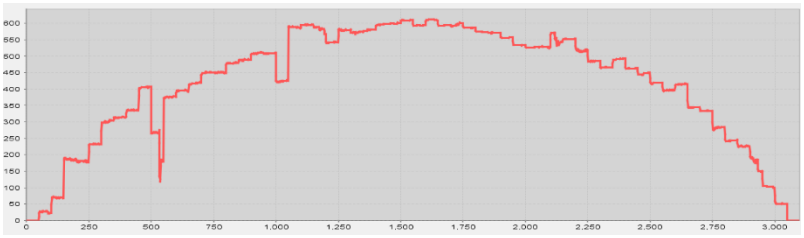

Figure 3.5: Errors and instability in FSR sensor output results.

It was assumed that these results were due to the force plate hitting each sensor's separating substrate, thus creating an incorrect contact between the conductive layers, in relation to the load (Figure 3.6a). To mitigate this risk, the force plate was increased in diameter to completely cover the active area and the separating substrate. Additionally, a layer of spongy biodegradable cellulose double-sided tape was placed in-between the force plate and the active area to compensate for any positional errors (Figure 3.6b). This creates a spongy layer that will fill the air gap more consistently when exposed to a load, even if slightly off centre.

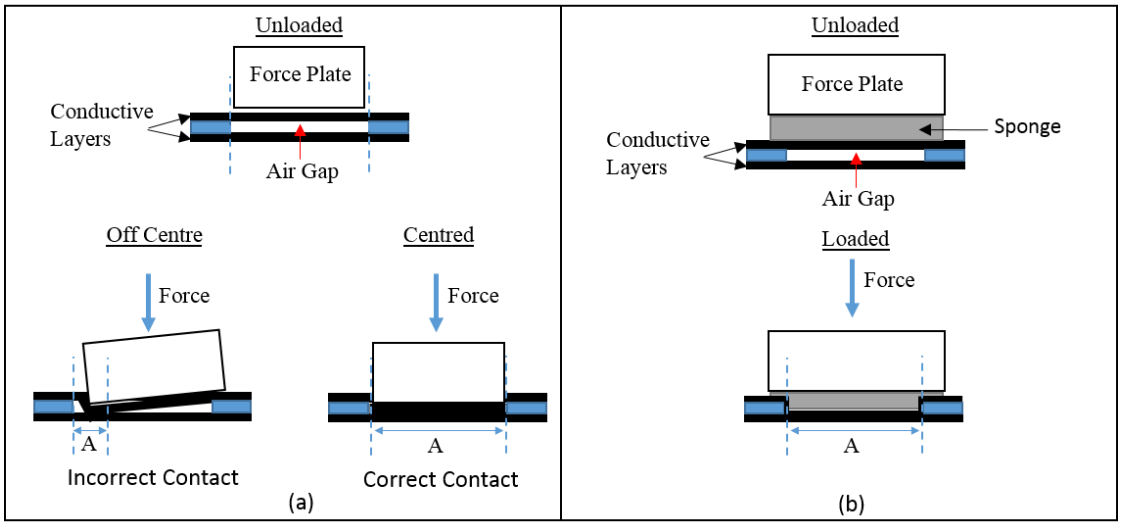

Figure 3.6: Sensor Configuration (a) Incorrect force plate positioning leading to an incorrect contact for load interpretation. (b) Added spongy tape layer that decreases the risk of incorrect contact due to force plate positioning.

This theory was tested by comparing the uncalibrated digital output of placing a 0.5 kg weight on the FSR sensor with and without the tape 12 times each. Figure 3.7 illustrates the results of the comparison. The results illustrate that the spongy layer between the force plate and the top layer decreased the standard deviation by a digital output of 119.69, therefore, increasing the repeatability of the sensor output.

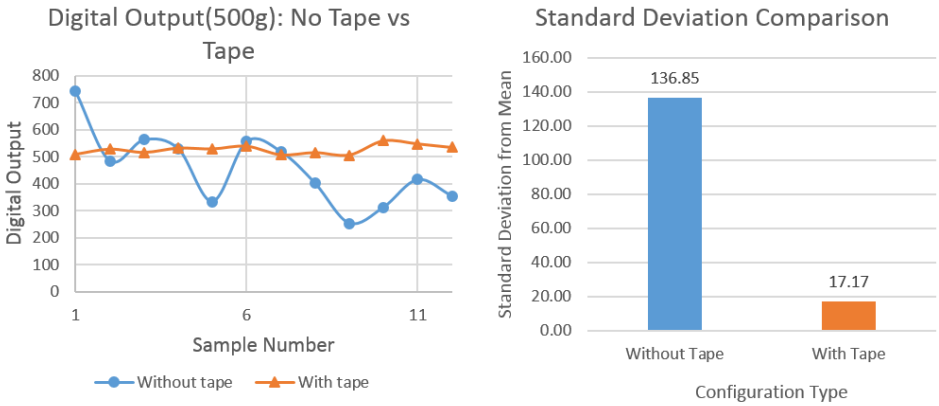

Figure 3.7: A comparison between 2 types of FSR configurations.

The FSR sensor was then tested within the basic ADC circuit again for analysis and it was found that the spongy tape layer solved the sporadic nature found previously, and increased the repeatability (Figure 3.8).

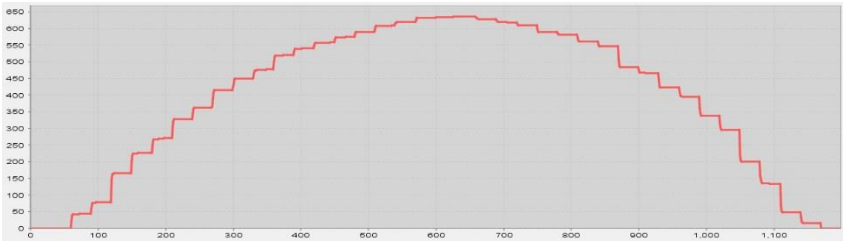

Figure 3.8: ADC results of FSR with spongy tape layer

This solution was implemented during the evaluation of the FSR and FlexiForce™ sensors. To obtain the most efficient sensor and setup, seven different configurations were compared (Table 3.3).

Table 3.3: Pressure sensor configurations for comparison.

CONFIGURATION NUMBER	SENSOR TYPE	SENSOR CONFIGURATION
1	FlexiForce™ A201 25lb (11 kg)	no added tape (Square force plate)
2	FlexiForce™ A201 25lb (11 kg)	1 mm thick tape layer (Square force plate)
3	FlexiForce™ A201 25lb (11 kg)	1 mm thick tape layer (Circular force plate)
4	FlexiForce™ A201 25lb (11 kg)	0.1 mm thick tape layer (Circular force plate)
5	FlexiForce™ A201 1lb (0.45 kg)	0.1 mm thick tape layer (Circular force plate)
6	FSR 400 Short Tail (20 N)	1 mm thick tape layer (Circular force plate)
7	FSR 400 Short Tail (20 N)	0.5 mm thick silicone layer (Circular force plate)

Each A201 and FSR 400 sensor type and configuration was subjected to loads ranging from 0 – 20 N and 0 – 7 N respectively. These ranges relate to a pressure range of 0 – 250 kPa for each sensor. Each configuration was tested three times to obtain the average performance. The loads in the SLI are dynamic due to natural shifts of the body's centre of gravity during gait. Therefore, the configuration that yields the lowest overall repeatability error and hysteresis error was selected. The results of the tests are presented in Table 3.4.

Table 3.4: Sensor Configuration Comparison.

AVERAGE REPEATABILITY AND HYSTERESIS PERCENTAGE ERROR							
Configuration Number	1	2	3	4	5	6	7
Repeatability Error (%)	6.07	7.09	3.69	3.73	1.78	1.80	1.22
Hysteresis Error (%)	8	4.78	7.7	3.12	2.28	7.6	8.69

The results show that configuration seven (0.5 mm silicone layer) produced the lowest repeatability error, but the highest hysteresis error. A high hysteresis may produce inaccurate SLI pressure readings due to the dynamic loading. Therefore, the sensor and setup of configuration five (FlexiForce™ A201 0.45 kg - 0.1 mm thick tape layer with circular force plate) was selected due to producing the lowest hysteresis error and second lowest repeatability error. Figure 3.9 illustrates the final selected sensor and the datasheet can be found in Appendix A (Section 11.1).

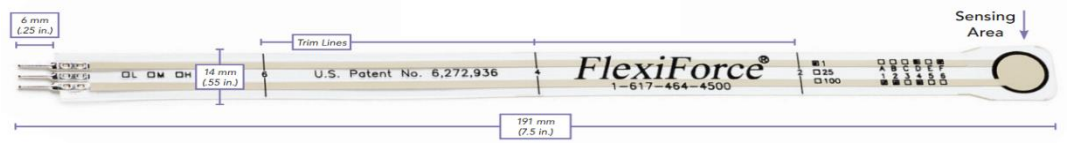

Figure 3.9: Socket Limb Interface Direct Pressure Sensor A201 (Tekscan®, 2016).

3.5.2 Gait Sensor Selection

During the gait cycle, it has been stated that the ground reaction forces reach 110 % of the body weight which, for an adult male of 85 kg, is approximately 1000 N (Su, Gard, Lipschutz, & Kuiken, 2010). These are the maximum loads found in the gait cycle and arise during the heel strike and toe-off phases of gait. Therefore, two force/load sensors needed to be selected, which are capable of measuring such loads. A 0.5 cm rise in heel or toe height is capable of shifting pressures on the RL, therefore, the sensors need to be thin enough so that they do not obstruct the natural gait cycle. It was found that the thinnest load sensor types were piezoresistive sensors and miniature load cells (strain gauge based). Both types were capable of measuring load within the required range, however, load cells have a metal structure and the thinnest found was 3.3 mm (Futek, 2017). This would cause a pressure point under the foot or potentially cause instability of the amputee. The Tekscan® A201 100 lb has the ability to measure up to 450 kg (4.4 kN) (dependent on circuitry configuration) and has a thickness of 0.2 mm. An additional advantage was that the sensors could be included in the order for the SLI pressure sensors, therefore, decreasing delivery costs. Therefore, Tekscan® A201 sensors were chosen to be used as the gait sensors for the application.

3.5.3 Temperature Sensor Selection

Section 2.7.3 highlighted the most common temperature sensors, with the appropriate dimensions, which can fit within the SLI. The characteristics of these sensors have been presented in Table 3.5 to compare and select the most practical and appropriate to use within the RLES.

Table 3.5: Temperature sensor characteristics (Enercorp, 2018; Minco, 2016).

TEMPERATURE SENSOR COMPARISON

	THERMISTOR	THERMOCOUPLE	RTD
Thickness (mm)	0.2 mm and larger	0.2 mm and larger	0.2 mm and larger
Range (°C)	-80 – 150	-270 to 1800	-260 – 850
Accuracy (°C)	±0.1	>1	±0.05
Thermal Response	Best	Low	Moderate
Stability	Moderate	Low	Best
Cost	Low	Low	Moderate
Advantages	- Simple Setup - Fast Response - Linear within 0 – 40 °C range	- Self-powered - Rugged	- Stable - Accuracy
Disadvantages	- Non-linear - Require linearization	- Non-linear - Cold junction compensation required - Low voltage readings (microvolts)	- Non-linear - Require linearization - Expensive - Low thermal response

The data gathered, illustrates that the RTD sensor has the greatest accuracy, however, the disadvantages of using this sensor is its moderate thermal response and its cost. The thermocouple offers a low cost, however, it has the lowest accuracy and stability and requires additional circuitry to amplify the analogue signals for calibration. The thermistor offers high accuracy, an adequate thermal response, a simple setup, linear measurement within the required range, and is inexpensive. Therefore, the thermistor was selected as the temperature sensor to track the RL skin temperature within the prototype RLES.

The Thermistor

A thermistor is manufactured from highly temperature sensitive ceramic materials. Its resistance changes in relation to an experienced change in temperature. There are two types of thermistors available; negative temperature coefficient (NTC) resistors and positive temperature coefficient (PTC) resistors, where resistance decreases or increases respectively as temperature increases. NTC thermistors are more commonly used as temperature sensors whereas PTC thermistors are mostly used in current limiting circuits, therefore, only NTC thermistors will be evaluated in this project. NTC thermistor resistance, in relation to a change in temperature, is calculated using equation 3:

$$R_T = R_0 e^{\beta(\frac{1}{T}-\frac{1}{T_0})} \quad [3]$$

Where, β is the linearisation constant and is determined by the material of the thermistor (value of β ranges between 3500 – 4600), T_0 is ambient temperature, T is the temperature exposed to the sensor, R_0 is the resistance at T_0, and R_T is the resistance for the measured temperature (R. S. Figliola, 2011).

There is minimal space between the prosthetic socket and the RL, therefore, any obstruction would create a pressure point on the RL skin and potentially harm the amputee. To conform as much as possible to the space provided (0 – 1.5 mm), the thermistor would need to be as thin and flat as possible to increase the surface contact area and distribute any pressure. Therefore 103 JT-025 thermistor from Semitec™, was selected since it featured a maximum thickness of 0.5 mm (only over the sensing area) and a width and length of 3.6 x 25 mm respectively (Figure 3.10). The datasheet can be seen in Appendix A (Section 11.2).

Figure 3.10: 103 JT-025 thermistor.

3.6 Electronic System Design

3.6.1 Power Supply Selection

Electric current needs to be passed through the sensor to create a voltage drop that can be measured. In biomedical devices, it is essential that the wearer has no risk of an electrical shock or injury. The majority of ADCs (microcontrollers) provide a 5 V output, which is utilised by the sensor. Section 3.2.2 presented an electrical current range of 1 – 16 mA, which is deemed safe if exposed to human skin. Therefore, utilising Ohms Law (Current = Voltage/Resistance), a 5 V supply is only capable of providing a current range of 0.005 – 5 mA to dry skin (100,000 Ω) or wet skin (1000 Ω) respectively. Therefore, a microcontroller was an adequate selection for the ADC of the RLES (Wallis et al., 1998).

Microcontrollers can be powered by a 5 – 16 V supply. They regulate this voltage input to output a constant 5 V or 3 V supply to the circuit. If a battery is used to power the microcontroller there exists a risk of battery depletion during the fitting procedure. Therefore, the power supply selected for the

prototype RLES was the 5 V supply provided by the Universal Serial Bus (USB) port of a laptop computer. This selection mitigates the risk of power loss, and creates a direct serial data line from the device to the software for interpretation.

3.6.2 Analogue to Digital Converter

Microcontrollers make it possible to convert analogue voltage readings, from sensors or other electrical components, to readable digital outputs that can be utilised within different software systems. There are numerous types of microcontrollers, however, it was decided that the Arduino Mega 2560 would be selected for the ADC. This is because it provides: a constant 5 V output; a sufficient number of analogue input and digital output pins; a USB connection for data transfer via a serial port; and user-friendly programming software for processing of obtained data. The Arduino Mega 2560 is illustrated in Figure 3.11.

(a)

TECHNICAL SPECIFICATIONS

Operating Voltage	5 V
Digital I/O Pins	54
Analogue Input Pins	16
Output Voltage Supply	3.3 V / 5 V
Clock Speed	16 MHz

(b)

Figure 3.11: (a) Arduino Mega 2560 microcontroller. (b) Technical specification.

Arduino offers an Arduino IDE (coding platform), which allows for code to be programmed onto the microcontroller. Therefore, signals from the temperature, pressure and gait transducers can be pre-processed before being transferred to the system software for display.

3.6.3 Transducer Circuit Design

The RLES circuit requires four sections of circuitry: 1) A voltage divider circuit, which sets how sensitive the voltage drop is to a required input parameter (temperature or force) range e.g. The voltage drop for intial force/temperature inputs may be too small (unobtainable), therefore, a VDC sets the sensitivity of the circuit to aquire an obtainable voltage drop for all required inputs; 2) An amplifier circuit, which stretches the voltage drop range (found from the VDC) over the entire capable voltage range (0 – 5 V) providing more calibration points, thereby increasing the calibration accuracy; 3) An ADC, which is used for the conversion of the 0 – 5 V analogue signal into a digital representation to be used within the software; 4) Peripheral circuits such as off/on switches, LED indicators, etc.

3.6.3.1 The Voltage Divider Circuit (VDC)

A VDC determines the initial sensitivity range of each transducer and is illustrated in Figure 3.12.

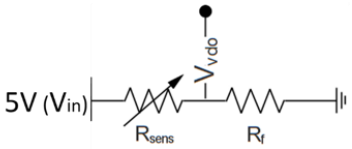

Figure 3.12: Voltage Divider Circuit.

V_{vdo} is the output voltage of the VDC. This is fed into the amplifier circuit and is calculated using equation 4:

$$V_{vdo} = V_{in} * \frac{R_f}{R_{sens} + R_f} \quad [4]$$

R_{sens} is the sensor's resistance relative to the parameter (pressure or temperature) magnitude that it is experiencing and R_f is a static resistor that determines the sensitivity of the sensor. Equation 4 states that R_f determines the impact that a change in R_{sens} has on V_{vdo}. As R_f increases the impact that R_{sens} has on the V_{vdo} decreases. The value of R_f for each sensor was selected so that the lowest parameter magnitude to be measured, creates a noticeable voltage drop that can be interpreted and quantised.

3.6.3.2 Signal Amplification

The chosen R_f value will allow for the lowest required parameter magnitude to be measured, however, the upper bound of the required parameter magnitude range may cause a voltage drop that falls below the maximum 5 V limit. This leaves a voltage range that is not being utilised. An amplification circuit is used to stretch the lower and upper bounds of the experienced voltage drop over the entire 0 – 5 V range. This increases the number of calibration points that can be made within the required voltage drop range, therefore, increasing the overall accuracy of the transducer output. This circuit is illustrated in Figure 3.13.

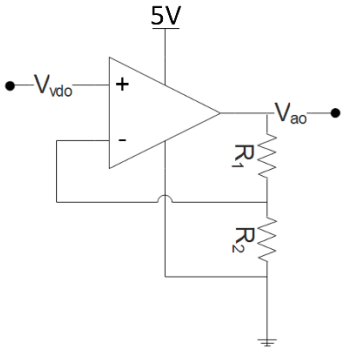

Figure 3.13: Signal Amplification Circuit. V_{ao} – Amplifier output voltage. R_1 & R_2 – Gain resistors.

The factor that this initial range is stretched by, is determined by the Gain of the amplification circuit. Gain is given by equation 5:

$$Gain = 1 + \frac{R_1}{R_2} \qquad [5]$$

The operational amplifier selected for the RLES application in this study was the LMC660CN (Figure 3.14) since it requires a low power of 5 V to operate and can amplify four individual sensors at once.

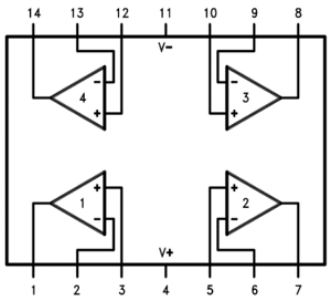

(a)

#	PIN DESCRIPTION	#	PIN DESCRIPTION
1	Amp 1 V_{ao}	8	Amp 3 V_{ao}
2	Amp 1 -	9	Amp 3 -
3	Amp 1 +	10	Amp 3 +
4	5 V pin	11	Ground
5	Amp 2 V_{ao}	12	Amp 4 V_{ao}
6	Amp 2 -	13	Amp 4 -
7	Amp 2 +	14	Amp 4 +

(b)

Figure 3.14: (a) LMC660CN Schematic (Texas Instruments, 1999) (b) Pin descriptions.

3.6.3.3 Pressure sensor functioning circuit

To test if each pressure sensor circuit is working correctly, each pressure sensor output was assigned to a specific digital output on the microcontroller.

If the lower limit of the pressure sensor is exceeded, the assigned digital pin closes an LED circuit, which illuminates an LED to illustrate the successful connectivity of the sensor. The LED circuit utilises a resistor to limit the current over the LED, as shown in Figure 3.15.

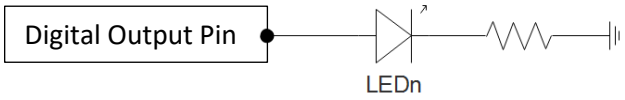

Figure 3.15: Pressure Sensor LED Circuit.

3.6.3.4 Final device schematics

Each transducer set (the combination of one pressure sensor and one temperature sensor) entails a VDC and amplification circuit for each sensor. Therefore, for illustration purposes, each transducer set will be assigned to TSn where n is the transducer set number. This is illustrated in Figure 3.16 .

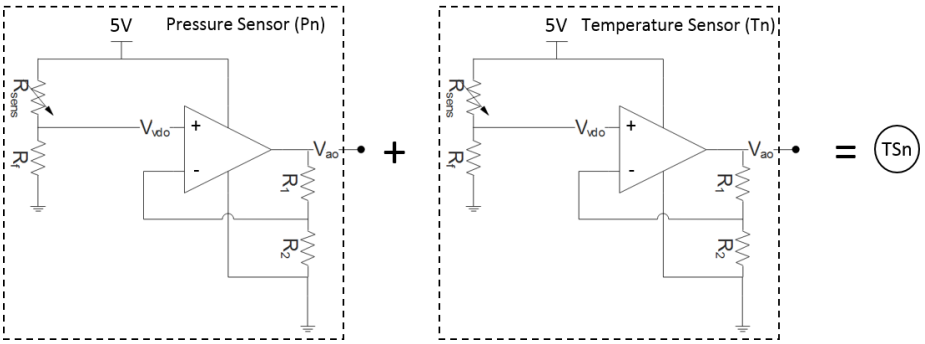

Figure 3.16: Transducer set circuit comprising of 1 pressure sensor circuit and 1 temperature sensor circuit (n - transducer set number).

Each gait force sensor circuit comprises of a VDC and an amplifier circuit and will be assigned to G_n where n is the gait sensor number. The schematics for the entire RLES device is illustrated in Figure 3.17

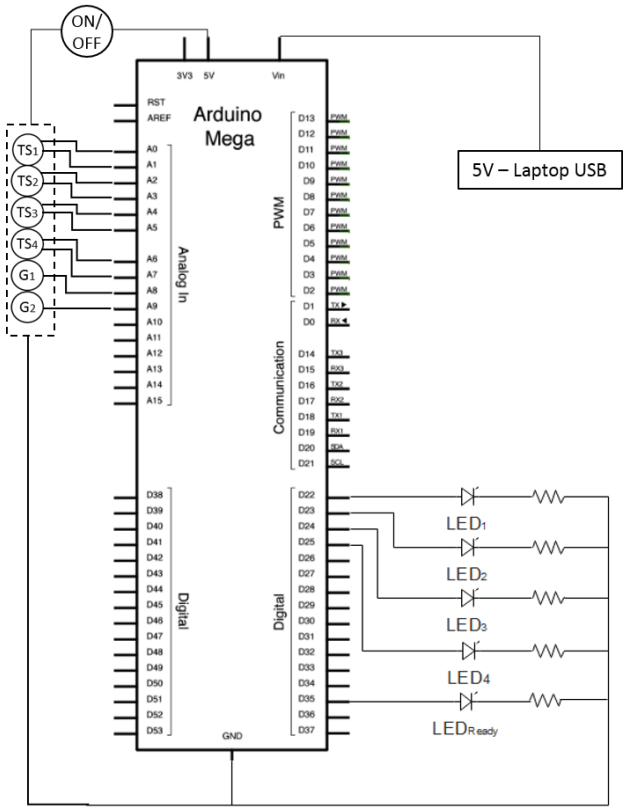

Figure 3.17: Circuitry Schematic (Arduino, 2015).

All the transducer sets and gait sensors are powered by the Arduino Mega 5 V pin. An ON/OFF switch was implemented within the power lead to the transducer sets, which can be used as an emergency stop if any electrical current is felt by the user. Each LED circuit relates to a specific TS_n sensor by the n value and will illuminate an LED if the related sensor is working correctly. The LED_{Ready} light illuminates if all sensors are working correctly. The ground pin on the Arduino Mega is used for grounding all circuits.

3.7 Mechanical System Design

The mechanical portion of the project is concentrated around human variability and ease of application.

3.7.1 Human Variability

The device is intended to fit TTAs of all heights and RL characteristics, and attach to any area that the user (prosthetist) wishes to analyse. In order to do so, the device sensor pad leads would need to change length i.e. elongate or shorten. All transducer sets are to extend from the control box using a ribbon connection, therefore, each transducer set is assigned three thin cables (Voltage Source for both pressure and temperature sensors, T_n signal, P_n signal). This is demonstrated in Figure 3.18:

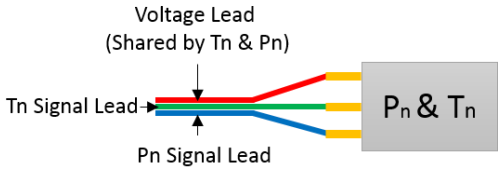

Figure 3.18: Transducer set leads.

To adapt the length of the leads from the control box to the RL, small strap clips were 3D printed from ABS plastic. The 3D model, the 3D printed version, and how they are used is shown in Figure 3.19.

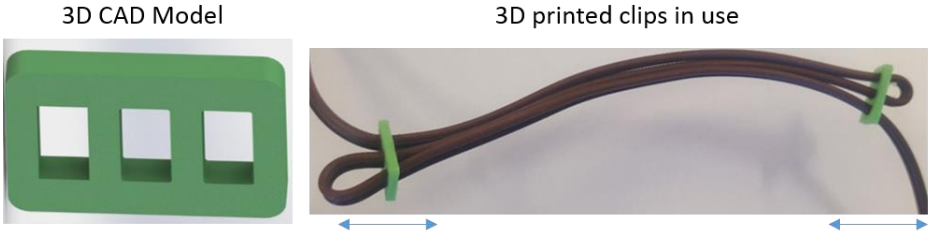

Figure 3.19: 3D printed lead clips for human variation in height and transducer set placements.

A design of the RLES device control box is not essential for the functioning and testing of the prototype, however, it needs to be easily attached to and removed from the TTA without causing any obstruction or adding excess weight that could offset the amputee's balance. Therefore, due to the rigidity and lightweight properties of ABS, the most feasible option for manufacturing was to 3D print the control box, since multiple iterative prints can be performed. A 3D model of the control box was designed using Solidworks 2016 and is shown in Figure 3.20.

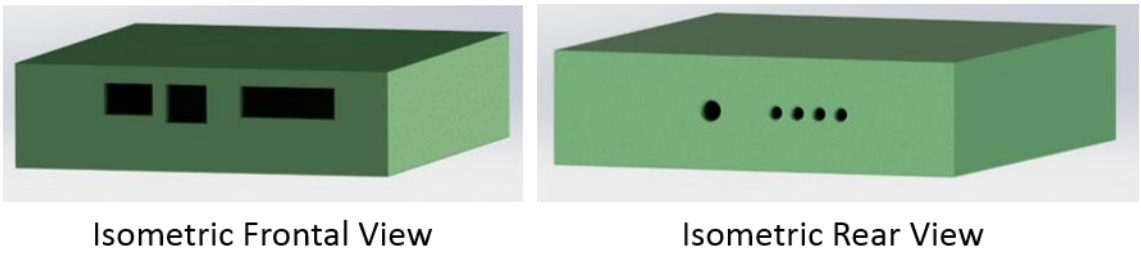

Figure 3.20: Control box 3D model.

A 3D printed belt clip was designed to be printed and attached to the control box for attaching the device to the TTA.

3.8 Software Design

The software is the most essential component of the system, since its function is interpreting the signals from the transducers as pressure, temperature and gait force measurements, and appropriately displaying the results for a user to understand. For the system to be practical to be used by a prosthetist, it needed to feature functions, which satisfy the objectives laid out in Section 1.5.1. The functions are summarised as follows:

- Amputee registration onto the system.
- Selection of RL areas for analysis.
- Allow the user to define pressure and temperature thresholds for each transducer set area.
- Alert the user if thresholds are exceeded to indicate vulnerability.
- Display of all RL analysis areas with corresponding pressure and temperature displays.
- Produce real-time pressure, temperature and gait data during the testing procedure.
- Real-time automatic generation of data statistics.
- Record and playback all data function for post-fitting analysis.
- Real-time individual sample index and playback of previously recorded results.
- An indication of maximum pressure and temperature sample numbers during the recording.
- Allow for single sensor selection for the in-depth analysis of a specific area.
- Allow for the display of all analysis areas simultaneously for a top-down view.

3.8.1 Graphical User Interface (GUI)

The efficiency and practicality of the system depends on the usability and functionality of the software. The GUI is broken up into three sections: the control panel; the single sensor analysis panel; and the all sensor analysis panel. The control panel (Figure 3.21) will always be visible throughout the use of the software so that essential functions are always available to the user. The function of each button is described within the caption of Figure 3.21.

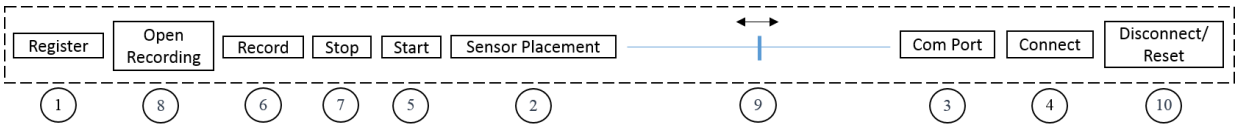

Figure 3.21: Software Control Panel Layout: 1 - Register subject on system. 2 - Select residual limb areas to analyse and allow user to set a user defined threshold of each pressure and temperature sensor in the area. 3 - Select the com port relating to the connection of the Arduino. 4 - Connect the software to the serial of the com port. 5 - Start the display/analysis of the of residual limb areas. 6 - Start recording of analysis. 7 - Stop recording and save analysis. 8 - Open a recording of a previous analysis. 9 - Select sample in recording to analyse. 10 - Disconnect from com port and restart software.

The single sensor analysis panel (Figure 3.22) and all sensor analysis panel (Figure 3.23) provides the user with all the information to perform an efficient analysis of the pressures and temperature being experienced at the SLI, while additionally allowing the inspection of the gait pattern. The single sensor panel provides an in-depth analysis of a specific RL area and displays the pressure and temperature pattern it experiences over the last 100 samples. Additionally, it provides statistical information such as the maximum, minimum and average pressure and temperature values over the entire session to gauge what the RL is experiencing. The all sensor panel provides the user with a top-down overview of the pressure and temperature magnitudes that all areas are experiencing at once as well as highlighting which sample produced the maximum magnitudes for future analysis.

Therefore, once a session is recorded, the user (prosthetist) can open up the recording and select a specific sample to analyse. This provides the ability to view the RL pressure and temperature values at the selected sample time as well as note if the amputee's gait pattern is correct. This view will provide an overview of how all areas are faring with regard to the current prosthetic fitment. Additionally, the user-defined threshold set for each sensor evaluates each magnitude and if this threshold is exceeded, the colour of the representing graphic will display red to alert the user.

Single Sensor Panel

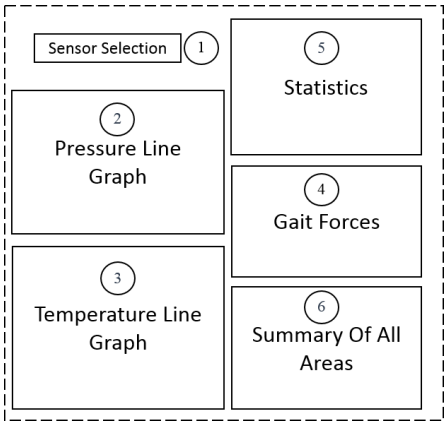

Figure 3.22: Single Sensor Analysis Panel Layout:

1- *Select sensor to analyse*
2- *Pressure line graph for previous 100 samples.*
3- *Temperature line graph for previous 100 samples.*
4- *Toe off & Heel strike GRFs for the previous 100 samples.*
5- *Statistics of selected sensor.*
6- *Current pressure and temperature values of all sensors*

All Sensor Panel

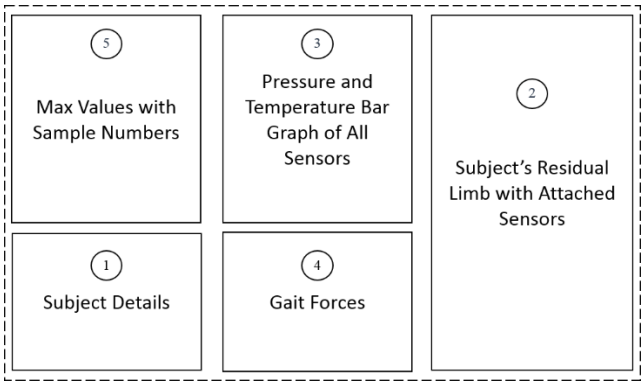

Figure 3.23: All Sensor Analysis Panel Layout:

1- *Subject details display panel.*
2- *Subjects residual limb with sensor placements.*
3- *Bar graph of both temperature and pressure values for all areas.*
4- *Toe off & Heel strike GRFs for previous 100 samples.*
5- *Max temperature and pressure values and their correlated sample number for all sensors*

3.8.2 Software Logic and Programming

Amputee registration on the software requires creating an amputee object. In computer programming, objects comprise of attributes that can be defined. The amputee registration function would save specific attributes to each amputee object such as their weight, age, height and sensor placements. Therefore, an object orientated programming language was selected. There are numerous object-oriented platforms for this type of programming, however, Java EE Swing was chosen for the creation of the software because of its capabilities such as: microcontroller integration ability; drag and drop GUI creations; multiple thread creation; and availability. The real-time property of the software needs to continually be reading in data from the device into a dataset, as well as using this dataset information to display appropriate visuals to the user. Therefore, two threads were designed for this application:

1- User interface thread
2- Serial port thread

3.8.2.1 User Interface Thread

This thread provides all the front-end functionality of the software and allows the user to register subjects, connect to the device, select sensor areas, define pressure and temperature thresholds, switch between panels, record/playback data and disconnect or restart the software. A flowchart of this thread is illustrated in Figure 3.24.

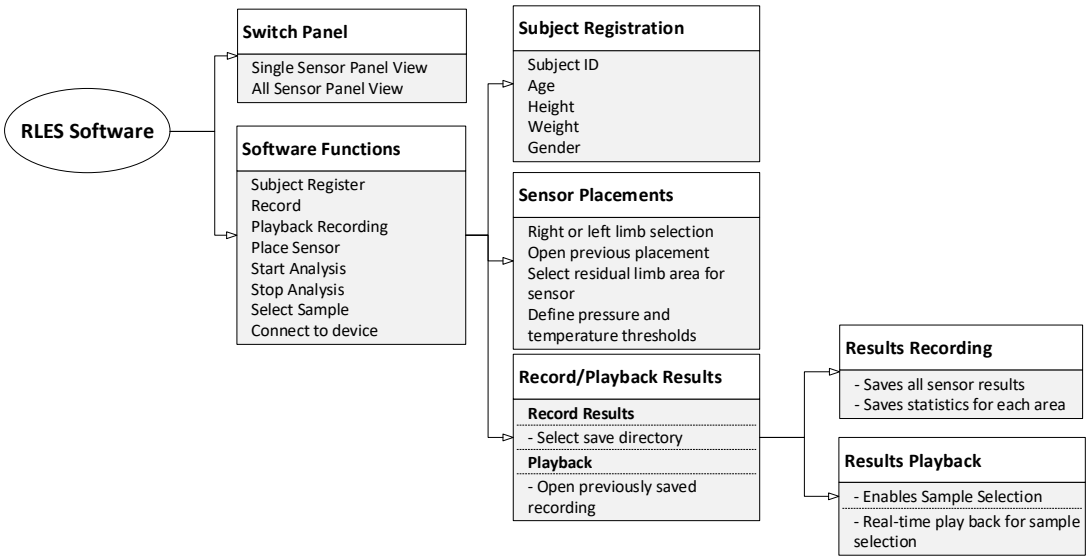

Figure 3.24: User interface thread functions and sub-functions.

3.8.2.2 Software Back-End

The back end of the software performs all the data storage and processing logic that is required to run the software.

Data Storage

The real-time display, recording and playback functions require the software to save, read and write data to large datasets. Each registered subject represents an object with attribute storage and inner data storage. These attributes and datasets are presented in Table 3.6 and Figure 3.25. The datasets for each transducer set sensor and each gait sensor contain large integer arrays to save the pressure, temperature, and gait force values found throughout the fitting process. Storing data in this way will allow the software to record all dataset information and allow the user to select specific sample values by indexing the dataset arrays as well as performing statistical calculations on each array.

Table 3.6: Attributes and datasets needed for each subject.

TRANSDUCER SET	GAIT SENSOR	SUBJECT DETAILS
- Pressure dataset - Pressure magnitude threshold - Temperature dataset - Temperature magnitude threshold - 2D x and y coordinates on image of residual limb	- Toe Off dataset array - Heel Strike dataset array	- Participant Identification Number - Age - Weight - Gender - Amputation Side

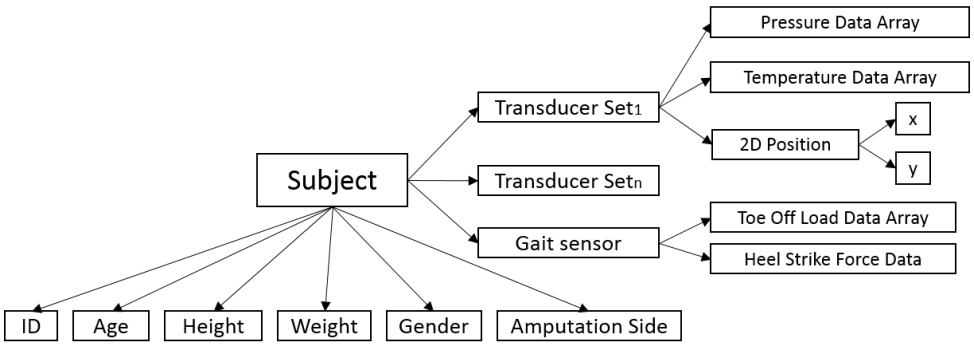

Figure 3.25: Subject Object Structure: Represented the attributes and datasets within each subject object where n is the transducer set number.

Processing Logic

The serial port thread is the process that runs continuously in the background once the connection is made between the software and the device. It is responsible for gathering the sensor signals, converting them from analogue signals into digital signals, and displaying them to the user in an appropriate manner via the GUI. Figure 3.26 displays the process logic design of the software.

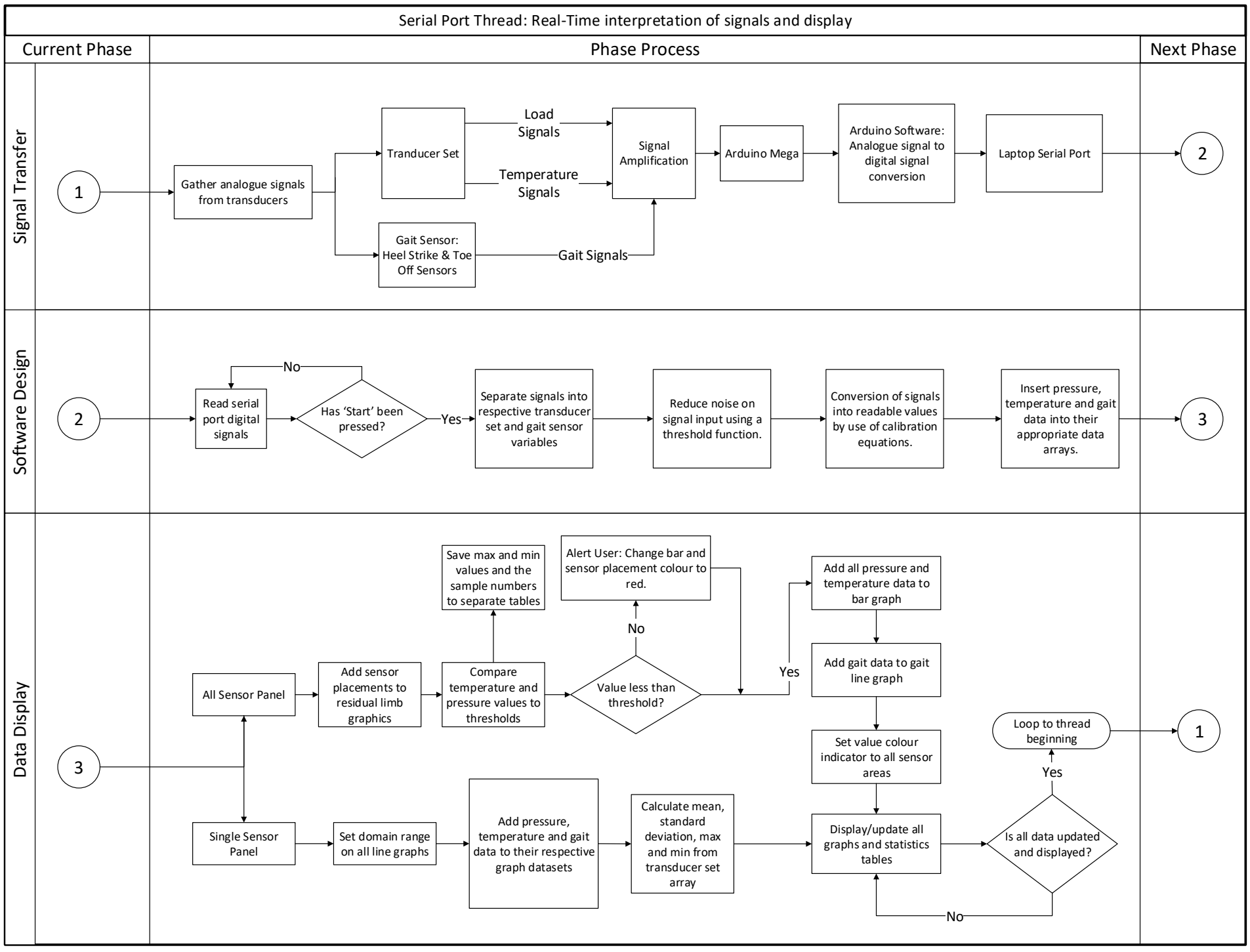

Figure 3.26: Signal Port Thread: Programming Logic.

3.8.2.3 Noise Reduction

Resistive-based analogue sensors such as the FlexiForce™ A201 sensor and 103 JT-025 thermistor suffer from noise, which is unwanted disturbances within the signal that induces small changes in input value. Therefore, to mitigate this noise and provide a stable input signal value, a threshold algorithm was developed and implemented. This analyses the input value change and if the change exceeds a defined threshold, then the input value will be updated, otherwise, the value will remain unchanged. The digital range provided by the Arduino Mega is 0 – 1024 (0 – 5 V), and the noise produced by the sensors related to a 0 – 5 digital value fluctuation. The threshold was set to the digital value of 5. This relates to 4.88 mV, which is insignificant compared to the maximum 5 V range and will not affect the accuracy of the sensor. The threshold algorithm is illustrated in Figure 3.27.

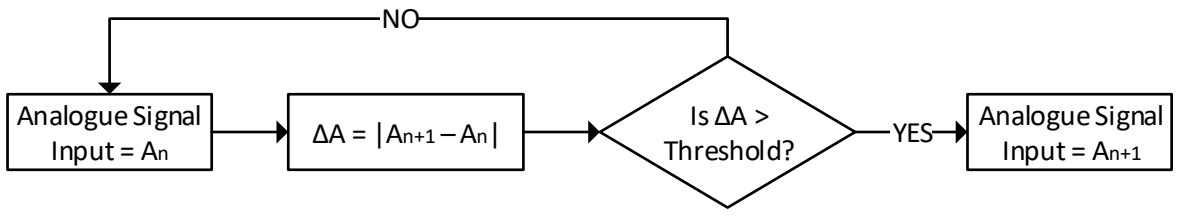

Figure 3.27: Threshold Algorithm.

3.9 Conclusions

Chapter 3 discussed appropriate design considerations, as well as investigated, evaluated and selected the most efficient sensors to be used within transducer sets of the RLES, and discussed the design of the RLES software. Chapter 4 discusses the development of the RLES and presents the finalized RLES prototype.

4 Design Outcomes

4.1 Introduction

This chapter illustrates the outcome of the final system development, which is separated into the following subsections:

1. The Device
    a. The Transducer Set
    b. The Gait Sensors
    c. The Circuitry
    d. The Control Box
2. The Graphical User Interface
    a. Subject Registration
    b. Single Sensor Panel
    c. All Sensor Panel
    d. The Control Panel

4.2 The Device

4.2.1 The Transducer Set

Figure 4.1 shows the final configuration and dimensions of each transducer set. The width of the entire configuration is 1.8 mm. This falls 0.3 mm above the range ruled out in the design considerations (Section 3.2), however, the 0.5 mm thickness of the 103 JT-025 thermistor falls only over the thermistor point (sensing area). The remainder of the thermistor is approximately 0.1 mm thick. Therefore, it is assumed that if a load is applied to the force plate, while the transducer set is attached to the RL, the 0.4 mm difference between the point and the remainder of the thermistor will be occupied instantly by the skin due to the skin's elasticity, and therefore mitigate the chance of a pressure point.

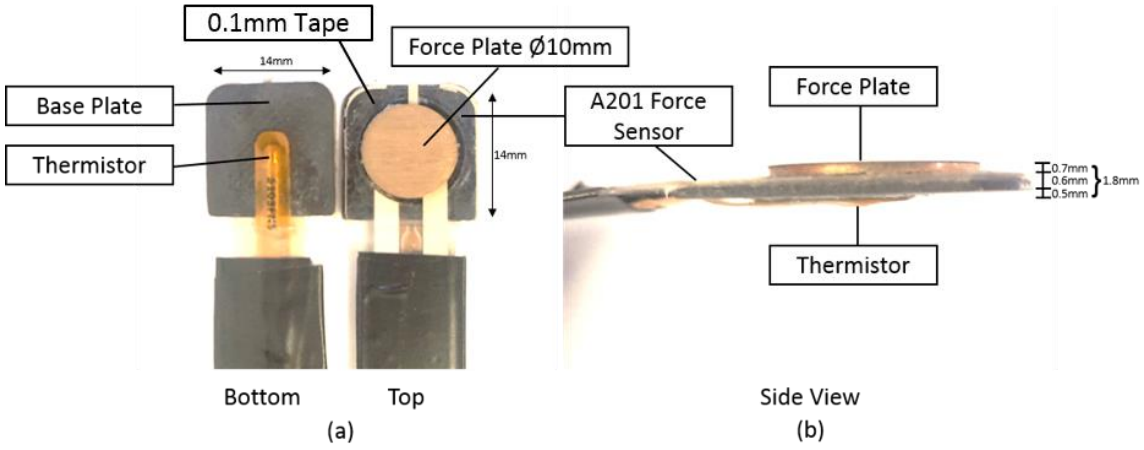

Figure 4.1: The Transducer Set. (a) Top and bottom view of transducer set displaying the force (pressure) and temperature sensor attachment to the base and force plate. (b) Side view showing the thickness of the transducer set.

4.2.2 Sensor Calibrations

Due to the variability between each sensor structure (slight resistance changes, etc.), each transducer set was calibrated to determine its ability to provide accurate and repeatable pressure and temperature measurements to the user.

4.2.2.1 Pressure Transducer Calibrations

Each pressure sensor was calibrated using the application of precision weights. To accurately apply the load directly onto the active area, a force transducer calibration structure was 3D printed out of ABS plastic (Figure 4.2). The force applicator (Figure 4.3), which fits within the calibration structure, was manufactured from Aluminium.

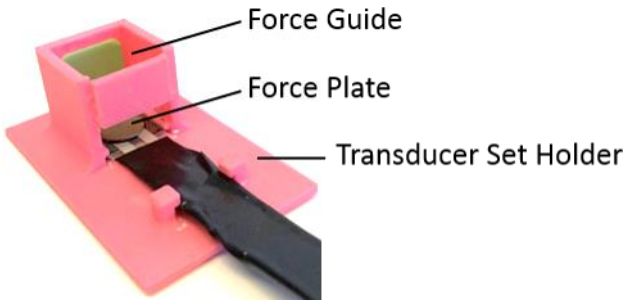

Figure 4.2: Force calibration structure. Holds each transducer set and provides a guide for the force applicator to fit, which directs the load onto the force plate of the transducer set.

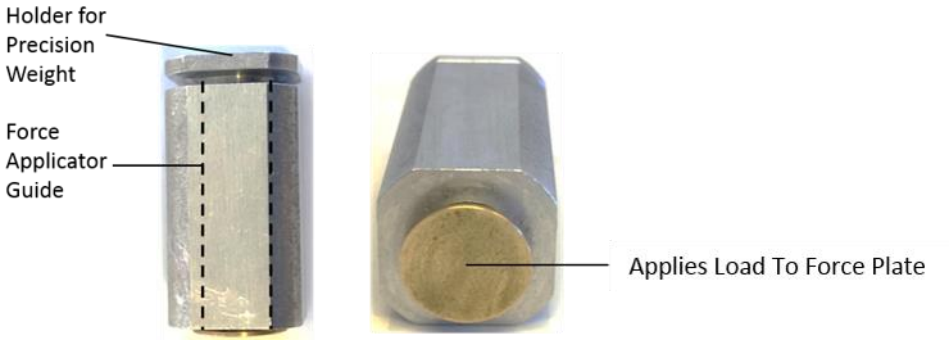

Figure 4.3: Force Applicator. Fits within the force guide of the calibration structure, holds the precision weight to calibrate, and directs the load onto the transducer set's force plate.

The pressure sensor calibration was performed by recording the digital value output from a load application of 0 – 2.4 kg in 0.1 kg increments. Figure 4.4 illustrates how each pressure sensor was calibrated and the application of the weights.

Figure 4.4: Weight application for calibration of pressure sensors.

The capability of the pressure sensor is dependent on its accuracy error and repeatability error. Therefore, after calibration, each pressure sensor was loaded up to a total range (TR) of 2 kg (250 kPa). The load output of each pressure sensor was tested three times and the average accuracy error and repeatability error was calculated (Table 4.1).

Table 4.1: Average accuracy and repeatability percentage error of device over 2 kg range.

WEIGHT (GRAMS)	100	200	300	400	500	1000	1500	2000	TR AVERAGE
Average Accuracy Percentage Error (%)	28.02	4.89	6.93	7.78	5.66	9.23	4.31	5.25	9.01
Average Repeatability Percentage Error (%)	0.32	0.44	0.37	1.29	1.50	2.93	5.91	4.40	2.14

The results were calculated using the following statistical equations (Figliola & Beasley, 2011):

$$Accuracy\ \%\ Error = \frac{|Weight\ Value - Sensor\ Value|}{Weight\ Value} \times 100 \quad [7]$$

$$Repeatability\ \%\ Error = \frac{2\ \times Standard\ Deviation}{Full\ Scale\ Output} \times 100 \quad [6]$$

The average accuracy error over the full range is 9.01% which satisfies the design objective (less than 10%) within Section 1.5.1. The repeatability error suggests that the device can produce repeatable results when subject to the same load. This accuracy result is similar to that of the F-Socket™ (Section 2.6.1, Table 2.3), furthermore, the 2.28% hysteresis error over this pressure range was calculated during the pressure sensor selection (Section 3.5.1, Table 3.4) which falls 9% below that of the F-Socket™, therefore, validating the transducer set configuration. Each pressure sensor has a brass 10 mm diameter force plate placed over the active area which experiences and directs the load. This load induces pressure on the force plate, which is pushed down onto the active area and interpreted by the sensor. Within the SLI the pressure felt by the force plate is induced by the inner surface of the socket/liner, and therefore equation 8 can be used to calculate the pressure being induced on the RL by the socket:

$$P_{socket}(kPa) = \frac{F_{forceplate}(N)}{A_{forceplate}(m^2)} \quad [8]$$

P is the pressure induced by the socket, A is the area of the force plate, and F is the force (weight (kg) times 9.81 m/s^2) experienced by the force plate. The results suggest that all sensors show inaccuracies at the initial change of resistance from the lower limit weight of 100 g, which relates to approximately 12 kPa of pressure. The literature review (Section 2.5.1) showed that capillary pressures are approximately 1.6 – 10 kPa, therefore, pressures that are of most importance, are pressures beyond this range. In the pressure range from 10 – 250 kPa it is seen that the average accuracy and repeatability error satisfies the requirement by falling in the range of 0 – 10%.

4.2.2.2 Temperature Transducer Calibrations

The calibration of each transducer set's temperature sensor involved attaching it in close proximity to a commercial RS1319A digital thermometer (accuracy error of ±0.75%), on the underside of an aluminium container. This container was then filled with boiling water and left to cool until the temperature on the RS1319A's sensor reached 40 °C, after which, the digital output produced by each thermistor was recorded at every 0.5 °C decrease in temperature until 27 °C (the ambient temperature over the calibration period). This process was repeated four times, and the average digital output at each step was calculated and assigned to its related temperature magnitude. The accuracy error of each temperature sensor was tested three times in the same manner. The average accuracy error of each temperature sensor is displayed in Table 4.2.

Table 4.2: Temperature sensors average accuracy error (%).

ACCURACY ERROR %				
Temperature (°C)	**T1 Error (%)**	**T2 Error**	**T3 Error (%)**	**T4 Error (%)**
27	0.74	0.37	0.74	0.37
30	0.00	0.20	0.33	0.67
35	0.00	0.51	0.00	0.06
40	0.75	0.41	0.30	0.10

4.2.3 The Gait Transducer

The 445 Newton A201 FlexiForce™ sensors were selected for the gait transducers to indicate the timing and phases of gait GRFs. They were both calibrated to 1.4 kN using an Instron machine (Strait Access Technologies, Cape Town). However, during the initial trial on a TTA, it was found that the sensing area of the sensor was not able to produce results if the gait of the amputee deviated slightly. Therefore, a system was created that increased the portion of the shoe sole that it would cover, as well as increasing the sensing area of both gait transducers (Figure 4.5). This system comprises of two 6 x 6 cm ABS pads with one of the pads having a slight circular extrusion with a similar diameter to the A201 FlexiForce™ activation area (9.53 mm). Figure 4.5 illustrates that if an external load is placed off the active area (but on the pad) a torque is created pushing the extrusion into the active area of the sensor below.

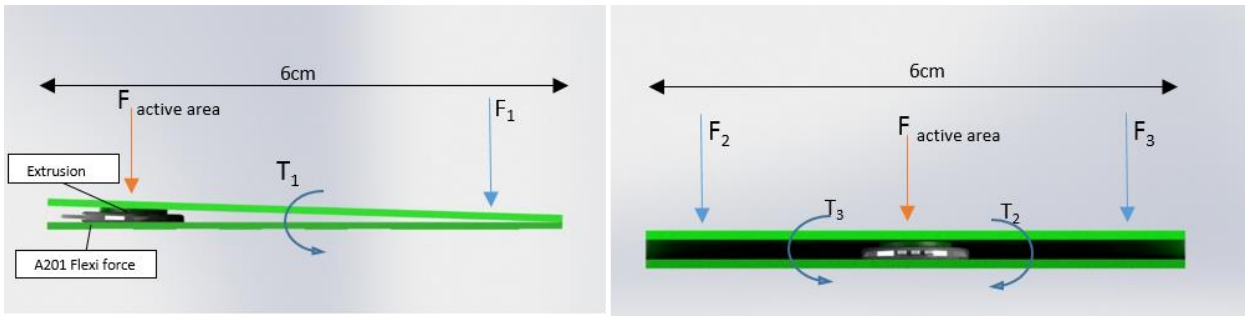

Figure 4.5: Gait sensor pads (Increases the sensing area of the A201 FlexiForce™ sensor). If F1, F2, or F3 is applied off the active area of the sensor, T1, T2, or T3 is generated which applies a force over the active area from the extrusion.

Because amputees have different shoe sizes and placement space, the fitment of the gait pads within the shoe (under the prosthetic foot) was not practical. Therefore, ABS plastic clips were 3D printed and a Velcro mechanism was used to attach the gait pads to the base of the shoe as shown in Figure 4.6.

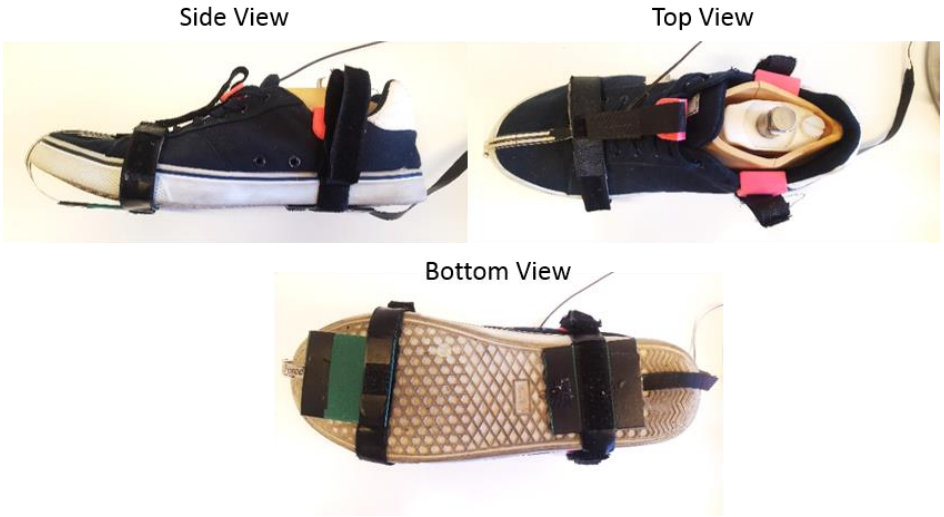

Figure 4.6: Gait pad shoe connection.

However, this configuration rendered the initial calibrations inaccurate because the distance between the force load and the extrusion could not be known. However, the sensors were kept calibrated as their output still provided the start, finish and the motion of the gait forces during the stance phase and an indication of what the GRF magnitudes may be. Future work should entail creating an insole strip of gait sensors that can attach to the base of all prosthetic feet

4.2.4 Device Circuitry

The circuitry schematic designed in Figure 3.17 was developed onto a PCB board. The circuitry is shown in Figure 4.7 with labels indicating each component of the device.

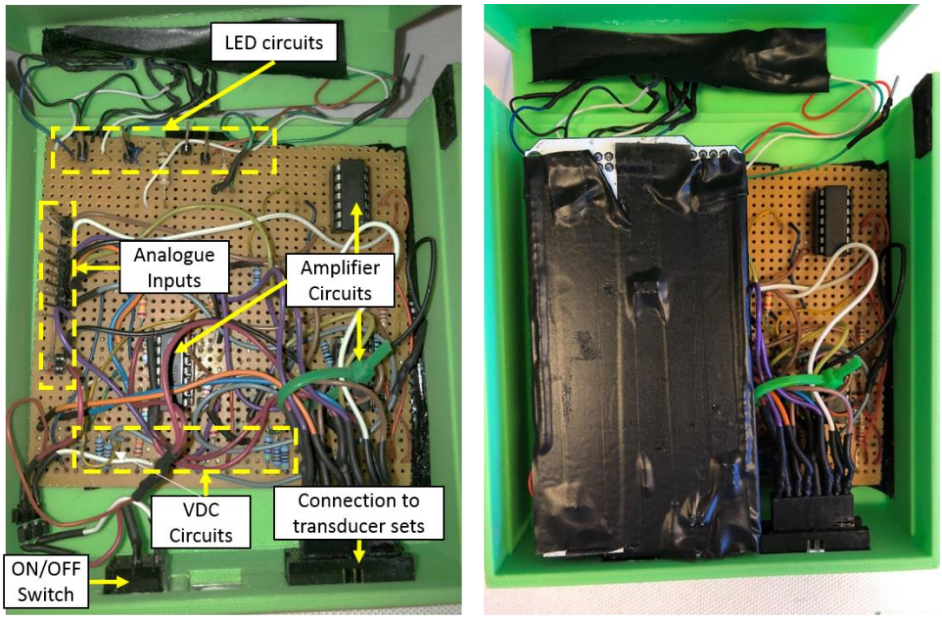

Figure 4.7: RLES device circuitry. (a) Circuitry illustrating individual subcircuits (no Arduino Mega attached) (b) Circuitry with attached Arduino Mega.

4.2.5 The Control Box

The control box was 3D printed from ABS plastic and can be seen in Figure 4.8. The box encloses the device circuitry and also entails an on/off switch, a serial connection port, a connection for the sensors as well as LED lights which inform the user that the RL pressure transducers are working.

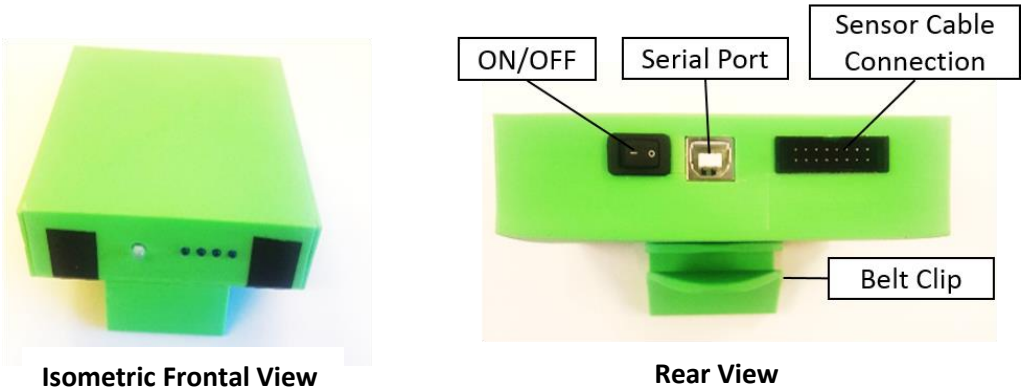

Figure 4.8: Control Box.

4.3 The Graphical User Interface (GUI)

The GUI of the RLES is an essential part of the system since it needs to provide the prosthetist with vital information in an appropriate manner to perform an accurate evaluation. The software offers two panels: the Single Sensor Panel and the All Sensors Panel (Figure 4.9). These panels provide the user with the SLI pressure and temperature information needed for an efficient RL evaluation. The software example given was extracted from a pilot software evaluation test on the RL of a TTA. Each label is explained in the Sections 4.3.1 - 4.3.5.

Single Sensor Panel

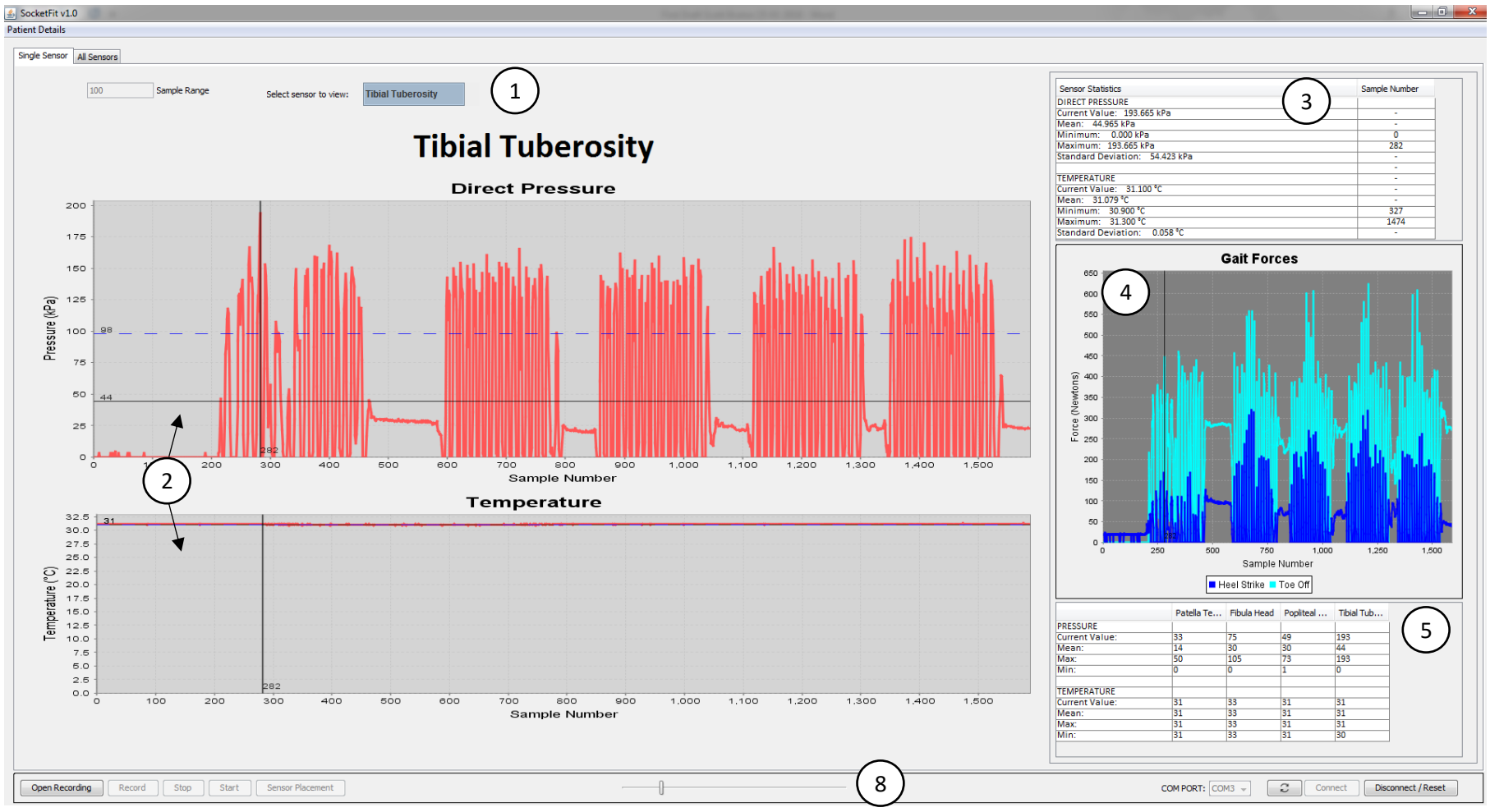

All Sensors Panel

Figure 4.9: GUI panels: Single Sensor Panel and All Sensors Panel.

4.3.1 Single Sensor Panel

The Single Sensor Panel (Figure 4.9) displays a more in-depth data analysis for a selected area of the RL and presents the user with the following information: The current selected sensor (Label 1); The recorded real-time pressure and temperature data over the entire testing procedure with the marked mean and standard deviation lines (horizontal lines) (Label 2); A statistics table displaying the current sample value, mean, minimum, maximum and standard deviation of the testing procedure (Label 3); The gait ground reaction forces (shown on both panels) (Label 4); An overview table displaying the current value, mean, maximum and minimum value of all other RL areas (Label 5). Each graph can be zoomed in which allows the user (prosthetist) to analyse the loading pattern on a particular area over each stride.

Additionally, the loading pattern of an area can be analysed with its related gait GRF curve, to evaluate the alignment of the entire prosthesis.

4.3.2 All Sensor Panel

The All Sensors Panel (Figure 4.9) of the software GUI, during a recording playback, presents the user with an overall evaluation of the RL at any specific time during the procedure. It provides the following information: The subject's details (Label 6); The maximum pressure and temperature values found in the recording (with their corresponding sample number), currently the maximum pressure sample for the tibial tuberosity is selected (Label 7); A slider to select a sample to analyse (sample 282 is selected in the figures) (Label 8); The recorded real-time pressures and temperatures over all areas corresponding to the specific chosen sample (Label 9); Illustrated positions of the transducer sets on the amputee's RL (Label 10); Colour indicators for different pressure (blue) or temperature (green) magnitudes and a red colour indicator to alert the user if a pressure or temperature has exceeded the threshold (Label 11).

4.3.3 Control Panel

The control panel of the software comprises buttons, which control the majority of the software functions (Figure 4.10).

Figure 4.10: Control Panel

It presents click buttons for the following functions: connecting to the COM port of the Arduino, which begins the signal transfer from the device to the software; sensor placement, which allows the user to select the RL limb side and areas of analysis; initiating the real-time pressure and temperature data display; recording the real-time pressure and temperature data; opening a recording of the data (the result of which is shown in Figure 4.9); and the selection of a sample to analysis (current selection, in Figure 4.9, is sample 282).

4.3.4 Subject Registration

The RLES software allows the user to save the amputee's details to the hard drive of a computer. This function is located in the drop-down menu "Patient Details", which is located at the top left corner of the software and is always available (Figure 4.9). The details comprise the amputee's identification number, age, height, weight and gender. Saving the details create new directory folders for each specific amputee, which can be loaded for future testing procedures (Figure 4.11).

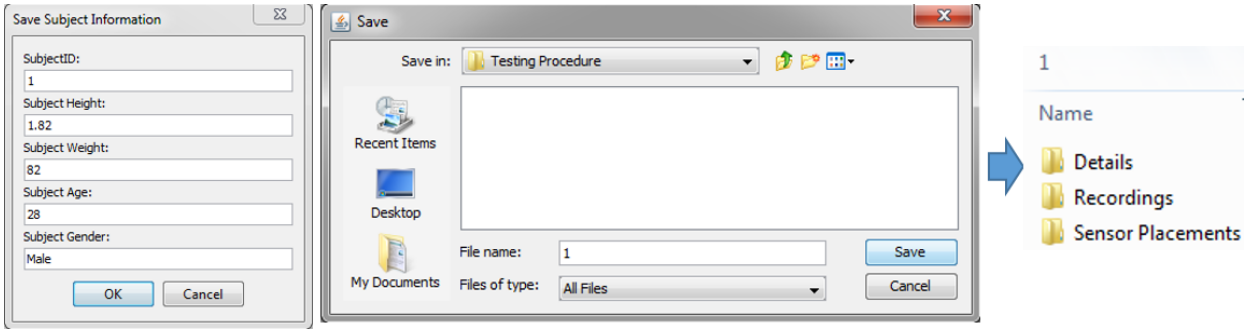

Figure 4.11: Saving subject's details.

4.3.5 Create/Load Sensor Placements

The software allows the user to select the amputation side of the patient, after which, it prompts the user to add areas to analyse (Figure 4.12).

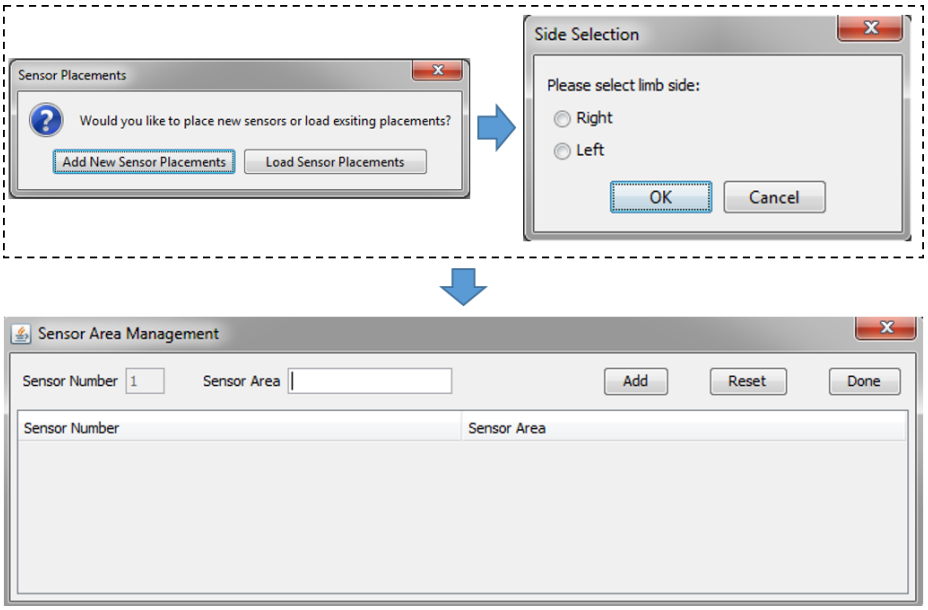

Figure 4.12: Sensor Area Panel.

The user then selects points on the RL image and sets the pressure and temperature threshold for that specific area (Figure 4.13). After confirming placement, a double circle icon appears in the selected area. The coloured circle icon comprises the number of the transducer set, an outer green ring (representing the temperature magnitude), and an inner blue circle (representing the pressure magnitude). The colour of the ring or circle represents the respective magnitudes. A zero pressure or temperature magnitude changes the colour of the related circle or ring to white. As the magnitudes approach the threshold, the colour become more blue or green respectively. If the magnitude exceeds the threshold, the related circle or ring turns red to alert the user (shown in Figure 4.9).

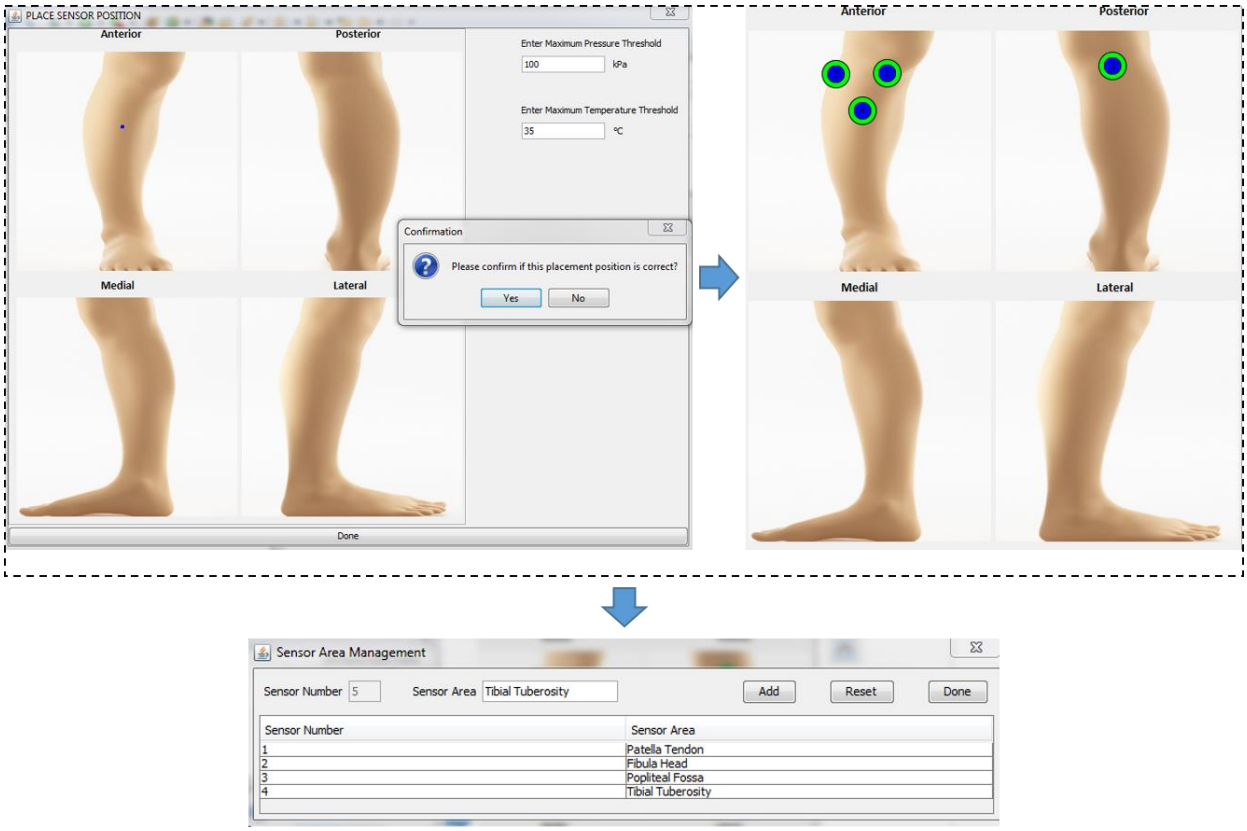

Figure 4.13: Sensor Placements.

4.4 Data Retrieval and System Sampling Rate

The Arduino Mega 2560 was used to convert the analogue voltage provided by the pressure loads and the temperatures for each transducer set, to digital values. The analogue signals are transferred to the ADC via a USB cable into a USB port of a laptop. However, during software analysis, it was found that the sampling rate was limited. The sampling rate is one of the most important aspects of the system since it determines the amount of data gathered for analysis and if the rate is too slow, large pressures may be missed which would render the system, as an evaluation tool, inefficient. The software is required to continually update the GUI with pressure and temperature data at a speed which is appropriate for real-time evaluation and which is allowable by the computer's processing power. The computational processing power to update all graphics of the RLES developed in this study, only allowed for a sampling rate of 10 Hz (1 sample per 100 ms) with faster rates rendering the software unable to update the real-time graphics quick enough. This limitation of the system was governed by the computer running the software as well as the efficiency of the software code, which utilises two threads for the graphical simulations (discussed in Section 3.8.2). Previous interface pressure measurement studies have utilised commercially built systems such as Tekscan's® F-Scan™ (Ali et al., 2013; Dumbleton et al., 2009; Eshraghi et al., 2014) or research developed systems (J Sanders et al., 1997; Zachariah & Sanders, 2001; Zhang et al., 1998). These systems have been seen to sample at a rate of 50 – 200 Hz, however, the research developed systems do not provide real-time graphical software for analysis and merely save data to be processed later.

The efficiency of the sampling rate is determined by its capability to gather enough samples to approximate the peak pressures found on the RL areas accurately. The average gait cycle time is approximately 1 - 1.2 seconds and studies by Seelen et al. (2003) and Jia et al. (2008) found that on average, the duration in which RL interface pressures exceed 80% and 90% of their peak pressure is 25% and 19.5% of the gait cycle respectively (Hermodsson, Ekdahl, Persson, & Roxendal, 1994). This duration equates to an average time period of approximately 200 – 300 ms, which will allow approximately two samples to be retrieved during this period. Therefore, it is assumed that a sampling rate of 10 Hz will be sufficient for retrieving an accurate approximation of the maximum pressure in each RL area. This assumption will be evaluated within Section 8.2. Future iterations of the software code should include multiple threads to run simultaneously, with a dedicated thread to update software graphics.

4.5 Final Residual Limb Evaluation System (RLES)

The final RLES is presented in Figure 4.14. The transducer sets (Label 2) attach to the skin of the RL of the TTA within the SLI and connects to the control box via a ribbon of cables. The gait pads (Label 3) attach to the underside of the shoe in the toe off and heel strike positions and are held in place using a Velcro™ and clip system. The control box (Label 1) attaches to the belt of the TTA and connects to the USB port on the computer via a 2 m USB data cable. The RLES software (Label 4) receives all information from the control box and displays them to the user via the GUI.

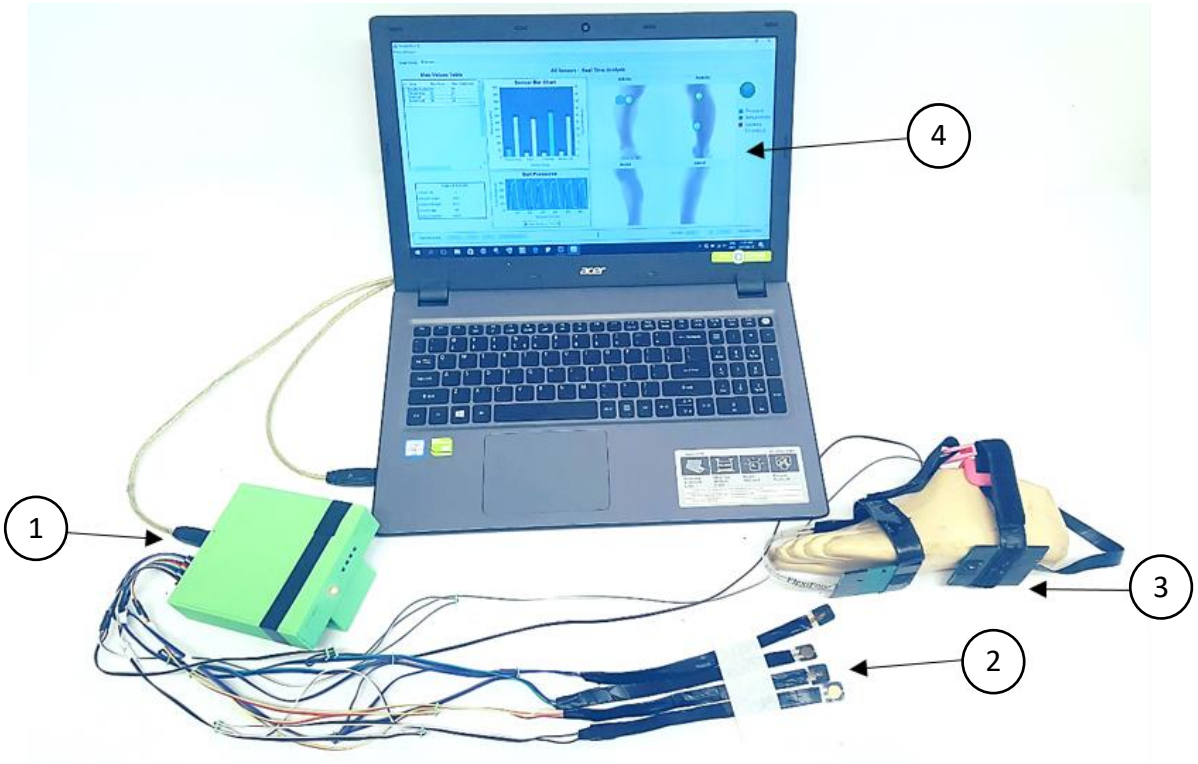

Figure 4.14: 1 - Control Box, 2 – Transducer Sets, 3 – Gait Pads, 4 – RLES Software.

4.6 Conclusions

The development of the RLES produced a device capable of retrieving accurate pressure and temperature readings, as well as gait phase knowledge and system software that provides the user with the ability to analyse the data gathered thoroughly. The software is tailored to the prosthetic fitting procedure by providing visual displays of the RL evaluation to the user. Chapters 5 – 8 entail the methods, experiments, and analysis, which tests the efficiency of the prototype RLES and evaluates its use within a real-world setting.

5 Experimental Methodology and Design

5.1 Introduction

The efficiency of the RLES is defined by its functionality and limitations. The following chapter describes the methodologies and procedures that were designed to identify and obtain these characteristics and analyse the RLES's ability to be used as an evaluation system within the prosthetic fitting procedure.

5.2 Experimental Overview

In Sections 4.2.2.1 and 4.2.2.2, the pressure and temperature sensors were calibrated, and their accuracy errors and repeatability errors were defined. However, the environment drastically changes within the SLI, therefore, the RLES needed to be evaluated within a real-world situation on TTAs. The following experimental methodology was designed to complete this evaluation and satisfy the objectives outlined in Section 1.5.2.

5.3 Research Hypothesis

The proposed research was performed to investigate the following hypothesis: "A tactile residual limb evaluation device and recording software can provide reliable socket-limb interface information, which can be used to identify vulnerable areas on the residual limb induced by the socket during the natural gait movements of trans-tibial amputees." Therefore, the reliability and repeatability of the RLES measurements needed to be calculated and validated to define the evaluation capabilities of the system.

5.4 Experimental Setup

The prototype RLES comprised four RL transducer sets to prove that a device of this nature is practical for use within the prosthetic fitment procedure. Therefore, the placement of each transducer set is important.

5.4.1 Transducer Set Placement Positions

It was assumed that the condition of the TTA's RL would be unknown before participating in the testing procedures. Therefore, to maintain consistency over all the study participants, four RL areas of expected pressures were chosen to be evaluated. These areas comprised of the fibula head (largest pressure expected), the popliteal fossa and patella tendon (common load-bearing areas), and the distal medial calf (lowest pressure expected). The fibula head (FH), the popliteal fossa (PF) and patella tendon (PT) areas were defined as constant areas to be tested over all participants, and the distal medial calf (DMC) was defined as a "movable area", whereby its transducer set could be moved to a skin problem area if presented. Figure 5.1 displays the selected areas to analyse on each TTA.

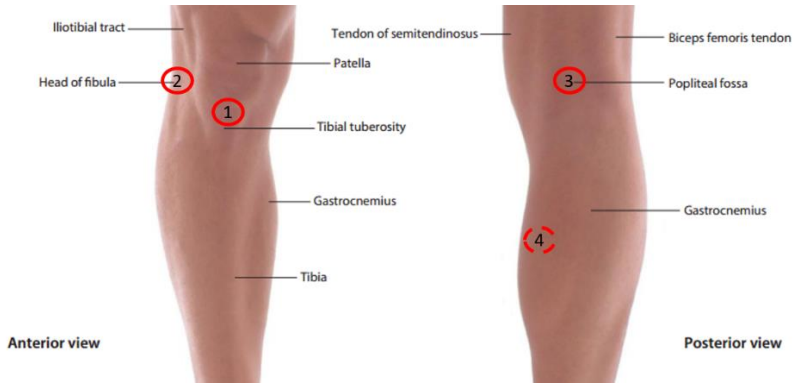

Figure 5.1: Selected areas for the transducer sets to analyse. Areas 1,2, and 3 are constant areas represented by full circles. Area 4 is a moveable area represented by a dashed circle (Drake et al., 2008).

5.4.2 Experimental Procedures

Three tests were designed to evaluate the study objectives, each with specific requirements, purpose, and considerations. All tests entailed attaching the transducer sets to the relevant sensing areas for the particular participant's RL and required the participant to don (attach) their own private prosthetic components (liner, socket, foot, etc) over the transducer sets.

5.4.2.1 Static Standing (SS) procedure

Purpose

Large interface pressure applied to skin areas can potentially constrict the subcutaneous blood flow to the cells and can cause reactive hyperaemia when unloaded. This leads to a common trend in skin temperature change. During the loading period, the area's skin temperature decreases due to a compromised blood supply or increases slightly due to a decrease in distance from the underlying muscle and blood vessel layer (Pye & Bowker, 1976). However, during the unloading period, reactive hyperaemia causes an increased blood flow to that area to compensate for the previous lack of blood which results in an increase of the area's skin temperature (Barnett & Ablarde, 1995; Kemuriyama, Niitsuma, Yano, & Komeda, 1998; Mak, Zhang, & Boone, 2001; Meijer et al., 1989; Pye & Bowker, 1976). Therefore, the purpose of the SS procedure is to validate whether the RLES can identify and replicate the trends found in literature, which would verify its ability to track skin temperature change.

Requirements

Studies that have researched skin temperature changes due to interface pressure follow a similar procedure namely: Attaching thermistors to analysis areas; recording the skin temperature before loading; statically loading the area for 5 - 10 minutes; relieving area of load; and recording temperature reaction to unloading for 5 - 10 minutes (Bader, 1990; Barnett & Ablarde, 1995; Pye & Bowker, 1976; Joan E Sanders, 2000). Therefore, a similar procedure needed to be recreated within the SLI of a TTA. Since a known load cannot be applied to the skin within the socket, it was decided that the static load was to be provided by the participant standing still while attempting to bear weight equally on each leg, and the resting period would entail the participant to sit for an appropriate amount of time. Therefore, the requirements of the SS procedure involved:

1. The SS test to be performed first to avoid prior temperature changes due to walking or other loading movements.
2. Flat ground for each participant to stand on.
3. The participant to rest for 10 minutes while sitting in a chair to allow for the skin temperature within the socket/liner to equalise.
4. Ambient temperature and initial temperature on the RL areas to be recorded.
5. The participant to stand for a 5 – 10 minutes period while the device records the temperature change under the standing pressures.
6. The participant to rest for 10 minutes while the device records the temperature change after load release.

Considerations

It was assumed that the participants recruited would be at different stages of recovery and could consist of amputees who are new to their prosthesis, experiencing discomfort on their RL, or are bilateral amputees who may have difficulty balancing on their prostheses for long periods of time. Therefore, the ideal standing duration for testing was set at 10 minutes but could decrease due to the amputee's capabilities.

Floor Plan

Figure 5.2 displays a top-down view of the space needed for the procedure, and the placement of the participant's feet while standing.

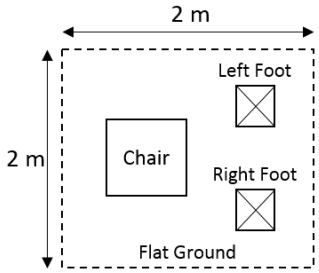

Figure 5.2: Static standing procedure floor plan and foot placement.

5.4.2.2 Straight Line Walk (SLW)

Purpose

The RL soft tissue is exposed to dynamic and repetitive loading from the prosthetic socket during walking. If large pressures are being placed on sensitive areas, there exists the potential for future skin complications. Therefore, the measurement of interface pressure is the most crucial evaluation parameter to obtain. Identification of these dynamic and repetitive loads will give the prosthetist insight into the pressure magnitudes which are continually applied during regular movements. Therefore, to quantify the repeatability of the RLES output, which indicates reliability, the RLES needed to be exposed to the same movement continually (repetitive loads). The method chosen to quantify the RLES's repeatability was a straight line walk, since it provided the highest probability of repetitive loads over each stride. The peak pressure points between strides were chosen to be used for comparison. The COV between peak pressure points would be calculated and compared to the COV found from other systems used in literature for validation of correct functioning and quantify the RLES's repeatability. The SLW procedure has been performed in the majority of SLI pressure measurement studies which involved measuring the pressures on the RL or in the socket during "normal walking", which is assumed to relate to straight line walking (E. Al-Fakih et al., 2016; Jia et al., 2008; Rae & Cockrell, 1971; J Sanders et al., 1997). Each stride consists of a loading (stance) and an unloading (swing) phase, which would allow the recording of many samples (1 sample = 1 stride) to be utilised within the repeatability analysis. Therefore, the purpose of the SLW procedure was to provide multiple peak pressure samples over a controlled and repeatable movement to the RLES to quantify its repeatability capabilities and evaluate its functioning against literature for validation.

Requirements

Each stride varies from the next and is seen to be more variable for amputees. Therefore, to minimise the variations and collect multiple peak pressure samples, the SLW procedure will entail the following:

1. 20 – 40 m of flat ground to walk on.
2. Appropriately spaced stride markers throughout the 20 – 40 m track, to minimise the stride variation.
3. The participant to walk the track, with each heel strike landing on the required marker.
4. The participant to rest at each end of the track for 10 seconds, to identify the start and end of the track on the recorded results.
5. The participant to repeat the walk 4 or more times (depended on participant capabilities) for the recording of a sufficient dataset size.

Considerations

The participants are most likely to be at different stages of recovery or prosthesis use and may have difficulty walking for long periods at a time. Therefore, the size of the SLW sample dataset (number of consistent strides performed) will be determined by the capabilities of the amputee to avoid injury or discomfort. Additionally, to account for acceleration and deceleration at the beginning and end of each track, the first and last three strides of each SLW track run will be removed from the sample dataset. Furthermore, the rest period between walking periods will be zeroed for appropriate data analysis.

Floor Plan

Figure 5.3 illustrates the floor plan of the SLW procedure.

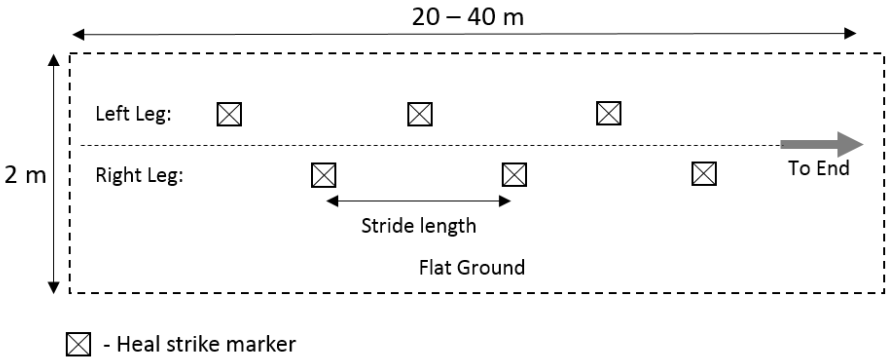

Figure 5.3: Straight Line Walk procedure floor plan.

5.4.2.3 Figure of 8 Walk (F8W)

A thorough literature review was conducted, which failed to produce any study that performed SLI pressure measurements on TTAs while turning or walking a figure-of-8 track. This indicates that the analysis of the pressures induced while turning with or pivoting about a prosthesis has been neglected in research (E. A. Al-Fakih et al., 2016). The F8W procedure's aim was to produce all natural walking motions and angles. This would induce the maximum pressures that are likely to be experienced by the amputee's RL on a day-to-day basis.

Purpose

As previously discussed the SLW procedure is used in the majority of SLI studies, however, natural day-to-day movements involve turning left and right (at natural walking speeds) which entail weight shifts on the RL dependent on whether the prosthesis is being used as the inside or outside turning leg. These everyday movements potentially produce much larger pressures on the RL soft tissue than a SLW due to the momentum of walking being carried into the turn. Therefore, the purpose of the F8W procedure was to produce SLI pressures induced by the natural walking movements for comparison with the SLW pressures to validate the assumptions and evaluate the RLES's ability to track natural walking movements. This evaluation would assess the RLES's ability to measure the pressures on a TTA's RL during specific movements, such as sporting actions, for tailoring the socket for the amputee's specific need.

Requirements

The requirements of the F8W test are less strict than the other two tests since it aims to produce the TTA's natural movement. However, the track should be the same for each participant to ensure consistency in testing. Therefore, the F8W procedure will entail:

1. A track area of level ground with a space that provides at least 5 m for turning and 10 m for straight walking in-between turns.

2. Two markers placed 5 m apart.
3. Left turn and right turn assigned to each marker.
4. The participant to walk from marker to marker turning left and right at the relevant marker.
5. The participant to repeat to track ten or more times (dependant on the participant's capabilities).

Considerations

Figure-of-8 walking involves sharp turning on both limbs. This may be difficult for amputees when pivoting on their prosthesis which is a concern for unilateral and even more so, bi-lateral amputees. Therefore, the sample size gathered would be completely dependent on the participant's capabilities, as each amputee may be at different stages of recovery or prosthesis use. This implemented precaution was to avoid any possibility of injury or risk. The F8W test would only be performed on participants that have the capability to do so.

Floor Plan

Figure 5.4 illustrates the floor plan and track for the F8W procedure.

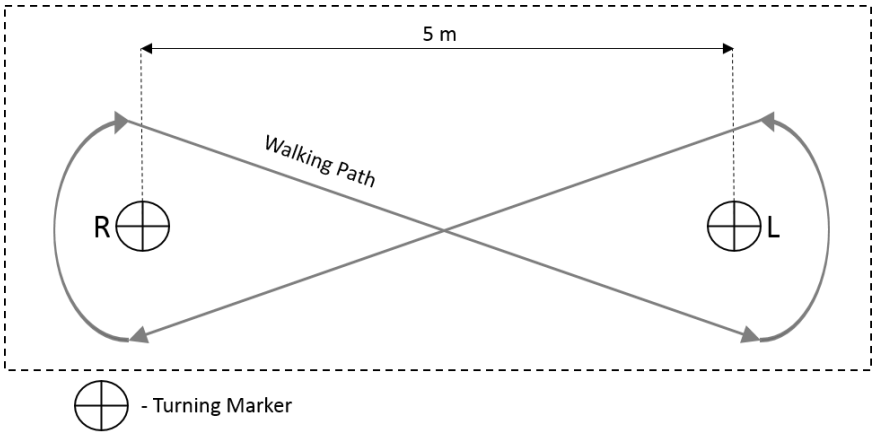

Figure 5.4: Figure-Of-8 Walk procedure floor plan. R – Right turn marker, L – Left turn marker.

5.5 Experimentation

The experimentation for each testing procedure followed the same preparation protocol.

5.5.1 Preparation Protocol

The preparation protocol presented in Figure 5.5 was to be performed at the beginning of each testing session.

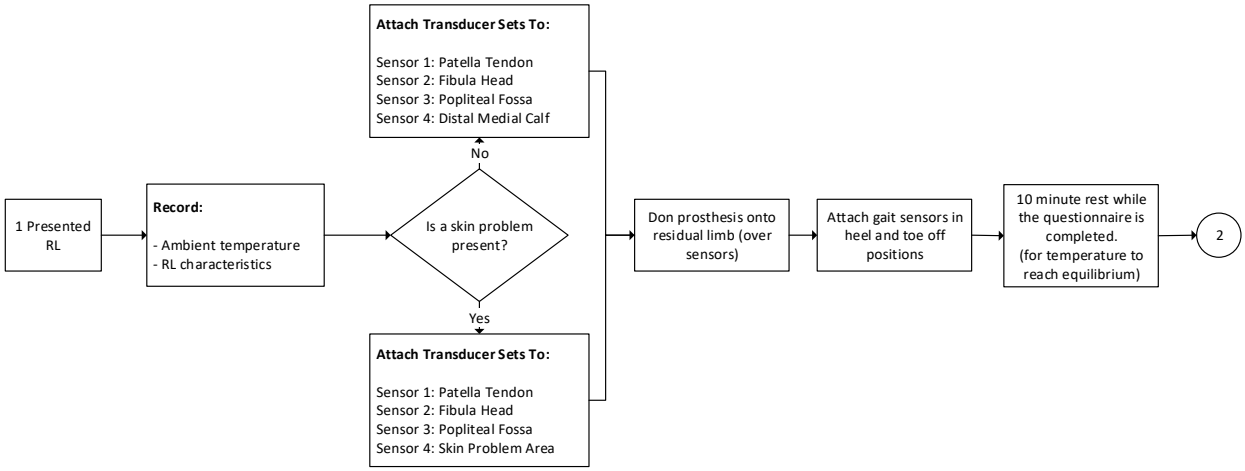

Figure 5.5: Testing Procedure Preparation Protocol.

5.5.2 Testing Protocol

The testing protocol was determined by the experimental procedure to be performed (Figure 5.6).

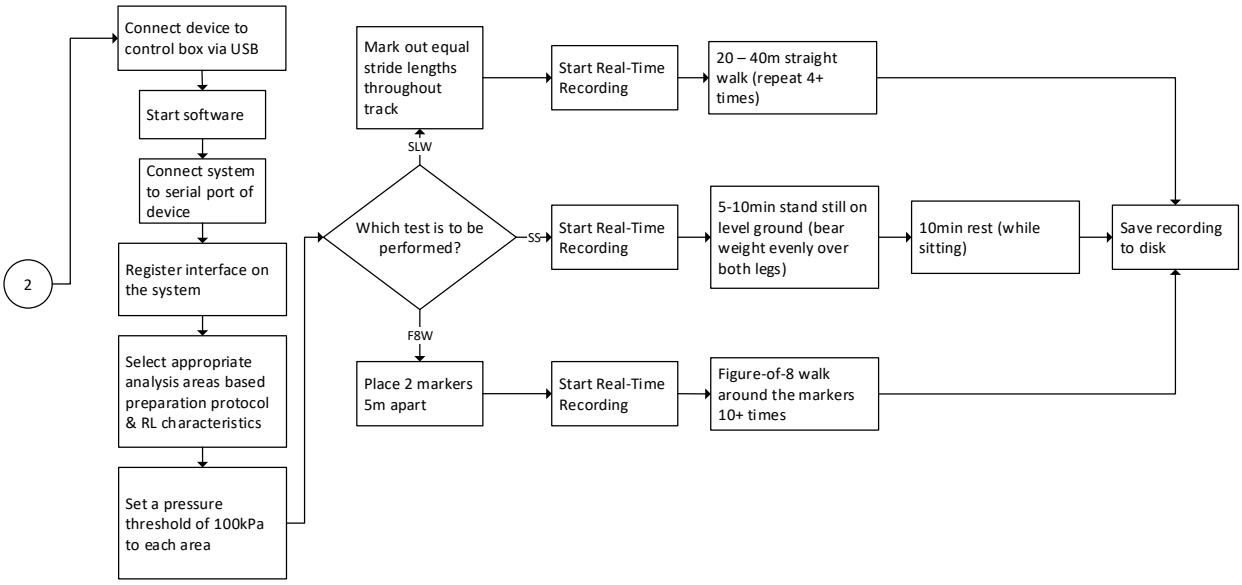

Figure 5.6: Testing Procedure Protocol.

5.6 Data Recording and Analysis

5.6.1 Data Recording

The control box was to be attached to each participant and connected to the software via a USB data cable to a laptop. Data would be sampled and recorded at 10 Hz during all tests. Each pressure and temperature sensor within all transducer sets has a pre-allocated double array size of 2049 rows and 1,048,576 columns. This equates to a storage of 214,853,224 samples on each test, which allows for a maximum sample recording time of approximately 6000 hours per session. Once the recording is stopped, all test and subject data is recorded to the hard drive.

5.6.2 Data Analysis

The software GUI presents a platform to analyse all data over the entire recording period. However, to perform additional statistical analysis on the results for system validation, the data files were set to save in a format which is compatible for import into Microsoft Excel to allow all data to be imported into tables for further analysis. This allowed for statistical analysis software, IBM SPSS Statistics 24, to be used for appropriate results comparison and illustration.

5.7 Required Study Population

The experimental procedures aimed at verifying and validating the RLES's ability to analyse the pressures and temperatures within the SLI of TTAs. Therefore, the subjects of the study population should satisfy the following criteria before being accepted into the study:

- Have a unilateral or bi-lateral trans-tibial amputation.
- Have a personal prosthesis to use in the study.
- Have the ability to walk and stand without support (crutch, support pole, etc).
- Be between the ages of 20 - 70 years old and weigh between 60 – 90 kg.
- Male or female.

5.8 Conclusions

Chapter 5 presented the study hypothesis and discussed the methodologies designed to evaluate it. RL areas to analyse were selected, experimental procedures were designed (each with their own purpose and requirements), and the protocol for the testing procedures were presented. These protocols were designed to produce reliable and appropriate results to be analysed. Chapter 6 discusses how the methodologies were implemented, the complications that arose, and the decisions made.

6 Experimental Implementation

6.1 Introduction

This chapter describes the creation of the study population, implementation of the experimental methodology, the complications that arose and recommendations for future methods.

6.2 Participant Recruitment and Study Population

Before study participant recruitment took place, ethical approval was acquired from the Human Research Ethics Committee (Appendix B - Figure 12.1). TTA participants were then recruited for the study via Vincent Pallotti (VP) private hospital (Cape Town, South Africa) and the private practice of Eugene Russouw, Orthotist and Prosthetist (Cape Town, South Africa).

6.2.1 Testing Venue

To decrease travel distance and expenses for participants, a venue for testing was requested at each practice to use after each participant's appointment. However, due to venue availability, only participants from Eugene Russouw's Orthotist and Prosthetist's practice could be tested after their check-up at the practice. Appropriate off-site venues were chosen for the VP participants dependent on their availability and location.

6.2.2 Amputee Participant Population

All available participants that satisfied the criteria in Section 5.7 were male (female candidates were not available during the recruitment process). In total five TTAs were recruited for the research study which entailed three uni-lateral and two bi-lateral amputees. Table 6.1 presents the details of each subject and their RL characteristics.

Table 6.1: Amputee population characteristics.

PARAMETER	SUBJECT #1	SUBJECT #2	SUBJECT #3	SUBJECT #4	SUBJECT #5
Gender	Male	Male	Male	Male	Male
Age	60	64	42	32	29
Weight (kg)	85	73	83	82	70
Height (m)	1.65	1.7	1.86	1.75	1.78
Amputation	Bi-lateral	Bi-lateral	Uni-lateral	Uni-lateral	Uni-lateral
Amputation Reason	Diabetes	Trauma	Trauma	Trauma	Trauma
Amputation Side	Right & Left	Right & Left	Right	Left	Right
Unusual Characteristics	N/A	Very bony fibula head on both RLs	Erythema on RL after removing prosthesis	Erythema on RL after removing prosthesis	Protruding fibula head
Skin Problem	N/A	N/A	Pressure Sore - Proximal Tibia (below tibial tuberosity)	Pressure Sore – Distal Tibia	N/A

The study aimed to determine if the RLES is capable of producing repeatable and reliable results to verify its capabilities as an evaluation tool (to be used in the prosthetic fitting procedure) by identifying vulnerable areas on the RL. Considering the variability in RL morphology, the seven RLs (from all five subjects) interface differently against their socket and are exposed to different pressures due to gait

variability between legs and different RL characteristics. Therefore, these interfaces are separated by the subject, amputation side, socket type and liner type. The collection of these interfaces makes up the study population which will be discussed in Section 6.2.3.

6.2.3 Interface Study Population

All subjects were required to perform all three testing procedures, however, the entire testing procedure duration was approximated to 1 - 1.5 hours for uni-lateral amputees and 2 - 3 hours for bilateral amputees (both RLs). The capabilities of each participant were unknown prior to testing, therefore, the following considerations had to be taken into account: the testing procedure duration; the participant time availability; the participant's capability to complete all three procedures in one testing slot; and the testing venue capabilities. To account for these possible scenarios two testing slots (over two separate days) were made available to each subject to allow for all tests to be completed. However, unavoidable complications arose when testing subjects 1, 2 and 3. These are listed below:

- Subject 1 was not available for a second testing session.
- Subject 2's prosthetic sockets from the first testing session were undergoing a re-design and modification, and the participant could only use previous prosthetic sockets for the second testing session.
- Subject 3 presented a pressure sore in the first testing session, but had different prosthetic components during the second testing session which had healed the pressure sore area.

These complications introduced new SLIs into the study population, which could not be grouped with results from the first testing session. However, the validation of each specific system function is solely dependent on the SLI that it is analysing, therefore, three separate study populations were made by grouping the related and appropriate interfaces. To distinguish between each interface, an identification code was given based on the subject number, amputation side, and interface number. An example is shown in Figure 6.1.

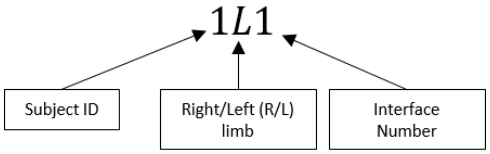

Figure 6.1: Identification code: Subject ID, Amputation Side, Interface Number.

A description of the interface socket and liner type can be found in Appendix C (Table 13.1). Table 6.2 displays the study population for each respective test.

Table 6.2: Study interface population for each test type.

TEST TYPE	SS	SLW	F8W
Study Population	• 1L1 • 1R1 • 2L1 • 2R1 • 3R1* • 4L1* • 5R1	• 1L1 • 2L2 • 2R2 • 3R1* • 3R2 • 4L1* • 5R1	• 1L1 • 2L2 • 2R2 • 3R2 • 4L1* • 5R1

** - Pressure sore visually present in interface.*

It must be noted that for a comparative study between the SLW and F8W, only the interfaces which appear in both the SLW and F8W populations that were tested sequentially on the same day with no modification to the interface or sensor placements are included in the F8W study population.

Furthermore, interface 3R1* was included in the SLW population since it presented a pressure sore and its results were compared to that of 3R2 (healed pressure sore area) to indicate the system's ability to identify pressure relief in the vulnerable area.

6.3 Transducer Set Placement

An example of the transducer set placements on the RL of the TTAs is shown in Figure 6.2.

TRANSDUCER SET PLACEMENTS (SUBJECT #2)

Patella Tendon (PT)	Fibula Head (FH)
	
Popliteal Fossa (PF)	**Distal Medial Calf (DMC)**
	

Figure 6.2: Transducer set placement and attachments.

Each transducer set was attached to its specific area using Tegaderm™ dressing. This allowed for placement to be kept within the socket and easy application and removal of each transducer set.

6.4 Gait Sensor Attachments

The gait sensor pads were attached to the underside of the participant's shoes via 3D printed clips and a Velcro™ system (Figure 6.3). The point of the arrows represent the position of the heel-strike and toe-off load sensor's active areas. The gait sensor pads are held to the underside of the shoe by a Velcro™ and clip mechanism, where Velcro™ strips are fed through 3D printed clips, to tighten the pad to the underside of the shoe, and then connected to hold the pads in place. Duct tape was wrapped around the shoe to mitigate any risk of slippage.

Figure 6.3 shows the attachment and use of the gait sensors throughout a single step. The attachment of the gait sensor pads to the underside of the shoe allowed correct heel-strike and toe-off positions to be obtained. However, the characteristics of shoe tread vary between shoe types which created difficult attachment surfaces. Future iterations should entail in-sole gait pads which can be inserted into the shoe at appropriate positions which would decrease the differences in attachment surfaces.

Figure 6.3: Gait sensor pad attachment.

6.5 Data Retrieval

For each testing procedure, the same laptop was used for data retrieval while the principal researcher was positioned next to the participant throughout the testing duration. The control box attached to the TTA's belt or pants and was connected to the USB 2 port of a laptop via a 2 m USB data cable. Figure 6.4 displays an example of how the data was retrieved from the device during the testing procedures.

Figure 6.4: Data retrieval during the F8W procedure.

6.6 Experimental Complications

To decrease the interruption between the socket and the limb, 0.2 mm diameter wires were used to connect the thermistor temperature sensors to the control box. However, during the testing procedure of 4L1, the subject pushed their RL into the socket to create suction and suspension and damaged the connection between three of the temperature sensors. Attempts to repair these connections before each subsequent testing procedure were performed, however, this damage appeared to be carried through to the second testing session and induced signal loss in certain areas. Table 6.3 displays the RL areas of the specific interface IDs that were excluded from the study datasets due to loss of signal connection. It must be noted that all other transducer sets within these testing procedures were functioning correctly and produced reliable results, and therefore could be used in the study.

Table 6.3: Interface areas and tests where temperature signal loss was encountered.

INTERFACE ID	RESIDUAL LIMB AREA	TEST
2R2	Popliteal Fossa	SLW, F8W
2L2	Fibula Head, Popliteal Fossa	SLW, F8W
3R2	Popliteal Fossa	F8W
5R1	Popliteal Fossa, Distal Medial Calf	F8W

6.7 Future Methodology Recommendations

The implementation of the experimentation showed good results, however, there were a few complications that arose. Therefore, the following list contains future recommendations for later studies:

- Decrease study time and limit one testing session per subject to mitigate the chance of variables changing during the second testing procedure.
- Increase the study population.
- Create more robust connections between transducer sets and control box.
- Create in-sole gait pads to minimise variability between connection surfaces.

6.8 Conclusions

The implementation of the test procedures and experimental methodologies were successful. Due to interfaces changing for certain subjects on the second testing period the link between testing procedures and interfaces was interrupted. However, the results for each individual test were still valid for specific testing purposes. The addition of new interfaces presented the opportunity to analyse the system's ability to compare pressure and temperature changes between correct and incorrect prosthetic fitment. However, for future studies, more provisions should be made to mitigate the risk of interruptions. Chapter 7 presents the results gathered from the experimental implementation.

7 Experimental Results

7.1 Introduction

This chapter presents the results gathered from the RLES during the SS, SLW and F8W procedures. The experimental results (Chapter 7) and the results analysis and discussion (Chapter 8) follow a structured process displayed in the flowchart of Figure 7.1.

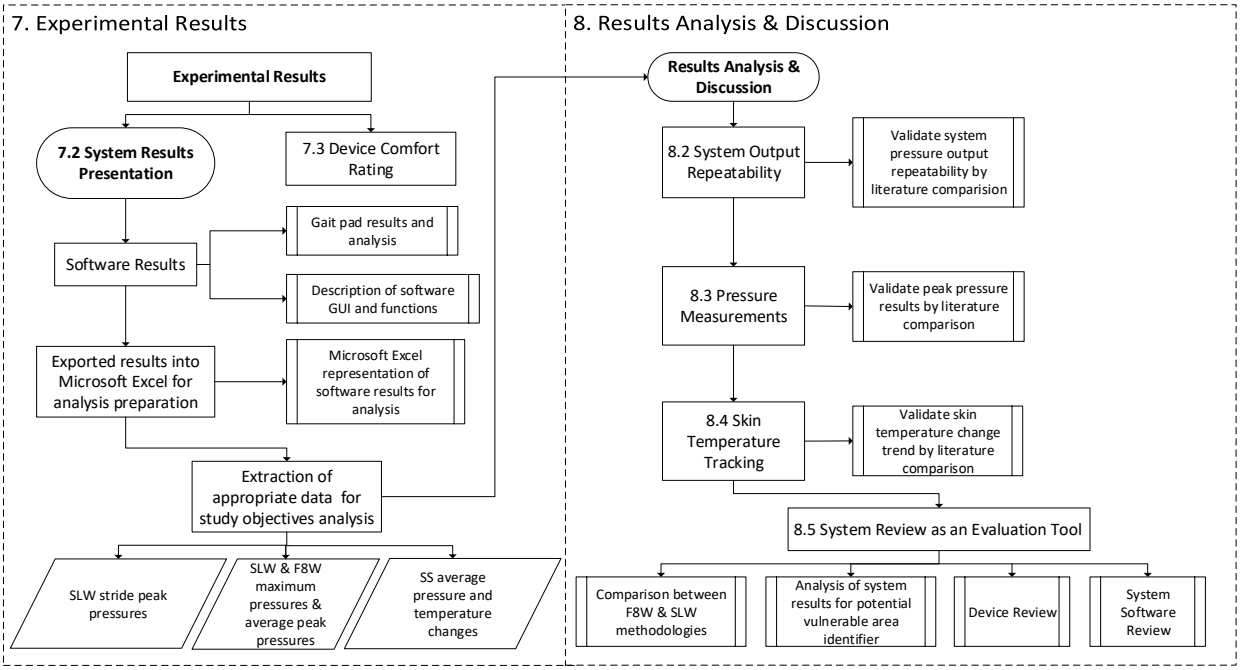

Figure 7.1: Experimental Results and Results Analysis & Discussion Flow Chart.

7.2 System Results Presentation

The RLES gathered all pressure, temperature and gait force data during every test. All data was recorded in multiple text files that are compatible with all data processing systems (Excel, MATLAB, etc). The following section describes how the GUI displays the results, interpretations of the GUI for prosthetic fitting analysis, and the raw data (imported into Excel and MATLAB tables and graphics) obtained from the experimental methodology for analysis in Chapter 8. For illustration purposes, extracts from selected interface datasets were chosen to visually display how the data is received and how it can be represented for each testing procedure.

7.2.1 Areas Analysed

As previously discussed in Section 5.4.1, if a participant presented a skin problem on their RL, the DMC's transducer set would be moved to this area for analysis. Two participants presented a pressure sore in different areas during testing, which introduced two additional areas to be analysed. All areas are discussed in Chapter 7 and 8, and therefore the following list presents the acronyms used for each:

- PT – Patella Tendon
- FH – Fibula Head
- PF – Popliteal Fossa
- DMC – Distal Medial Calf
- ProxTib – Proximal Tibia (Pressure sore present in Interface 3R1)
- DT – Distal Tibia (Pressure sore present in Interface 4L1)

7.2.2 Gait Pad Results

To analyse the efficiency of the gait pads in identifying gait phases, timing, and load transfers, ten strides of gait data from interface 1L1's SLW procedure were averaged and displayed in Figure 7.2

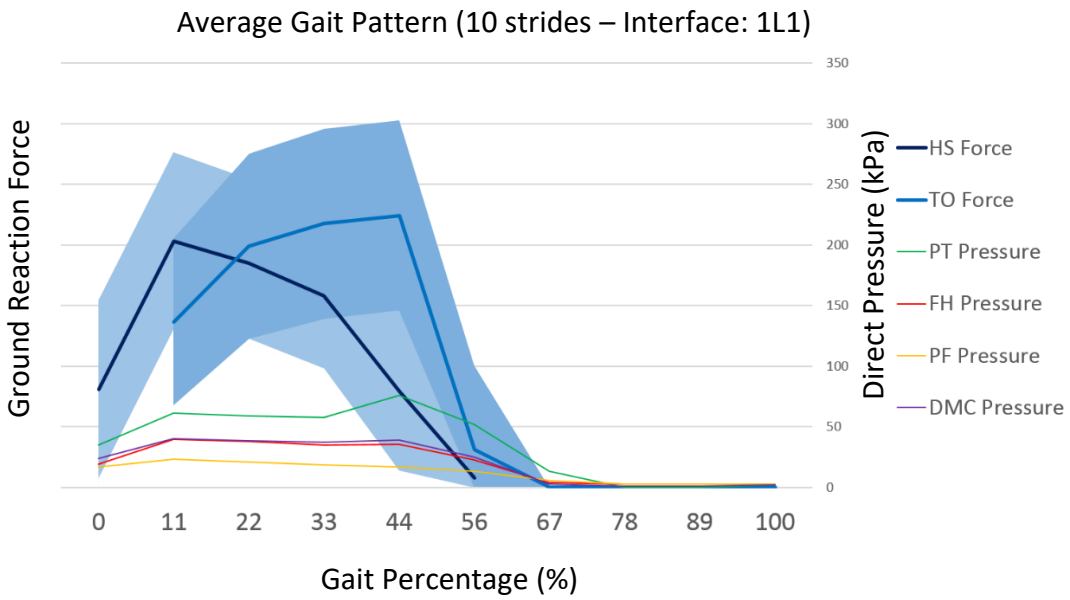

Figure 7.2: System gait cycle results: The gait force representation is created by 2 load sensors placed under the heel and toe of the shoe. These sensors produced the HS (Heel Strike) force and TO (Toe Off) force data respectively. The light and dark blue bands surrounding the HS and TO force curves resemble the standard deviation (over the 10 strides) at each point. The sampling frequency was approximately 10 Hz. PT, FH, PF, and DMC pressure curves indicate how the load transfer throughout the stance phase of gait effects the specific area pressure.

The results show that the GRF data from the gait pads produce a similar pattern to that of a usual TTA's GRF curve and transfer load patterns found in literature (as discussed in Section 2.3.3). However, they highlight that the sampling frequency only retrieves approximately seven samples during the stance phase. The objective of the prototype gait pads was to indicate the timing and phases (heel strike, foot flat, toe off, etc) of gait GRFs. This gait curve approximation was produced successfully since the first and second peaks fall within the respective normal ranges of 10 - 20% and 40 - 50% and the foot flat phase begins at 11% (between 5 - 15%). However, what is most important to evaluate, is whether the system was capable of retrieving an accurate approximation of the interface pressures in each RL area. This evaluation will be performed in Section 8.2 when determining the COV between RL area peak pressures (between strides), since if the sampling rate is too low, the COV will increase due to peak pressure data being missed.

7.2.3 Socket-limb Interface Pressure and Temperature Results

To illustrate the raw data shown to the user from the RLES software and the Excel represented data (used for analysis), Figure 7.3 - 7.7 display extracts from appropriate interface results. Interface 3R1 was chosen to illustrate the results obtained from a walking test since it entailed a vulnerable area identification with a pressure sore present and allowed for the illustration of the software threshold alert function. Interface 1L1 was chosen to illustrate the SS procedure and the system's ability to track skin temperature change. Figure 7.3 and 7.4 displays the raw data presented by the RLES software to the system user and Figure 7.5 displays the Excel representation of the exported data for analysis. The selected sample displayed from the test procedure is 1241 (shown in all figures), at this point it can be seen that the pressures found over the ProxTib area exceeded 100 kPa (the user-defined pressure threshold) and that the bar

representing the related pressure and the pressure sensor 4's position icon (inner circle) has turned red on the GUI. This alerts the user that this specific area threshold has been exceeded and allows the user to view that specific sample while analysing the pressures of all other areas relative to the problem area as well. The position in gait, when the large pressure occurred at the proximal tibia, can also be identified which provides extra information to the user when changing the prosthesis alignment for a potential solution. A pressure sore was present in this area which the RLES identified as vulnerable due to large pressure loads. Therefore, if the RLES was used during the fitting procedure, this pressure sore could have potentially been avoided.

7.2.3.1 Software Pressure and Temperature Results from SLW (Interface 3R1)

Software GUI (All Sensors Panel)

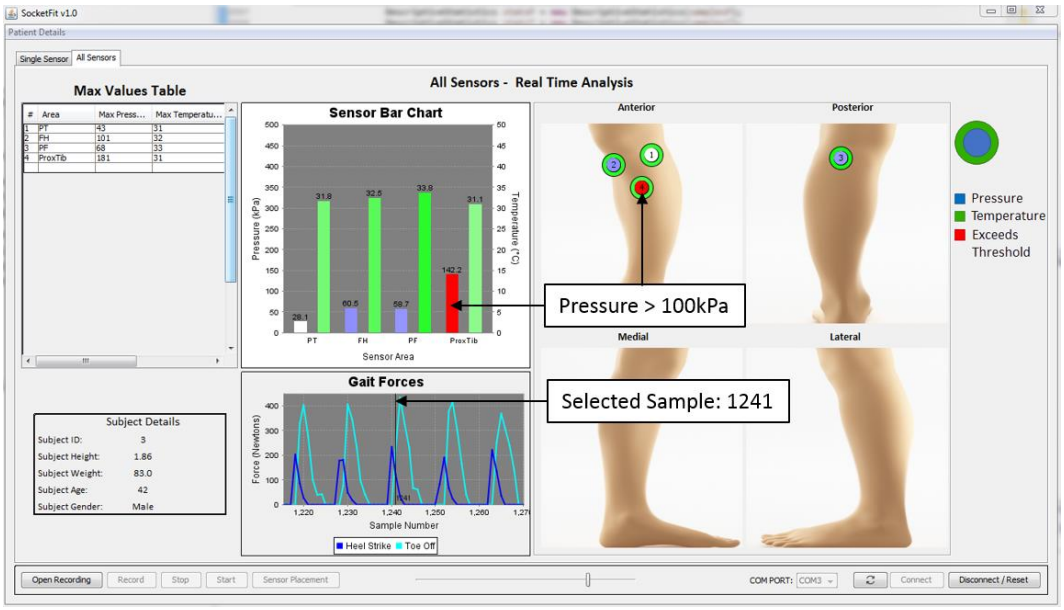

Figure 7.3: Software GUI (All Sensors Panel) of the SLW procedure of interface 3R1. A vulnerable area is identified at the ProxTib area. Software indicates that this pressure occurred during the load transfer between the heel and toe during gait.

Software GUI (Single Sensor Panel)

Figure 7.4: Software GUI (Single Sensor Panel) of the SLW procedure of interface 3R1. Software allows user to analyse the vulnerable area in depth by displaying the pressure in this area during numerous strides and gives statistical information about this area.

Excel Representation

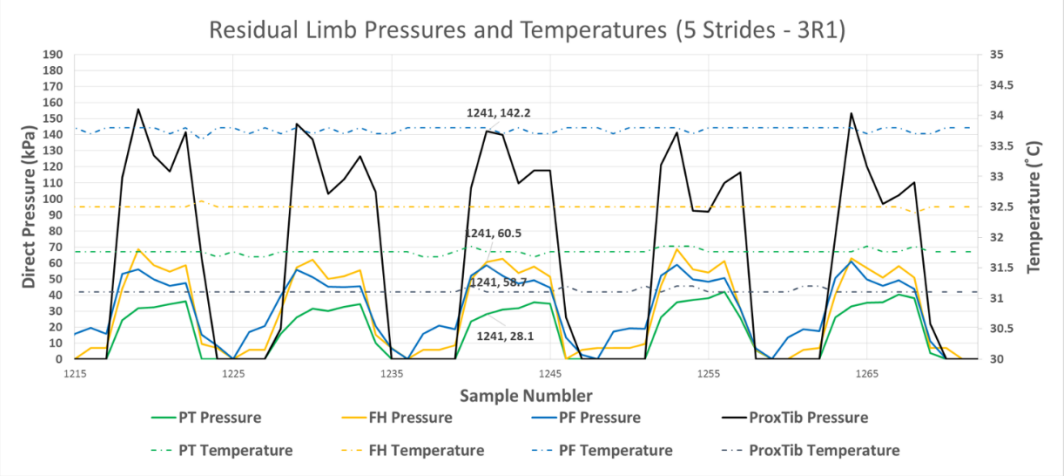

Figure 7.5: Excel representation of the recorded software data from the SLW procedure of interface 3R1. The figure displays the combination of all the software data for interface 3R1 over the samples 1215 – 1270. Each area is represented by a colour where the sold line and dotted line represent direct pressure and temperature respectively. The dynamic loading of each area throughout each stride can be viewed. The selected sample is 1241, and it can be seen that pressures exceeding 100 kPa are present on the ProxTib (pressure sore present) throughout the entire stride, while pressures from other areas never cross this threshold.

7.2.3.2 Software Pressure and Temperature Results from Static Standing Procedure

Figure 7.6 displays how the RLES software allows the user to analyse the skin temperature for specific RL areas. It can be seen that the skin temperature decreases during the standing (static loading) phase and increases during the resting (unloading) phase. Figure 7.7 illustrates the Excel representation of the combined static standing test data extracted from the software for interface 1L1. Currently, the RLES software saves all data as text files in specific folders, but the excel combination needs to be performed manually. Future software iterations will entail an Excel import button which will automatically collect all the data from the testing procedure and create an excel report of the information.

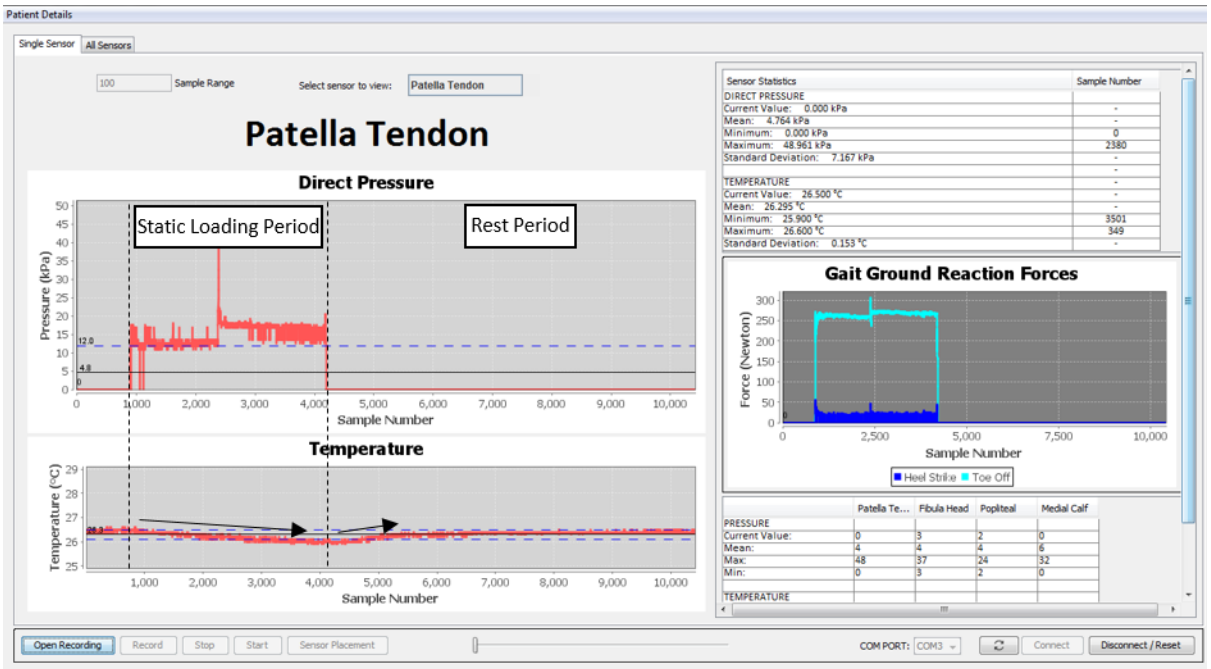

Figure 7.6: Static standing procedure results (Single Sensor Panel) for interface 1L1. The extract displays the system's ability to track the change in temperature of an area due to static pressure. The decrease and increase in skin temperature can be seen during the static loading period and rest period respectively represented by the arrows.

Excel Representation of Software Results

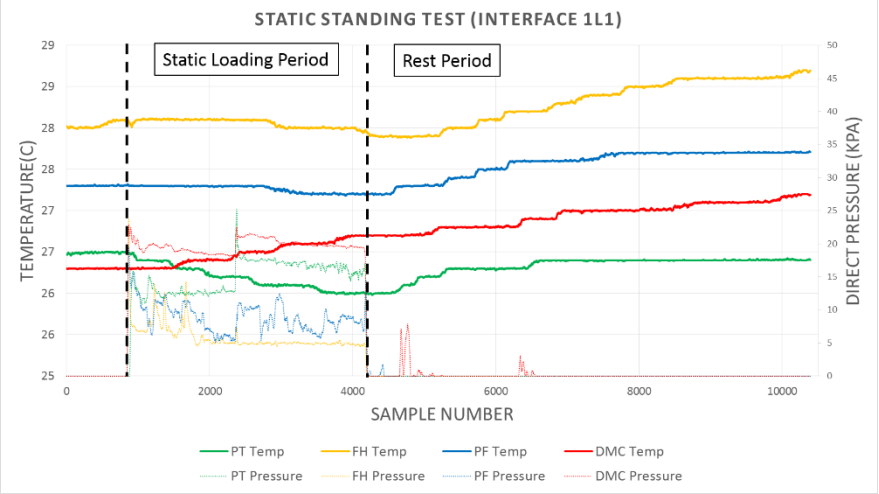

Figure 7.7: Excel representation of SS procedure of interface 1L1.

7.2.4 Results Selection and Summary of Analysis Variables

The RLES presented a large amount of data to analyse, as seen in Figure 7.5 and 7.7, therefore, only the data which can evaluate the project objectives (Section 1.5) were chosen.

7.2.4.1 Results selected for repeatability test

To determine the repeatability of the system, the peak pressure from each stride within the SLW test was chosen since it is a variable that is most likely to be repeated over consecutive strides of similar length and speeds. As discussed in Section 5.4.2.2, the COV was extracted from the results to be validated by literature to indicate the devices ability to produce repeatable results successfully. The programming software, MATLAB, was used to separate strides within the results and identify the peak pressures found over all SLW tests. All SLW peak pressure data can be seen in Appendix D (Section 14.1). Figure 7.8 displays a graphical representation of the peak pressure results of the SLW for interface 1L1.

Straight Line Walk Peak Pressures (Interface 1L1)

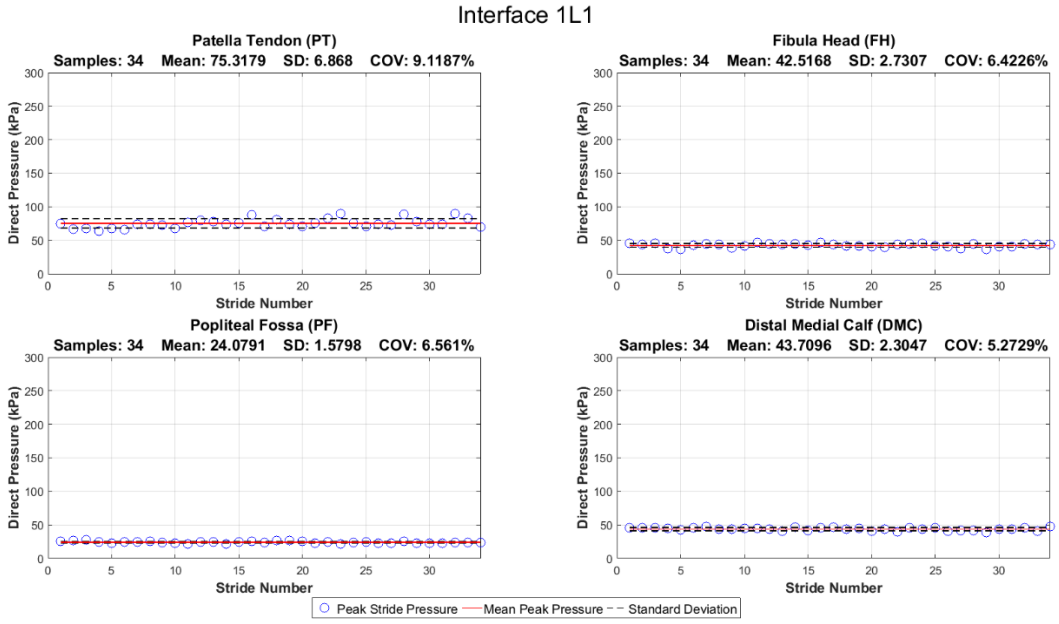

Figure 7.8: Straight Line Walk peak pressures (Interface 1L1). Peak pressures over all residual limb areas are displayed with the mean, standard deviation, and COV. The sample number represents the number of strides analysed.

Prior to data analysis, the normality of all SLW peak pressure datasets was calculated using the IBM SPSS Statistic 24 software which utilises the Shapiro-Wilk normality test method (Shapiro & Wilk, 1965). Normality of a dataset means that each data sample found within the dataset is not significantly different from the other samples within the dataset and is normally distributed around the dataset mean (p-value > 0.05). If a dataset is not normality distributed after the first analysis, outliers were identified and removed and the dataset was tested for normality again. Outlier removal was performed only once, and the samples that were removed are presented in Appendix E (Section 15.2). Table 7.1 displays the peak stride pressure mean, the standard deviation (SD), p-value (p) and the 95% confidence interval (CI) of the mean, calculated with the Statistics 24 software, for all SLW tests over all RL areas.

Table 7.1: Statistical information of all peak pressure SLW datasets.

NORMALITY P VALUES OF ALL PRESSURE SENSORS SUBJECT TO A RANGE OF PRESSURES (KPA)

INTERFACE ID	Strides	PT Mean ± SD (p) (95% CI)	FH Mean ± SD (p) (95% CI)	PF Mean ± SD (p) (95% CI)	DMC/Skin Problem Mean ± SD (p) (95% CI)
Interface 1L1	34	75.32 ± 6.87 (0.063) (72.9 – 77.7)	42.52 ± 2.73 (0.109) (41.5 – 43.5)	24.08 ± 1.58 (0.362) (23.5 – 24.6)	43.71 ± 2.30 (0.338) (42.9 – 44.5)
Interface 2R2	56	28.29 ± 2.27 (0.101) (27.7 – 28.9)	254.38 ± 41.87 (0.000)	25.96 ± 1.27 (0.124) (25.6 – 26.3)	26.0 ± 1.55 (0.126) (25.6 – 26.4)
Interface 2L2	55	48.86 ± 5.16 (0.524) (47.5 – 50.3)	95.87 ± 22.36 (0.006)	21.64 ± 1.16 (0.288) (21.3 – 21.9)	23.14 ± 1.14 (0.669) (22.9 – 23.4)
Interface 3R1*	33	38.0 ± 2.25 (0.607) (37.2 – 38.8)	65.72 ± 3.65 (0.285) (64.4 – 67.0)	60.14 ± 3.37 (0.332) (58.9 – 61.3)	151.35 ± 9.78 (0.071) (147.9 – 154.8)
Interface 3R2	39	23.06 ± 1.27 (0.057) (22.7 – 23.5)	62.69 ± 6.36 (0.200) (60.6 – 64.7)	24.07 ± 0.94 (0.174) (23.8 – 24.3)	103.21 ± 16.39 (0.731) (97.9 – 108.5)
Interface 4L1*	35	N/A	60.05 ± 6.24 (0.100) (57.9 – 62.2)	N/A	138.33 ± 13.83 (0.615) (133.6 – 143.1)
Interface 5R1	34	25.76 ± 3.18 (0.110) (24.7 – 26.9)	229.86 ± 11.86 (0.081) (225.7 – 233.9)	53.78 ± 1.46 (0.059) (53.3 – 54.3)	27.36 ± 1.43 (0.593) (26.9 – 27.9)

*N/A – Not available due to signal loss, * - Pressure sore present in interface.*

The purpose of the SLW was to quantify the repeatability of the RLES output at different pressures by exposing each sensing area to repetitive loads and calculating the mean, standard deviation and COV between strides. Pressures were expected to vary over RL areas due to load distribution and gait variation between interfaces and therefore, each area was to be analysed separately over all strides. Validating the repeatability of RLES results, at different pressure exposures, throughout a sufficient range of pressures, would prove reliability of the results and allow the SLW and F8W results to be compared in Section 8.5.1. The descriptive statistics presented in Table 7.1 for each area allows for the repeatability of the device to be analysed when exposed to different pressures.

Dr Bohland[2] and the Mr Meyer[3] have stated that due to the nature of this study, a power analysis of the sample was not required. A power analysis only applies to a comparative analysis study and only if inferences were made between differences in population means. Therefore, the 95% CI presented in Table 7.1 (generated by SPSS Statistics 24 software), is considered reliable in approximating the range of the true pressure mean in each area.

It must be noted that Interface 4L1 does not have pressure measurements for the PT and PF areas. This is due to incorrect positioning of these transducer sets, which fell in the space between the subject's hypobaric membrane rim (which is used for suction) and the RL. Therefore, no pressure measurements

[2] Dr Florian Bohland (PhD in Finance) of PwC South Africa
[3] Mr Shakeel Meyer of the Statistical Science Department at UCT

were recorded for these areas, however, the FH and the pressure sore area measurements were still valid.

Normality was found for all datasets (p - value > 0.05) except for the FH area of interfaces 2R2 and 2L2. The cause of this was found to be the exceptionally bony prominences of Subject 2's FHs which caused pressure points to be created on the brass pressure plates of each transducer set from the sockets inner surface. The results from these two interfaces were sporadic and 2R2's results exceeded the devices maximum pressure limit (can be seen in Appendix D, Section 14.1,Figure 14.3, Interface 2R2 - FH). Therefore, these two area datasets were removed from the analysis since they were outliers due to anatomical exceptions. A similar behaviour was found at the FH of interface 5R1, however, this was expected since prior to testing, the subject expressed previous problems with pressure in the FH area due to an exceptionally bony prominence. A re-design of the socket had been performed to relieve this pressure point and the peak pressure results obtained from the testing procedures appeared to all fall within the system's measurement capabilities. The results from 2R2, 2L2 and 5R1 highlight a limitation of the device's pressure functionality when exposed to curvature.

7.2.4.2 Results selected for the comparison between different walking tests

As there was no previous research found on TTA's SLI pressures while turning or pivoting, it was assumed that the maximum pressures found and the SD between peak pressures would increase since the movements involved are less repeatable than the SLW. The F8W test was performed in order to induce all natural forward walking movements and angles that a participant could perform. The evaluation of this assumption would identify the system's ability to track natural walking movements. To compare variability between tests, the peak pressures found over both the SLW and F8W procedures (performed sequentially within the same testing session and with no modification to the transducer set placements) were extracted for analysis. Figure 7.9 displays all of the stride peak pressures over all analysed areas found during the F8W test for interface 1L1.

Figure-of-8 Walk Peak Pressures (Interface 1L1)

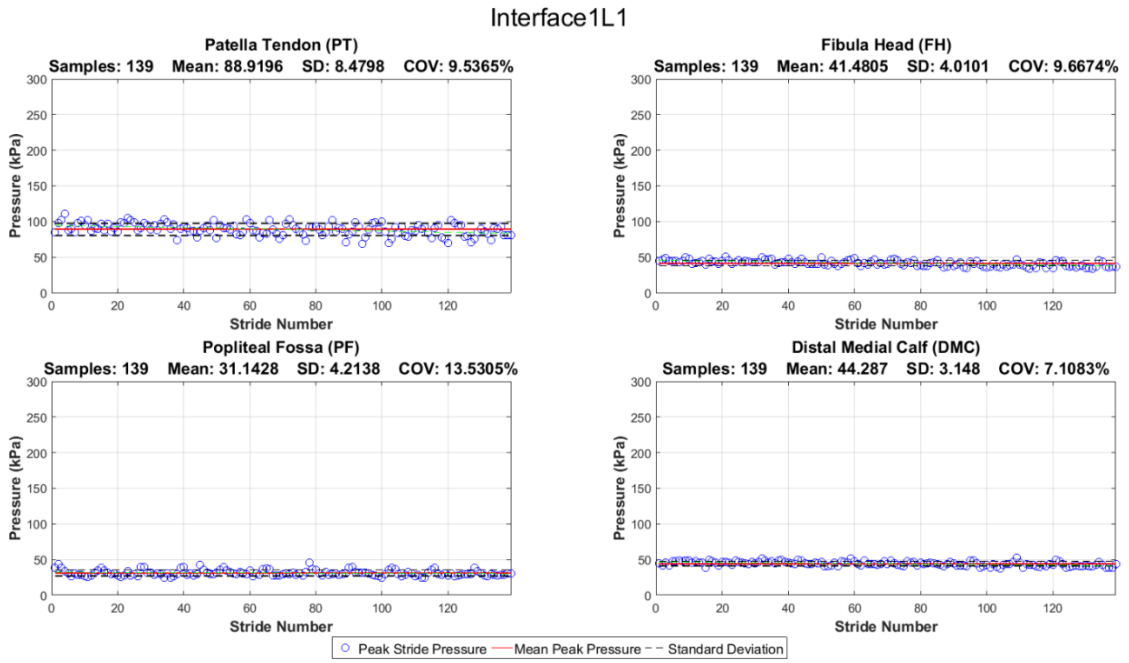

Figure 7.9: Figure-of-8 stride peak pressures (Interface 1L1). Peak pressures over all residual limb areas are displayed with the mean, standard deviations, and COVs. The sample number represents the number of strides analysed.

All comparable interface SLW and F8W peak pressure results can be seen in Appendix D (Section 14.3). However, to illustrate a summary of these results, the average peak pressures and their standard deviations over these SLW and F8W tests have been collected and presented in Figure 7.10 for analysis.

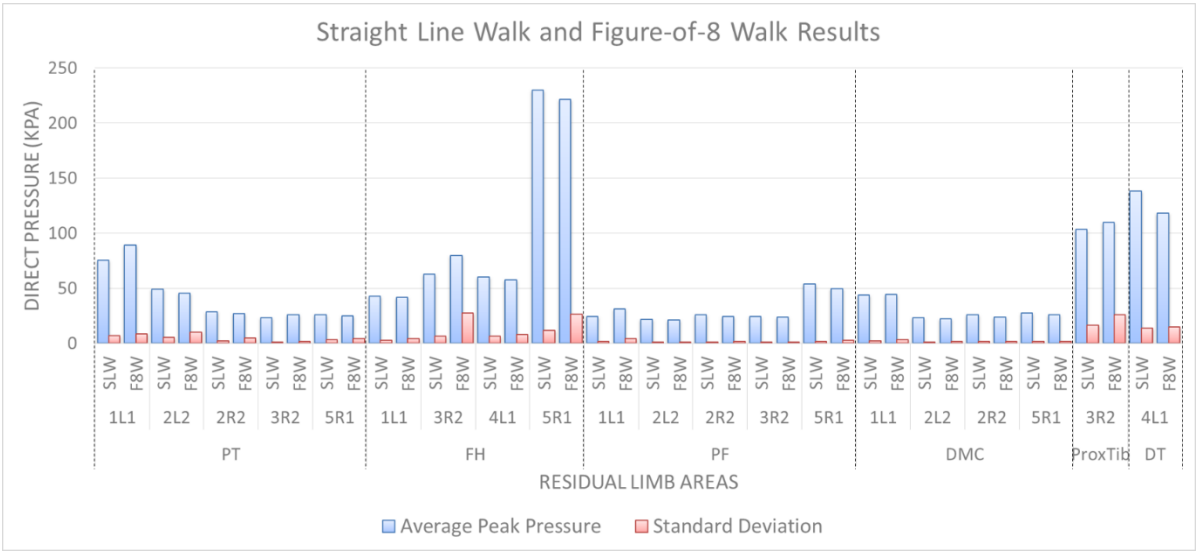

Figure 7.10: Summary of the average peak pressures and standard deviations over all RL areas and interfaces for the SLW and F8W tests. Vertical dashed lines separate each RL area.

To compare maximum pressures found for assumption evaluation, the maximum pressure results over each area and each test are displayed in Figure 7.11.

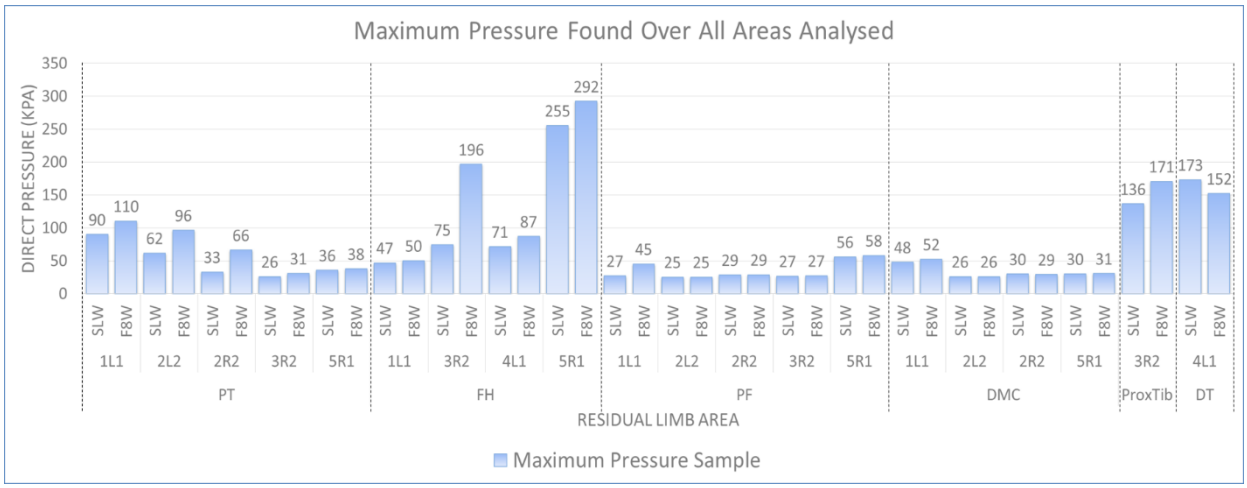

Figure 7.11: Overall maximum pressure found over residual limb areas and interfaces in each SLW and F8W tests. Vertical dashed lines separate each RL area.

In the majority of all RL areas, the F8W produced the largest pressures when compared to the SLW. This satisfies the previous assumption. A more in-depth analysis will be performed in Chapter 8.

7.2.4.3 Results Selected to Evaluate Temperature Change Tracking Under Loading and Unloading

During the development of the device, the temperature sensors were calibrated to within a 1% accuracy error. However, to determine if the design of the transducer set and attachment method efficiently allows the thermistor to measure the area's skin temperature, the trends of temperature change under loading and unloading of the SS test needed to be analysed and compared to literature. It was expected for each skin area to experience a slight increase or decrease in temperature during the loading period and an increase of in temperature during the unloading period (due to reactive hyperaemia).

To evaluate the RLES's skin temperature tracking ability, the temperature changes over the RL areas from the SS procedure results are presented in Table 7.2. For additional analysis, temperature changes over all walking tests are presented in Appendix D (Section 14.4). The SS results show that the temperature in all areas experienced a slight change in temperature due to loading, and on pressure relief, the temperatures increased by an average of 0.48 °C (over all RL areas). This differential temperature change trend has been seen in literature and suggests that the RLES's temperature sensors were able to identify the reactive hyperaemia produced after pressure loading. Validation on this result will be performed in Section 8.4.

Table 7.2: Static Standing Test Results.

STATIC STANDING TEST

Interface (Ambient Temperature)	Area	Average Loading Pressure (kPa)	Temp Before Loading (°C)	Temp After Loading (°C)	Temp Change After Loading (°C)	Temp After Rest (°C)	Temp Change After Rest (°C)	Total Temp Change (°C)
1R1 (22.3 °C)	PT	34.01	26.50	26.49	-0.01	27.10	0.61	0.60
	FH	19.50	27.29	27.40	0.12	28.39	0.98	1.10
	PF	29.55	30.39	30.50	0.11	31.52	1.02	1.13
	DMC	18.20	28.20	28.20	0.00	28.50	0.30	0.30
1L1 (22 °C)	PT	15.06	26.49	26.00	-0.49	26.41	0.41	-0.08
	FH	5.78	28.07	27.95	-0.13	28.69	0.75	0.62
	PF	8.81	27.30	27.20	-0.10	27.71	0.51	0.41
	DMC	19.69	26.30	26.70	0.40	27.19	0.49	0.89
2R1 (22 °C)	PT	5.92	28.30	28.40	0.10	28.70	0.30	0.40
	FH	4.24	27.35	27.61	0.26	27.61	0.00	0.26
	PF	14.70	29.80	30.10	0.30	30.30	0.20	0.50
	DMC	8.95	28.40	28.40	0.00	28.70	0.30	0.30
2L1 (22 °C)	PT	32.26	26.94	27.24	0.30	27.13	-0.11	0.19
	FH	32.64	28.69	28.72	0.03	29.30	0.59	0.62
	PF	20.98	29.11	29.49	0.38	29.49	0.00	0.38
	DMC	14.89	26.31	26.50	0.20	26.31	-0.19	0.01
3R1 (20 °C)	PT	23.27	30.66	29.73	-0.93	31.29	1.56	0.63
	FH	64.16	31.88	31.31	-0.57	32.07	0.76	0.19
	PF	44.27	33.40	33.10	-0.31	33.69	0.60	0.29
	ProxTib*	16.28	30.99	30.41	-0.58	31.03	0.62	0.04
4L1 (21 °C)	PT	28.26	28.21	28.47	0.25	28.39	-0.08	0.17
	FH	17.70	30.00	30.10	0.10	30.03	-0.07	0.03
	PF	2.65	31.20	31.30	0.10	31.80	0.50	0.60
	DT*	36.12	28.10	27.73	-0.37	29.80	2.07	1.70
5R1 (19.4 °C)	FH	28.45	28.41	28.08	-0.33	29.00	0.92	0.59
	PF	28.29	31.01	31.05	0.05	31.68	0.63	0.68
Average		**22.10**			**-0.04**		**0.53**	**0.48**

** - Indicates pressure sore visibly present in area, Temp - Temperature.*

7.3 Comfort Rating of the Device

After all testing procedures were performed each subject was asked to answer the following question related to the comfort of the prototype's transducer sets within their SLI, "How did the measurement device feel during the testing procedure?" The answers they could give were: "comfortable", "tolerable", or "uncomfortable", which were related to the scores of 2, 1 and 0 respectively. The comfort rating given by all subjects was tabulated and presented in Table 7.3.

Table 7.3: Device comfort rating by subjects

SUBJECT ID	ANSWER	SCORE
1	Comfortable	2
2	Comfortable	2
3	Comfortable	2
4	Tolerable	1
5	Tolerable	1
Total		8/10

7.4 Conclusions

Chapter 7 displayed how the RLES software can be used during a fitting procedure and the results that can be extracted from the system. Appropriate data was selected from each testing methodology and presented to evaluate all objectives and criteria of the system. Chapter 8 analyses and evaluates these results and determines if the RLES and its functionality are practical, useful and viable to be used as a prosthetic fitting evaluation tool.

8 Results Analysis and Discussion

8.1 Introduction

The following chapter presents the analysis and discussion of the results obtained in Chapter 7. The analysis evaluated the objectives of the RLES and compared the data produced with results found in similar studies from literature for the validation of its functionality.

8.2 System Output Repeatability

Repeatability is determined by the precision of a transducer's output when exposed to the same input over numerous tests. However, within the SLI the pressures expected in each transducer set area were unknown before testing, therefore, the transducer sets were positioned in specific areas with the highest probability of yielding pressures throughout the normal interface pressure range (0 – 300 kPa). The combined RL area pressure results gathered from the SLW procedures (of all interfaces) resulted in a range of pressures being found from 20 – 230 kPa. Therefore, to display the repeatability of the device over pressures within this range, the mean peak pressures found were sorted from smallest to largest with their SD and COV presented in Table 8.1.

Table 8.1: SLW peak pressures over all areas and interfaces.

INTERFACE	AREA	MEAN PEAK PRESSURE (KPA)	STANDARD DEVIATION (SD) (± KPA)	COV (%)
2L2	PF	21.64	1.16	5.35
3R2	PT	23.06	1.27	5.51
2L2	DMC	23.14	1.14	4.90
3R2	PF	24.07	0.94	3.91
1L1	PF	24.08	1.58	6.56
5R1	PT	25.76	3.18	12.34
2R2	PF	25.96	1.27	4.89
2R2	DMC	26.00	1.55	5.96
5R1	DMC	27.36	1.43	5.21
2R2	PT	28.29	2.27	8.03
3R1	PT	38.03	2.25	5.91
1L1	FH	42.52	2.73	6.42
1L1	DMC	43.71	2.30	5.27
2L2	PT	48.86	5.16	10.56
5R1	PF	53.78	1.46	2.72
4L1	FH	60.05	6.24	10.39
3R1	PF	60.14	3.37	5.60
3R2	FH	62.69	6.36	10.15
3R1	FH	65.72	3.65	5.56
1L1	PT	75.32	6.87	9.12
3R2	ProxTib	103.21	16.39	15.88
4L1	DT*	138.33	13.83	10.00
3R1	ProxTib*	151.35	9.78	6.46
5R1	FH	229.86	11.86	5.16
Average				7.16

*SLW peak pressure statistics sorted by mean peak pressures from smallest to largest. * - Indicates pressure sore visibly present in area.*

These results show that the average COV recorded was 7.16% over the entire range of pressures found. Previous inter-subject interface pressure studies which presented the average peak pressures and COVs for each area (for each subject) have calculated COVs of less than 10% between peak pressures such as Zhang et al. (1998) and Sanders and Daly (1999). These studies found a 8.73% and 6.8% COV using research developed sensory systems which sampled data at 125 Hz and 200 Hz for each study

respectively. Neumann et al. (2005) used the F-Socket™ in SLI pressure measurements on a trans-femoral amputee (above knee amputation) and obtained a COV of 5.4% during a walking study. The mean COV between these systems is 6.94% with an SD of 1.7%. The prototype RLES presented in this study obtained a COV that falls within 1 SD of this literature mean. This validates that the RLES produces repeatable measurements over any stride, therefore, satisfying the repeatability objective of the system. Additionally, this supports the assumption made in Section 4.4 that a sampling rate of 10 Hz is sufficient to produce an accurate approximation of the peak pressures being induced in each area. However, for future iterations of the system a faster sampling rate would increase its efficiency and analysis capabilities.

8.3 Pressure Measurements

Numerous SLI pressure measurement studies have been performed on TTAs, and RL pressure ranges have been found to vary significantly. These results vary due to the multiple uncontrollable variables that take place while walking (discussed in Section 2.5.1.3). Additionally, the RL pressures found are determined by the placement of the sensors which varied between studies. This suggests that the pressure magnitudes found within this study cannot be compared to a defined range approximated from literature for validation. Therefore, the evaluation of the results were performed by comparing pressures found to the expected pressure trend within the RL area for validation.

The study population comprised of unilateral and bilateral TTAs. No study was found that presents SLI pressures on the RL of bilateral amputees. Additionally, the gait characteristics of bilateral amputees have been found to differ from unilateral amputees in walking speeds, kinematic and kinetic data (Su et al., 2007). Therefore, the SLW pressure measurements of only the unilateral amputees were compared with literature. Table 8.2 illustrates the average peak pressures found over the RL areas of the unilateral amputees within this study (all of which utilised PTB sockets in their interfaces). It must be noted that pressure sores were found on interfaces 3R1 and 4L1, and therefore the average peak pressures of these areas were combined.

Table 8.2: Average peak pressures over interfaces which utilized PTB sockets.

RL AREA	PT	FH	PF	DMC	PRESSURE SORE AREAS
PTB (3R1,3R2,4L1,5R1)	28.94	104.58	45.99	27.36	144.84 (3R1*,4L1*)

** - Indicates pressure sore visibly present in interface.*

The largest pressures were found over areas that were experiencing pressure sores which were situated at the proximal tibia (3R1) and the distal tibial (4L1) on the RL anterior. These areas contain subcutaneous bone and are sensitive to pressure which makes them common sites for the development of pressure sores (James, 1991; Levy, 1980). The pressures in these areas exceed the 100 kPa threshold presented by Reswick and Rodgers (1976) and will be evaluated in more detail in Section 8.5.2. Over the healthy RL areas, the largest pressures found were over the FH which was expected due to its bony prominence. The second largest pressures were found over the PF which was expected since other studies, which did not measure the FH pressures, found the largest pressures over the PF area (Goh et al., 2003a; J Sanders et al., 1997; Zhang et al., 1998). Interestingly, the PT area experienced similar but slightly larger pressures than the DMC area. It was expected that due to the nature of the PTB socket design (which generally comprises of a patella tendon bar (Figure 2.4)) this area would experience larger pressures. However, on inspection of the study participant's PTB socket inner surfaces (Appendix C, Section 13.2.2), all sockets did not entail a patella tendon bar. This potentially explains the results since the load is not being

concentrated within the PT area. The DMC experienced the lowest pressures, which was expected, and has been found in most studies (Convery & Buis, 1998; Joan Sanders & Daly, 1993; Shikh et al., 2007; Zhang et al., 1996). The pressure results found in the study correspond with the trends found in literature, and therefore validates that the results received from the RLES are reliable to be used for evaluation.

8.4 Skin Temperature Tracking

The loading and unloading of interface pressures onto skin produces a certain trend in skin temperature change. It is expected that the loaded area's skin temperature should experience a slight change (either a decrease or increase depending on load and underlying soft tissue temperature) during static loading of more than 10 kPa, and on load relief reactive hyperaemia would produce a noticeable increase in skin temperature above its initial value by increasing blood flow (Barnett & Ablarde, 1995; Pye & Bowker, 1976). The SS procedure was performed to simulate this skin temperature change and evaluate the system's ability to track it. Excluding the interfaces with pressure sores, the SS procedure results have been gathered from Section 7.2.4.3 and displayed in Figure 8.1 for literature comparison.

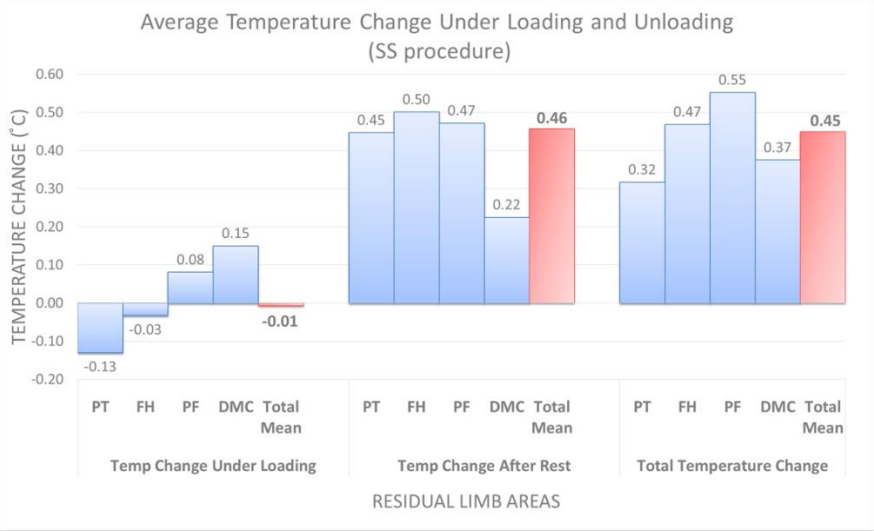

Figure 8.1: Average temperature change under loading and unloading (SS results).

The temperature change under loading (Figure 8.1) indicates that areas which are more vascular and comprise of more muscle volume, such as the PF and DMC, tend to experience a slight increase in temperature, whereas the areas with less subcutaneous soft tissue volume, such as the PT and FH, experience a slight decrease in temperature. This result corresponds with a study by Pye and Bowker (1976), who found that the distance between the skin surface and the warmer tissues nearer the central blood core plays an important role in determining skin temperature. The PT and FH are bony anatomical sites which have smaller soft tissue volumes than the PF and DMC, therefore, when exposed to interface pressures, the constriction of skin blood vessels have a more significant effect on the skin temperature change. When the PF and DMC areas are exposed to interface pressures, the distance between the skin surface and the underlying muscle mass (calf muscle) or vascular network (popliteal artery and vein) decreases and these warm tissues start to increase the skin temperature slightly.

After the static standing load was released by sitting on a chair, a common reaction over all areas was noticed whereby the skin temperature rose due to reactive hyperaemia throughout the ten minutes of rest. The average total temperature change due to the reactive hyperaemia, after loading-induced ischemia, was +0.45 °C. A similar increase was found in a study conducted by Sanders (Joan E Sanders, 2000) who performed a similar research methodology. This study investigated the skin temperature change due to reactive hyperaemia (after 5 min after loading) on the anterior aspect of the tibia of a TTA

and found a temperature increase of 0.34 °C. Investigations on other parts of the body have been performed by researchers such as Wong et al. (Wong, Stotts, Hopf, Dowling, & Froelicher, 2010) who found a 0.76 °C increase at the heel (in 18 subjects), and Schubert et al. (1991) who found a 0.46 °C increase at the sacrum (in 9 subjects) due to reactive hyperaemia. Therefore, the SS results corresponds with existing research. Additionally, the total temperature change throughout the walking procedures was tabulated in Table 14.2 (Appendix D, Section 14.4) for interfaces which performed both the SLW and F8W sequentially. However, the total walking time varied slightly between each subject (due to their capabilities) with an average of 5.4 minutes. This walking duration produced an average temperature increase of 1.14 °C over all RL areas which corresponds to the results of a five minute walk in a similar ambient temperature of 20 °C obtained from a study by Mathur et al. (2016). These results indicate that the temperature sensors of each transducer set had sufficient contact with the RL area's skin for measurement and tracking of the temperature change under pressures.

8.5 System Review as an Evaluation Tool

Sections 8.2 - 8.4 verified that the RLES could successfully measure the pressure and temperatures on the RL within the SLI. Sections 8.5.1 and 8.5.2 analyse the capabilities of the system as an evaluation tool by comparing results from the standard SLW methodology to a more real-life movement such as the F8W as well as identifying variables and trends for possible vulnerable area identification.

8.5.1 The Comparison of Peak Pressures between the SLW and F8W Procedures

The mean peak pressure and maximum peak pressure results from both the F8W and SLW procedures were presented in Section 7.2.4.2 (Figure 7.10 and Figure 7.11). The assumption is that the F8W methodology would produce larger maximum pressures on RL areas (due to pivoting and turning against the momentum of walking) that would be missed if only focusing on a standard SLW. To evaluate this assumption Figure 8.2 presents the change in the maximum pressure from SLW to F8W.

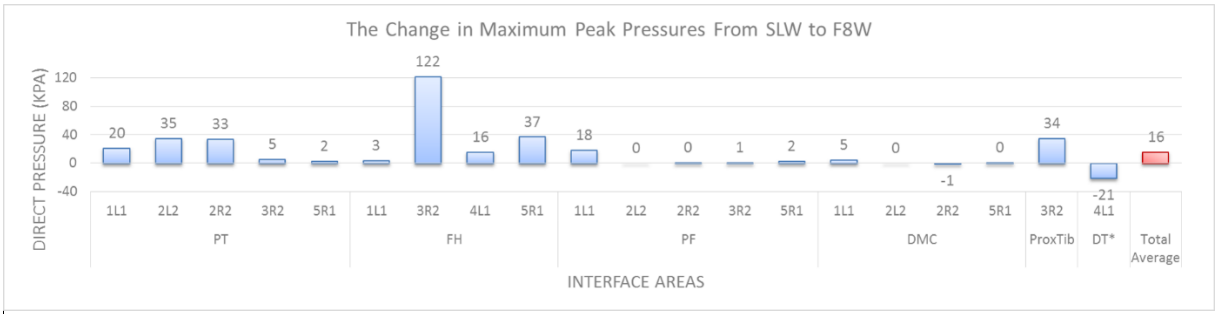

Figure 8.2: The change in the maximum peak pressures found between the SLW and F8W (F8W – SLW).

The average maximum pressure increase is approximately 16 kPa over all areas (18 kPa excluding DT*), however, in the FH area of 3R2 the maximum pressure difference was 122 kPa. These high pressures found during the natural walking movement (F8W) of the TTA cannot be found by SLW methodology alone. Interestingly, the only area which experienced significantly lower pressures during F8W than during the SLW was the DT of interface 4L1, which was an area that was experiencing a pressure sore. To investigate this further, the change in the maximum pressures, average peak pressures and standard deviations from SLW to F8W were tabulated for all interfaces from Table 14.1 (Appendix D). Due to the size of the datasets, for illustration purposes, only the percentage (%) pressure change from SLW to F8W results will be shown. These were calculated as the percentage differential change in pressures from SLW results to F8W results using equation 9:

$$\%Change = \left(\frac{F8W - SLW}{SLW}\right) \times 100 \quad [9]$$

The results are shown in Table 8.3 with each area's total average percentage change illustrated in Figure 8.3.

Table 8.3: Pressure Measurement Percentage (%) Difference (From SLW to F8W).

RESIDUAL LIMB AREA	INTERFACE	MAX PRESSURE % CHANGE [SLW, F8W]	AVERAGE PEAK PRESSURE % CHANGE [SLW, F8W]	SD % CHANGE [SLW, F8W]
PT	1L1	22.7 [90,110]	18.1 [75.3,88.9]	23.5 [6.9,8.5]
	2R2	101.1 [33,66.4]	-4.9 [28.3,26.9]	113.5 [2.3,4.8]
	2L2	56.0 [61.8,96.5]	-7.3 [48.9,45.3]	97.6 [5.2,10.2]
	3R2	19.0 [25.9,30.8]	12.9 [23.1,26]	37.8 [1.3,1.8]
	5R1	5.9 [35.7,37.8]	-3.3 [25.8,24.9]	33.4 [3.2,4.2]
	Average	**40.9**	**3.1**	**61.2**
FH	1L1	7.4 [46.8,50.3]	-2.4 [42.5,41.5]	46.9 [2.7,4.0]
	3R2	163.4 [74.6,196.4]	27.4 [62.7,79.9]	335.2 [6.4,27.7]
	4L1	21.9 [71.5,87.1]	-4.3 [60,57.5]	24.2 [6.2,7.7]
	5R1	14.4 [255.4,292.2]	-3.8 [229.9,221.2]	123.1 [11.9,26.5]
	Average	**51.8**	**4.2**	**132.3**
PF	1L1	67.2 [27.1,45.3]	29.3 [24.1,31.1]	166.7 [1.6,4.2]
	2R2	1.0 [28.6,28.9]	-7.0 [26,24.1]	17.1 [1.3,1.5]
	2L2	0.0 [25.3,25.3]	-2.2 [21.6,21.2]	8.9 [1.2,1.3]
	3R2	2.2 [26.8,27.4]	-0.6 [24.1,23.9]	42.7 [0.9,1.3]
	5R1	3.7 [56,58.1]	-7.9 [53.8,49.5]	81.5 [1.5,2.7]
	Average	**14.8**	**2.3**	**63.4**
DMC	1L1	9.6 [47.8,52.4]	1.3 [43.7,44.3]	36.6 [2.3,3.1]
	2R2	-2.6 [29.8,29]	-9.1 [26,23.6]	14.2 [1.5,1.8]
	2L2	0.0 [26,26]	-3.6 [23.1,22.3]	29.6 [1.1,1.5]
	5R1	1.3 [30.2,30.6]	-5.4 [27.4,25.9]	8 [1.4,1.5]
	Average	**2.1**	**-4.2**	**22.1**
DT*	4L1	**-12.2** [173.2,152.1]	**-14.7** [138.3,118]	**6.9** [13.8,14.8]
ProxTib	3R2	**25.0** [136.4,170.5]	**6.4** [103.2,109.8]	**58.5** [16.4,26]
Total Average		**20.4**	**-0.5**	**57.4**
Total Average (Excluding DT)		**26.9**	**2.4**	**67.5**

** - Indicates pressure sore visibly present in area. Values within the square brackets represent the pressure (kPa) results from the SLW and F8W procedures.*

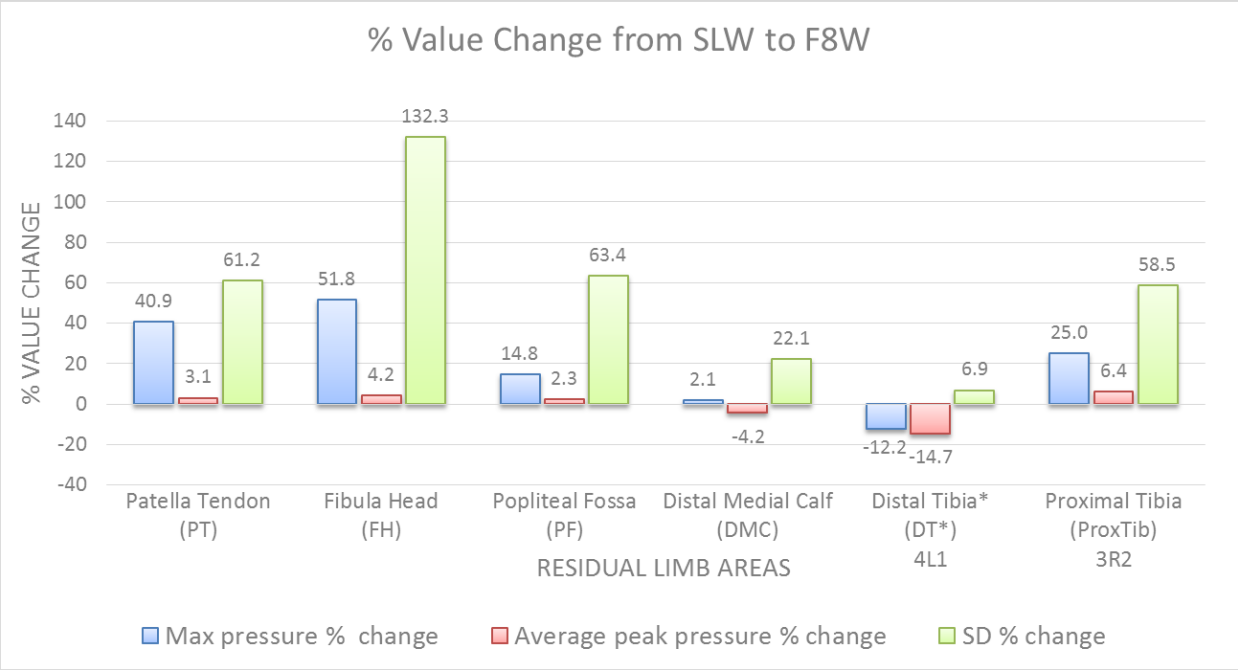

Figure 8.3: Total averaged percentage (%) direct pressure change from the SLW results to the F8W results for all subjects and areas.

These results support the assumption showing that there was an increase in the maximum peak pressure (26.9% increase) and SD (67.5% increase) in all areas excluding the DT* of interface 4L1. Interestingly it was found that at the DT* of Interface 4L1, the percentage SD change was the smallest of all tests with a value of 6.9% and both the maximum and mean peak pressure decreased by 12.2% and 14.7% respectively. The 12.2% decrease in maximum peak pressure suggests that during straight line walking, which is the most common movement, this area endures the largest pressures. Additionally, the average 67.5% SD increase over all other (healthy) areas suggests that there exists some relief between stride peak pressures during some movements. However, the DT* area (interface 4L1) had the smallest percentage SD change suggesting that these large pressures are consistently endured during any walking movement without relief. This potentially highlights a reason for the pressure sore development. Therefore, the method of comparing SLW to F8W walking pressures could potentially form an additional method of identifying areas that are vulnerable to future pressure sores, however, additional studies would be required.

The increase in maximum peak pressures and peak SDs, support the assumptions made and potentially validates the RLES's ability to track any natural movements performed by the TTA while wearing the device. This increases the potential of the system since the RL can be analysed during desired movements required by the amputee, such as specific sporting movements, which could improve the tailoring of the socket design for the specific TTA's needs.

8.5.2 Potential Vulnerable Area Identifiers.

In Section 2.5.1.2 the Reswick and Rogers Pressure-Time Curve (Figure 2.11) was discussed which illustrates a safe interface pressure threshold to avoid pressure sores. This curve indicates that surface pressures above 100 kPa are potentially dangerous which has been used as a threshold in previous TTA interface pressure measurement studies (Convery & Buis, 1998). Therefore, during the SLW and F8W procedures, the user-defined pressure threshold was set to 100 kPa to produce an alert if an area's pressure exceeded this value. All areas which produced an alert were tabulated for analysis in Table 8.4.

Table 8.4: Interface areas found with maximum pressures greater than 100 kPa.

PRESSURES FOUND ABOVE 100 KPA

STRAIGHT LINE WALK > 100 KPA							
INTERFACE	**Area**	**Max Pressure Found (kPa)**	**Average Peak Pressure (kPa)**	**SD (kPa)**	**%SD**	**Temperature Change (°C)**	**Pressure Sore (Y/N)**
3R1	**ProxTib***	**174**	**151.3**	**9.8**	**6.5**	**0.1**	**Y**
3R2	ProxTib	136.4	103.2	16.4	15.9	0.4	N
4L1	**DT***	**173.2**	**138.3**	**13.8**	**10**	**0.3**	**Y**
5R1	FH	255.4	229.9	11.9	5.2	0.7	N
FIGURE 8 > 100 KPA							
INTERFACE	**Area**	**Max Pressure Found (kPa)**	**Average Peak Pressure (kPa)**	**SD (kPa)**	**%SD**	**Temperature Change (°C)**	**Pressure Sore (Y/N)**
1L1	PT	110.4	88.9	8.5	9.6	0.6	N
3R2	FH	196.4	79.9	27.7	34.7	0.7	N
3R2	ProxTib	170.5	109.8	26	23.7	0.7	N
4L1	**DT***	**152.1**	**118**	**14.8**	**12.5**	**0**	**Y**
5R1	FH	292.2	221.2	26.5	12	1	N

** - Indicates pressure sore visibly present in area.*

These results show that the area that experienced the highest pressure was the FH of interface 5R1. This area was not experiencing any skin problems, however, as discussed in Section 7.2.4.1, the subject did express that, prior to testing, problems were faced with high pressures falling on the FH area. Additionally, this subject felt a slight pressure sensation in FH area due to the transducer set. Therefore,

this large pressure reading was expect due to the bony protrusion in the area. With the exclusion of the FH area of interface 5R1, the areas that were enduring average peak pressures greater than 100 kPa were all experiencing or had experienced a pressure sore. The interface areas that were experiencing a pressure sore at the time of testing are each enclosed in a border in Table 8.4. As discussed in Section 6.2.3 interface 3R1 presented a pressure sore on the ProxTib* area during the first testing period, and by the second testing session, the interface was modified (3R2) to relieve this area from pressure. The pressure relief from this modification can be seen in Table 8.4 (SLW results) where the maximum and mean peak pressure decreased by 37.6 kPa and 48.1 kPa respectively in 3R2. Even though the mean peak pressure was still slightly above 100 kPa (103 kPa) the pressure relief was enough to heal the area suggesting that the mean peak pressure threshold for this specific area (of Subject 3) lies between 103.2 kPa and 151.3 kPa. Additionally, the percentage SD increased from 6.5 to 15.9 and the change in temperature increased from 0.1 °C to 0.4 °C suggesting that there was a greater change in peak pressures from stride to stride offering slight relief to that area which could help with regaining efficient blood flow.

The last area whose average peak pressure exceeded 100 kPa was the DT* of interface 4L1 which was also experiencing a pressure sore. The pressure change between SLW and F8W in the area was discussed in Section 8.5.1, however, an additional interesting observation can be seen between the temperature change of the skin problem areas (4L1 DT* and 3R1 ProxTib*) and the healthy areas. The skin problem areas recorded the lowest temperature change over any walking procedure. The DT* of interface 4L1 experienced a large temperature increase during the SS procedure (+1.7 °C), this could potentially be due to the inflammation that was present around the pressure sore (seen in Figure 13.7 of Appendix C) which could have caused the initially large temperature increase. However, this reaction was not noticed in any other interface area. The ProxTib* of 3R1 did not have any inflammation around the pressure sore area (seen in Figure 13.8 of Appendix C) and only experienced a temperature increase of 0.04 °C in the SS test and a 0.1 °C increase in the SLW test which is very small and does not correspond with temperature changes of healthy skin areas found in literature (discussed in Section 8.4). A potential reason for this was found through research performed on thermal responses of skin to applied pressure by Mahanty and Roemer (1979) who found that damaged tissue does not exhibit the normal temperature increase characteristic during reactive hyperaemia. This suggests that a small change in skin area temperature after a walking methodology may potentially indicate damaged tissue which could be identified using the RLES software. A comparison between the ProxTib* area of 3R1 and follow-up interface 3R2, shows that in 3R2 there is a difference of 0.3 °C in the SLW results. The temperature change at the ProxTib area in 3R2 continues to increase by 0.7 °C in the F8W. This suggests that the pressure was compromising the blood flow to the ProxTib* area in 3R1 and the pressure relief in 3R2 corrected this problem. This compromised blood flow in 3R1 could potentially have been identified by using the RLES before a pressure sore developed.

The results suggest that pressure above 100 kPa can be used as a valid indicator of vulnerable areas, however, it is still unclear if skin temperature change is an appropriate indicator of pressure sore development. Additional studies are needed to be performed on the temperature measurement of the RL to determine skin temperature trends and values which indicate vulnerability to all skin problem types.

8.5.3 Overall Device Review

The results presented in Section 7.3 indicate the level of comfort experienced by the participants wearing the device's transducer sets on their RL in the SLI. The results show that three of the five subjects felt the device was comfortable and the remaining two felt it was tolerable but not uncomfortable.

The device functioned as intended and provided reliable and repeatable pressure and temperature measurements. It was concluded that the transducer set design allowed the temperature sensors to have sufficient contact with the skin for temperature tracking and that the 3D printed base, layer of spongy tape and brass pressure plate attached to the TekScan® A201 pressure sensors allowed for efficient pressure measurements. However, it was found that the pressure transducer design was still sensitive to sharp curvatures and in some RL areas, too thick and caused slight pressure points in the SLI. These design issues need to be solved in future design iterations. The control box, enclosing the circuitry, and the cables connecting the transducer sets, did not cause any discomfort to the amputee, however, tensions placed on the cables while the amputees donned their socket and while walking caused some connections to be damaged which had to be repaired continually. Therefore, future iterations should investigate wireless (Bluetooth, etc) pressure and temperature sensors for communication with the control box. The prototype device functioned efficiently to prove its purpose. However, many upgrades would still need to be implemented before the final product is produced.

8.5.4 Software Review

The prototype software performed successfully and efficiently as an evaluation tool for prosthetic fitting. It provided functions such as: registering the participant on the system; selecting areas for analysis; real-time pressure and temperature value displays in each area; real-time toe-off and heel-strike GRFs; the recording and playback of the prosthetic fitting procedure; real-time statistics of each area; and allowed for the export of data into Excel and MATLAB which was used for the results presentation and analysis of this study. The limitation of the software was the allowable sampling frequency which was limited at 10 Hz, however, code optimisation can increase this frequency. Future iterations of the device and software should entail a sock/sleeve of with a matrix of embedded transducer sets to produce a full pressure and temperature map of the amputee's RL for analysis.

8.6 Conclusions

The RLES performed satisfactorily and was able to produce a reliable evaluation of the amputee's RL within the socket and liner. The results satisfied all objectives and proved the practicality of the use of a RLES within the prosthetic fitting procedure. However, numerous limitations need to be improved in future iterations.

9 Conclusions and Recommendations

The presented study highlighted that there is a high prevalence of skin problems found on the RLs of amputees caused by an incorrect prosthetic socket fitment, prosthetic component selection or prosthesis alignment. This problem is due to the nature of the prosthetic fitting procedure being a completely empirical process and depends solely on the expertise and experience of the prosthetist. Thorough research was focused on the development of these skin problems and current solutions available, to find a solution. It was found that current commercially available products only analyse direct pressures on the RL. This neglects the importance of skin temperature and gait analysis, and entails software which is not tailored for the prosthetic fitting procedure. Therefore, the presented study aimed to design, develop and experimentally validate a novel RLES to potentially be used within the prosthetic fitting procedure. This system was required to accurately and reliably measure the pressures and temperatures on the RL of a TTA, produce gait phase data, present all data in real-time via a developed and tailored software, and identify potentially vulnerable areas.

The RLES presented in this study completed all device, software and research objectives (presented in Section 1.5) to meet this aim. This chapter discusses the conclusions of the objectives and presents recommendations for future work of this nature.

9.1 Conclusions

A thorough evaluation was performed during the design phase of the system to select the most efficient and appropriate sensors for the application. Design considerations were taken into account to provide for the variability of the amputee and ensure safety. The software was designed for ease of use, and each function was tailored to provide efficient and appropriate RL evaluation capabilities. The developed device comprised of transducer sets which when attached were deemed tolerable within the SLI by the participants of the study. The length of the transducer set cables was adjustable which provided for all RL dimensions and the control box was lightweight, did not provide any obstruction, and attached efficiently to the amputee. The developed system software met all the required objectives (Section 1.5.1) and allowed for the efficient analysis, recording and playback of the real-time RL pressure and temperature data as well as the timing and phases of the related gait GRFs. Additionally, the pressure and temperature transducers produced accuracy and repeatability errors of less than 10% during calibrations. The developed system met all design objectives as well as provided the necessary functions to perform an efficient RL evaluation.

The RLES was experimentally evaluated by attaching the transducer sets to RL areas on TTAs and analysing its efficiency and practicality by completing the research objectives (Section 1.5.2). A literature comparison validated the reliability of the pressure and temperature readings, since the COV between peak pressures (over numerous strides) fell within a COV range found in previous studies. The RLES proved that it could efficiently track skin temperature by producing an expected skin temperature change trend under loading and unloading found in literature. The RLES system was then used to perform a novel comparison test between the SLW and F8W methodologies and found that it was capable of tracking the natural movements of the TTA, and highlighted the potential importance of the F8W procedure in the evaluation of a prosthetic fitment. Additionally, it was able to identify areas of vulnerability by reporting large pressures over all areas which presented pressure sores.

In conclusion, the design development and evaluation of the prototype RLES was successful and confirms the hypothesis that a tactile RLES and recording software can provide reliable SLI information which can

be used to identify vulnerable areas on the RL induced by the socket during the natural gait movements of TTAs.

9.2 Recommendations

The aim of the presented study was met, however, the following section presents recommendations to improve all aspects of the system and its testing methodology.

9.2.1 System Design

- Each transducer set comprised of an ABS base plate, a layer of spongy tape, and a brass force plate to compensate for curvature within the SLI. However, this setup created a pressure point over the fibula head within Interface 2L2 and 2R2 which causes sporadic results. An alternative transducer set structure should be investigated, which could provide reduced thickness and a more stable pressure measurement over bony prominences of sharp curvatures.
- The number of transducer sets could be increased to increase the resolution of the RL area analysis. Multiplexers could be used to increase the number of analogue signal inputs that are capable of the microcontroller which then would need to be accommodated for within the software code.
- The GUI could be updated to include a 3D model of the RL with a pressure and temperature mapping overlay. This would require an increased resolution of areas analysed.

9.2.2 Experimental Methodology

- Complications were encountered when testing participants over two separate days. The methodology could be changed to focus on a single procedure, or the device attachment method could be improved which would decrease the preparation time before procedures.
- For future works, the RLES could be used by a skilled prosthetist to compare the results between a poorly fitting and a correct fitting prosthetic socket to determine the efficiency of the results within the fitting procedure.
- Most studies do not perform SLI pressure measurements during a figure-of-8 walking method. The presented study found interesting results when comparing the SLW data to the F8W data and suggested that this comparison may be an efficient fitment evaluation method that can be used within the fitment procedure. Future studies could be performed investigating this evaluation method.
- Future iterations would require a larger study population to draw statistic validation and analysis of the RLES function.

10 References

Akers, W., & Sulzberger, M. (1972). The friction blister. *Plastic & Reconstructive Surgery*, *50*(1), 98.

Al-Fakih, E. A., Abu Osman, N. A., & Mahmad Adikan, F. R. (2016). Techniques for interface stress measurements within prosthetic sockets of transtibial amputees: A review of the past 50 years of research. *Sensors (Switzerland)*, *16*(7). https://doi.org/10.3390/s16071119

Al-Fakih, E., Abu Osman, N. A., Mahamd Adikan, F. R., Eshraghi, A., & Jahanshahi, P. (2016). Development and Validation of Fiber Bragg Grating Sensing Pad for Interface Pressure Measurements Within Prosthetic Sockets. *IEEE Sensors Journal*, *16*(4), 965–974. https://doi.org/10.1109/JSEN.2015.2495323

Al-Fakih, E., Osman, N. A. A., Eshraghi, A., & Adikan, F. R. M. (2013). The capability of fiber Bragg grating sensors to measure amputees trans-tibial stump/socket interface pressures. *Sensors (Switzerland)*, *13*(8), 10348–10357. https://doi.org/10.3390/s130810348

Ali, S., Abu Osman, N. A., Eshraghi, A., Gholizadeh, H., Abd Razak, N. A. Bin, & Wan Abas, W. A. B. Bin. (2013). Interface pressure in transtibial socket during ascent and descent on stairs and its effect on patient satisfaction. *Clinical Biomechanics*, *28*(9–10), 994–999. https://doi.org/10.1016/j.clinbiomech.2013.09.004

Ali, S., Osman, N. A. A., Mortaza, N., Eshraghi, A., Gholizadeh, H., & Wan Abas, W. A. B. Bin. (2012). Clinical investigation of the interface pressure in the trans-tibial socket with Dermo and Seal-In X5 liner during walking and their effect on patient satisfaction. *Clinical Biomechanics*, *27*(9), 943–948. https://doi.org/10.1016/j.clinbiomech.2012.06.004

Amputee Coalition. (2016). Limb Loss Statistics - Amputee Coalition. Retrieved January 14, 2018, from https://www.amputee-coalition.org/limb-loss-resource-center/resources-filtered/resources-by-topic/limb-loss-statistics/limb-loss-statistics/

Appoldt, F., Bennet, L., & Renato, C. (1968). Stump-socket pressure in lower extremity prostheses. *Jounal of Biomechanics*, *1*(4), 247–257. Retrieved from https://www.sciencedirect.com/science/article/pii/0021929068900201

Appoldt, F., Bennett, L., & Contini, R. (1969). Socket Pressure as a Function of Pressure Transducer Protusion. *Bulletin of Prosthetics Research*, *10*(11), 236–249.

Arduino. (2015). Arduino Mega. Retrieved January 1, 2017, from https://www.arduino.cc/en/Tutorial/AnalogWriteMega

Artificial Limb. (2006). Artificial Limb. Retrieved from http://www.madehow.com/Volume-1/Artificial-Limb.html

Bader, D. L. (1990). The recovery characteristics of soft tissues following repeated loading. *Journal of Rehabilitation Research & Development.*, *27*(2), 141. https://doi.org/10.1682/JRRD.1990.04.0141

Bar, C. A. (1991). Evaluation of cushions using dynamic pressure measurement. *Prosthetics and Orthotics International*, *15*(3), 232–240.

Barnard, S. (2017). Amputations. Retrieved from http://slideplayer.com/slide/12347270/

Barnett, R., & Ablarde, J. (1995). Skin vascular reaction to short durations of normal seating. *Archives of Physical Medicine and Rehabilitation*, *76*(6), 533–540. https://doi.org/10.1016/S0003-9993(95)80507-9

Beil, T., Street, G., & Covey, S. (2002). Interface pressures during ambulation using suction and vacuum-assisted prosthetic sockets. *Journal of Rehabilitation Research and Development*, *39*(6), 693–700.

Berger, N. (2010). Analysis of Amputee Gait. *Atlas of Limb Prosthetics: Surgical, Prosthetic, and Rehabilitation Principles*, (1), 2–12.

Biometrics. (2017). Prosthetic Process. Retrieved from http://biometricsct.com/prosthetic-limbs-and-

braces/prosthetic-process/

Boone, D., Kobayashi, T., Chou, T., Arabian, A., Coleman, K., Orendurff, M., & Zhang, M. (2013). Influence of malalignment on socket reaction moments during gait in amputees with transtibial prostheses. *Gait and Posture*, *37*(4), 620–626. https://doi.org/10.1016/j.gaitpost.2012.10.002

Boutwell, E., Stine, R., Hansen, A., Tucker, K., & Gard, S. (2012). Effect of prosthetic gel liner thickness on gait biomechanics and pressure distribution within the transtibial socket. *The Journal of Rehabilitation Research and Development*, *49*(2), 227. https://doi.org/10.1682/JRRD.2010.06.0121

Butcher, M., & Thompson, G. (2009). Dressings can prevent pressure ulcers: Fact or fallacy? The problem of pressure ulcer prevention. *Wounds UK*, *5*(4), 80–93.

Chan K, T. E. (1990). No use of lower limb prosthesis among elderly amputees. *Annals of the Academy of Medicine*, *19*(6), 811–816.

Chang, W., & Seireg, A. (1999). Prediction of ulcer formation on the skin. *Medical Hypotheses*, *53*(2), 141–144. https://doi.org/http://dx.doi.org/10.1054/mehy.1998.0733

Charkoudian, N. (2013). Skin blood flow in adult human thermoregulation : How it works, when it does not, and why? *Mayo Foundation for Medicial Education and Research*, *78*(May), 1–13.

Collier, M., & Moore, Z. (2006). Etiology and Risk Factors. In *Science and Practice of Pressure Ulcer Management* (pp. 27–35). Springer, London. Retrieved from https://link.springer.com/chapter/10.1007/1-84628-134-2_4

Convery, P., & Buis, A. (1998). Socket/stump interface dynamic pressure distributions recorded during the prosthetic stance phase of gait of a trans-tibial amputee wearing a hydrocast socket. *Prosthetics and Orthotics International*, *22*, 193–198. https://doi.org/10.3109/03093649909071 62

Cutti, A., Perego, P., Fusca, M., Sacchetti, R., & Andreoni, G. (2014). Assessment of lower limb prosthesis through wearable sensors and thermography. *Sensors (Switzerland)*, *14*(3), 5041–5055. https://doi.org/10.3390/s140305041

Derek, H., Mary, C., Marion, D., & Leszek, W. (1977). Frictional Properties Of Skin. *The Journal Of Investigative Dermatology*, *69*(3), 303–305.

DesGroseilliers, J., Desjardins, J., Germain, J., & Krol, A. (1978). Dermatologic problems in amputees. *Canadian Medical Association Journal*, *118*(5), 535–537.

Dillingham, T., Pezzin, L., MacKenzie, E., & Burgess, A. (2001). Use and Satisfaction with Prosthetic Devices Among Persons with Trauma-Related Amputations: A Long-Term Outcome Study. *American Journal of Physical Medicine & Rehabilitation*, *80*(8), 563–571.

Drake, R., Vogl, W., Mitchell, A., Tibbitts, R., & Richardson, P. (2008). *Gray's Atlas of Anatomy* (2nd ed.). Elsevier.

Dudek, N., Marks, M., & Marshall, S. (2006). Skin Problems in an Amputee Clinic. *American Journal of Physical Medicine & Rehabilitation*, *85*(5), 424–429. https://doi.org/10.1097/01.phm.0000214272.01147.5a

Dudek, N., Marks, M., Marshall, S., & Chardon, J. (2005). Dermatologic conditions associated with use of a lower-extremity prosthesis. *Archives of Physical Medicine and Rehabilitation*, *86*(4), 659–663. https://doi.org/10.1016/j.apmr.2004.09.003

Dumbleton, T., Buis, A., McFadyen, A., McHugh, B., McKay, G., Murray, K., & Sexton, S. (2009). Dynamic interface pressure distributions of two transtibial prosthetic socket concepts. *The Journal of Rehabilitation Research and Development*, *46*(3), 405. https://doi.org/10.1682/JRRD.2008.01.0015

Dunk, A. M., & Gardner, A. (2015). The contribution of pressure gradients to advancing understanding of deep tissue injury to sacral regions. *Wound Practice and Research*, *23*(3), 116–122.

Enercorp. (2018). Comparision of Thermistors, Thermocouples and RTD's, 1–4. Retrieved from http://www.enercorp.com/temp/Thermistors_comparision.html

Eshraghi, A., Abu Osman, N. A., Gholizadeh, H., Ali, S., & Abas, W. A. B. W. (2014). Interface Stress in Socket/Residual Limb with Transtibial Prosthetic Suspension Systems During Locomotion on Slopes and Stairs. *American Journal of Physical Medicine & Rehabilitation / Association of Academic Physiatrists*, *94*(1), 1–10. https://doi.org/10.1097/PHM.0000000000000134

Ferreira, A., Correia, V., Mendes, E., Lopes, C., Vaz, J. F. V., & Lanceros-Mendez, S. (2017). Piezoresistive Polymer-Based Materials for Real-Time Assessment of the Stump/Socket Interface Pressure in Lower Limb Amputees. *IEEE Sensors Journal*, *17*(7), 2182–2190. https://doi.org/10.1109/JSEN.2017.2667717

Figliola, R., & Beasley, D. (2011). *Theory and Design for Mechanical Measurements* (5th ed.). Clemson: John Wiley & Sons, Inc.

Fleer, B., & Bennett, W. (1962). Construction of the Patellar-Tendon-Bearing Below-Knee Prosthesis. *Artificial Limbs*, *6*(2), 25–73. Retrieved from http://www.oandplibrary.org/al/pdf/1962_02_025.pdf

Friedel, F., & Tarakhchyan, H. (2017). Prosthetic Prescription, 1–13. Retrieved from https://www.physio-pedia.com/Prosthetics

Futek. (2017). Futek. Retrieved from http://www.futek.com/files/pdf/Product Drawings/llb130.pdf

Geoface. (2017). Integumentary System Anatomy. Retrieved January 1, 2017, from http://geoface.info/ef8714/integumentary-system-anatomy

Goh, J., Lee, P., & Chong, S. (2003a). Static and dynamic pressure profiles of a patellar-tendon-bearing (PTB) socket. *Proceedings of the Institution of Mechanical Engineers.*, *217*(2), 121–126. https://doi.org/10.1243/09544110360579330

Goh, J., Lee, P., & Chong, S. (2003b). Stump/socket pressure profiles of the pressure cast prosthetic socket. *Clinical Biomechanics*, *18*(3), 237–243. https://doi.org/10.1016/S0268-0033(02)00206-1

Goossens, R., Zegers, R., Vandijke, G., & Snijders, C. (1994). Influence of Shear on Skin Oxygen-Tension. *Clinical Physiology*, *14*(1), 111–118. https://doi.org/10.1111/j.1475-097X.1994.tb00495.x

Hagberg, K., & Brånemark, R. (2001). Consequences of non-vascular trans-femoral amputation: A survey of quality of life, prosthetic use and problems. *Prosthetics and Orthotics International*, *25*(3), 186–194. https://doi.org/10.1080/03093640108726601

Hermodsson, Y., Ekdahl, C., Persson, B., & Roxendal, G. (1994). Gait in male trans-tibial amputees: a comparative study with healthy subjects in relation to walking speed. *Prosthetics and Orthotics International*, *18*, 68–77. https://doi.org/10.3109/03093649409164387

Highsmith, J., & Jason, K. (2011). Identifying and Managing Skin Issues With Lower-Limb Prosthetic Use. *InMotion - A Publication of the Amputee Coalition*, *21*(1), 41–43.

Hollinger, A., & Wanderley, M. (2006). Evaluation of Commercial Force-Sensing Resistors, 1–4.

Horgan, O., & MacLachlan, M. (2004). Psychosocial adjustment to lower-limb amputation: A review. *Disability and Rehabilitation*, *26*(14–15), 837–850. https://doi.org/10.1080/09638280410001708869

Huff, E., Ledoux, W., Berge, J., & Klute, G. (2008). Measuring Residual Limb Skin Temperatures at the Skin-Prosthesis Interface. *Journal of Prosthetics and Orthotics*, *20*(4), 170–173. https://doi.org/10.1097/JPO.0b013e3181875b17

Interlink Electronics™. (2016). FSR 400 Series Data Sheet. Retrieved from https://cdn2.hubspot.net/hubfs/3899023/Interlinkelectronics November2017/Docs/Datasheet_FSR.pdf

James, W. (1991). Principles of limb fitting and prostheses. *Annals of the Royal College of Surgeons of England*, *73*(3), 158–162. https://doi.org/10.1016/B978-1-85617-803-7.50022-5

Jia, X., Suo, S., Meng, F., & Wang, R. (2008). Effects of alignment on interface pressure for transtibial amputee during walking. *Disability and Rehabilitation: Assistive Technology*, *3*(6), 339–343.

https://doi.org/10.1080/17483100802044634

Kanellos, G., Papaioannou, G., Tsiokos, D., Mitrogiannis, C., Nianios, G., & Pleros, N. (2010). Two dimensional polymer-embedded quasi-distributed FBG pressure sensor for biomedical applications. *Optics Express*, *18*(1), 179–186. https://doi.org/10.1364/OE.18.000179

Kemuriyama, T., Niitsuma, J., Yano, H., & Komeda, T. (1998). An Analysis of Skin Temperature Changes under Pressure Loading and Relief by Animal Experiments. *ZEEE Engineering in Medicine and Biology Society*, *20*(July), 423–445. https://doi.org/10.1177/0022427810397950

Klute, G., Huff, E., & Ledoux, W. (2014). Does activity affect residual limb skin temperatures? *Clinical Orthopaedics and Related Research*, *472*(10), 3062–3067. https://doi.org/10.1007/s11999-014-3741-4

Kobayashi, T., Orendurff, M., Zhang, M., & Boone, D. (2013). Effect of alignment changes on sagittal and coronal socket reaction moment interactions in transtibial prostheses. *Journal of Biomechanics*, *46*(7), 1343–1350. https://doi.org/10.1016/j.jbiomech.2013.01.026

Koc, E., Tunca, M., Akar, A., Erbil, A. H., Demiralp, B., & Arca, E. (2008). Skin problems in amputees: A descriptive study. *International Journal of Dermatology*, *47*(5), 463–466. https://doi.org/10.1111/j.1365-4632.2008.03604.x

Kokate, J., Leland, K., Held, A., Hansen, G., Kveen, G., Johnson, B., … Iaizzo, P. (1995). Temperature-modulated pressure ulcers: A porcine model. *Archives of Physical Medicine and Rehabilitation*, *76*(7), 666–673. https://doi.org/10.1016/S0003-9993(95)80637-7

Lai, C., & Li-Tsang, C. (2009). Validation of the Pliance X System in measuring interface pressure generated by pressure garment. *Burns*, *35*(6), 845–851. https://doi.org/10.1016/j.burns.2008.09.013

Laing, S., Lee, P., & Goh, J. (2011). Engineering a trans-tibial prosthetic socket for the lower limb amputee. *Annals of the Academy of Medicine Singapore*, *40*(5), 252–259.

Lara, S. (2007). The Effect of Surface Curvature and a Gel Liner Interface on Performance Properties of the Tekscan F - Socket System. Retrieved January 1, 2017, from https://smartech.gatech.edu/bitstream/handle/1853/14750/presentation_schrock.pdf

Laszczak, P., Jiang, L., Bader, D., Moser, D., & Zahedi, S. (2015). Development and validation of a 3D-printed interfacial stress sensor for prosthetic applications. *Medical Engineering and Physics*, *37*(1), 132–137. https://doi.org/10.1016/j.medengphy.2014.10.002

Laszczak, P., McGrath, M., Tang, J., Gao, J., Jiang, L., Bader, D. L., … Zahedi, S. (2016). A pressure and shear sensor system for stress measurement at lower limb residuum/socket interface. *Medical Engineering and Physics*, *38*(7), 695–700. https://doi.org/10.1016/j.medengphy.2016.04.007

Levy, S. W. (1980). Skin problems of the leg amputee. *Prosthetics and Orthotics International*, *4*(1), 37–44. https://doi.org/10.1001/archderm.1962.01590010071009

Linder-Ganz, E., Engelberg, S., Scheinowitz, M., & Gefen, A. (2006). Pressure-time cell death threshold for albino rat skeletal muscles as related to pressure sore biomechanics. *Journal of Biomechanics*, *39*(14), 2725–2732. https://doi.org/10.1016/j.jbiomech.2005.08.010

Lyon, C., Kulkarni, J., Zimerson, E., Van Ross, E., & Beck, M. (2000). Skin disorders in amputees. *Journal of the American Academy of Dermatology*, *42*(3), 501–507. https://doi.org/10.1016/S0190-9622(00)90227-5

Mak, A., Zhang, M., & Boone, D. A. (2001). State-of-the-art research in lower-limb prosthetic biomechanics-socket interface: a review. *Journal of Rehabilitation Research & Development.*, *38*(2), 1–14. Retrieved from http://www.ncbi.nlm.nih.gov/pubmed/11392649

Mathur, N., Glesk, I., & Buis, A. (2016). Skin Temperature Prediction in Lower Limb Prostheses. *IEEE Journal of Biomedical and Health Informatics*, *20*(1), 158–165. https://doi.org/10.1109/jbhi.2014.2368774

Meijer, J., Schut, G., Ribbe, M., Goovaerts, H., Nieuwenhuys, R., Reulen, J., & Schneider, H. (1989). Method for the measurement of susceptibility to decubitus ulcer formation. *Medical & Biological Engineering & Computing*, *27*(5), 502–506. https://doi.org/10.1007/BF02441469

Meulenbelt, H., Geertzen, J., & Jonkman, M. (2009). Determinants of Skin Problems of the Stump in Lower-Limb. *Archives of Physical Medicine and Rehabilitation*, *90*(1), 74–81. https://doi.org/10.1016/j.apmr.2008.07.015

Meulenbelt, H., Geertzen, J., Jonkman, M., & Dijkstra, P. (2011). Skin problems of the stump in lower limb amputees: 1. A clinical study. *Acta Dermato-Venereologica*, *91*(2), 173–177. https://doi.org/10.2340/00015555-1040

Minco. (2016). RTD, Thermocouple, or Thermistor?, *1*(1), 1–10.

Mueller, S., & Hettinger, T. (1954). Measuring the pressure distribution in the socket of the prostheses. *Orthpadie-Technik Heft*, *9*(222), 5.

Naylor, P. (1955). The skin surface and friction. *The British Journal of Dermatology*, *67*.

Neumann, E. S., Wong, J. S., & Drollinger, R. L. (2005). Socket : Measurement. *American Academy of Orthotists and Prosthetists*, *17*(1).

Papira, Y., Hsu, K.-H., & Wildnauer, R. (1975). The mechanical properties of stratum corneum: I. The effect of water and ambient temperature on the tensile properties of newborn rat stratum corneum. *Biochimica et Biophysica Acta*, *399*(1), 170–180.

Patterson, R., & Fisher, S. (1986). Sitting pressure-time patterns in patients with quadriplegia. *Archives of Physical Medicine and Rehabilitation*, *67*(11), 812–814. Retrieved from http://www.embase.com/search/results?subaction=viewrecord&from=export&id=L17186209%5Cnhttp://rug.on.worldcat.org/atoztitles/link/?sid=EMBASE&issn=00039993&id=doi:&atitle=Sitting+pressure-time+patterns+in+patients+with+quadriplegia&stitle=ARCH.+PHYS.+MED.+

Pearson, J., Holmgren, G., March, L., & Oberg, K. (1973). Pressures in critical regions of the below-knee patellar-tendon-bearing prosthesis. *Bulletin of Prosthetics Research*, *10*(19), 52–76. Retrieved from http://www.ncbi.nlm.nih.gov/pubmed/4767330

Peery, J., Ledoux, W., & Klute, G. (2005). Residual-limb skin temperature in transtibial sockets. *The Journal of Rehabilitation Research & Development*, *42*(2), 147. https://doi.org/10.1682/JRRD.2004.01.0013

Pirouzi, G., Abu Osman, N., Eshraghi, A., Ali, S., Gholizadeh, H., & Wan Abas, W. (2014). Review of the socket design and interface pressure measurement for transtibial prosthesis. *Scientific World Journal*, *2014*. https://doi.org/10.1155/2014/849073

Polliack, A., Sieh, R., Craig, D., Landsberger, S., McNeil, D., & Ayyappa, E. (2000). Scientific validation of two commercial pressure sensor systems for prosthetic socket fit. *Prosthetics and Orthotics International*, *24*, 63–73. https://doi.org/10.1080/03093640008726523

Pye, G., & Bowker, P. (1976). Skin temperature as an indicator of stress in soft tissue. *Engineering in Medicine*, *5*(3), 58–60. https://doi.org/10.1243/EMED_JOUR_1976_005_022_02

Quigley, M. (2010). Prosthetic Management: Overview, Methods, and Materials. *Atlas of Limb Prosthetics: Surgical, Prosthetic, and Rehabilitation Principles Prosthetic*, 1–25.

Radcliffe, C. W. (1962). The Biomechanics of Below-Knee Prostheses in Normal , Level , Bipedal Walking. *Artificial Limbs*, *6*, 16–24.

Rae, J., & Cockrell, J. (1971). Interface pressure and stress distribution in prosthetic fitting. *Bulletin of Prosthetics Research*, *10*(16), 64–111.

Rajtukova, V., Hudak, R., Zivcak, J., Halfarova, P., & Kudrikova, R. (2014). Pressure distribution in transtibial prostheses socket and the stump interface. *Procedia Engineering*, *96*, 374–381. https://doi.org/10.1016/j.proeng.2014.12.106

Reswick, J. B., & Rogers, J. E. (1976). Experience at Rancho Los Amigos Hospital with devices and

techniques to prevent pressure sores. *Bed Sore Biomechanics*, *2*, 301–310. https://doi.org/10.1007/978-1-349-02492-6_38

Sacks, A. (1989). Theoretical prediction of a time-at-pressure curve for avoiding pressure sores. *Journal of Rehabilitation Research & Development.*, *26*(3), 27–34.

Sae-Sia, W., Wipke-Tevis, D. D., & Williams, D. A. (2005). Elevated sacral skin temperature (Ts): A risk factor for pressure ulcer development in hospitalized neurologically impaired Thai patients. *Applied Nursing Research*, *18*(1), 29–35. https://doi.org/10.1016/j.apnr.2004.03.005

Sanders, J., Bell, D., Okumura, R., & Dralle, A. (1998). Effects of alignment changes on stance phase pressures and shear stresses on transtibial amputees: Measurements from 13 transducer sites. *IEEE Transactions on Rehabilitation Engineering*, *6*(1), 21–31. https://doi.org/10.1109/86.662617

Sanders, J., Cagle, J., Harrison, D., & Karchin, A. (2012). Amputee socks: How does sock ply relate to sock thickness? *Prosthetics and Orthotics International*, *36*(1), 77–86. https://doi.org/10.1177/0309364611431290

Sanders, J., & Daly, C. (1993). Measurement of Stresses in Three Orthogonal Directions at the Residual Limb-Prosthetic Socket Interface. *IEEE Transactions on Rehabilitation Engineering*, *1*(2), 79–85. https://doi.org/10.1109/86.242421

Sanders, J., Daly, C., & Burgess, E. (1993). Clinical measurement of normal and shear stresses on a trans-tibial stump: characteristics of wave-form shapes during walking. *Prosthetics and Orthotics International*, *17*(1), 38–48. https://doi.org/10.3109/03093649309164353

Sanders, J. E. (2000). Thermal response of skin to cyclic pressure and pressure with shear: a technical note. *Journal of Rehabilitation Research and Development*, *37*(October), 511–515.

Sanders, J. E., & Daly, C. H. (1999). Interface pressures and shear stresses: sagittal plane angular alignment effects in three trans-tibial amputee case studies. *Prosthetics and Orthotics International*, *23*(1), 21–29.

Sanders, J., & Goldstein, B. (1995). Skin response to mechanical stress: Adaptation rather than breakdown - a review of the literature. *Journal of Rehabilitation Research & Development.*, *32*(3), 214. Retrieved from http://web.a.ebscohost.com.ezproxy.uct.ac.za/ehost/delivery?sid=10865d4c-266d-40e6-9d85-97a075979575%40sessionmgr4008&vid=3&ReturnUrl=http%3A%2F%2Fweb.a.ebscohost.com%2Fehost%2Fdetail%2Fdetail%3Fvid%3D2%26sid%3D10865d4c-266d-40e6-9d85-97a075979575%2540ses

Sanders, J., Lam, D., Dralle, A., & Okumura, R. (1997). Interface pressures and shear stresses at thirteen socket sites on two persons with transtibial amputation. *Journal of Rehabilitation Research & Development.*, *34*(1), 19–43.

Schubert, V., & Fagrell, B. (1991). Evaluation of the Dynamic Cutaneous Postischemic Hyperemia and Thermal Response in Elderly Subjects and in an Area at Risk for Pressure Sores. *Clinical Physiology*, *11*(2), 169–182.

SD, M., & RB, R. (1979). Thermal response of skin to application of localized pressure. *Archives of Physical Medicine and Rehabilitation*, *60*(12), 584–590.

Seelen, H., Anemaat, S., Janssen, H., & Deckers, J. (2003). Effects of prosthesis alignment on pressure distribution at the stump/socket interface in transtibial amputees during unsupported stance and gait. *Clinical Rehabilitation*, *17*(7), 787–796. https://doi.org/10.1191/0269215503cr678oa

Semitec. (2017). JT Thermistor. Retrieved January 1, 2017, from https://www.mouser.com/ds/2/362/jtthermistor-2647.pdf

Shapiro, S. S., & Wilk, M. B. (1965). An Analysis of Variance Test for Normality (Complete Samples). *Biometrika*, *52*(3), 591–611.

Shea, D. (1975). Pressure Sores: Classification and Mangement. Orlando.

Shem, K., Breakey, J., & Werner, P. (1998). Pressures at the Residual Limb-Socket Interface in Transtibial Amputees with Thigh Lacer-Side Joints. *Journal of Prosthetics and Orthotics*, *American A*.

Shikh, S., Abu Osman, noor A., & Latif, L. A. (2007). Validating the efficiency of hydro-cast sockets through pressure distribution and gait analysis. *22nd European Photovoltaic Solar Energy Conference , 3-7 September 2007 , Milan , Italy*, *30*(September), 5–8.

Sprigle, S., Linden, M., McKenna, D., Davis, K., & Riordan, B. (2001). Clinical skin temperature measurement to predict incipient pressure ulcers. *Advances in Skin & Wound Care*, *14*(3), 133–137. Retrieved from http://www.ncbi.nlm.nih.gov/pubmed/11905978

Stekelenburg, A., Gawlitta, D., Bader, D., & Oomens, C. (2008). Deep Tissue Injury: How Deep is Our Understanding? *Archives of Physical Medicine and Rehabilitation*, *89*(7), 1410–1413. https://doi.org/10.1016/j.apmr.2008.01.012

Su, P.-F., Gard, S., Lipschutz, R., & Kuiken, T. (2007). Gait characteristics of persons with bilateral transtibial amputations. *The Journal of Rehabilitation Research and Development*, *44*(4), 491. https://doi.org/10.1682/JRRD.2006.10.0135

Su, P.-F., Gard, S., Lipschutz, R., & Kuiken, T. (2010). The Effects of Increased Prosthetic Ankle Motions on the Gait of Persons with Bilateral Transtibial Amputations. *American Journal of Physical Medicine & Rehabilitation / Association of Academic Physiatrists*, *89*(1), 34–47. https://doi.org/10.1097/PHM.0b013e3181c55ad4

Swain, I., & Bader, D. (2002). The measurement of interface pressure and its role in soft tissue breakdown. *Journal of Tissue Viability*, *12*(4), 132–146. https://doi.org/10.1016/S0965-206X(02)80022-5

Tekscan®. (2016). FlexiForce™. Retrieved from https://www.tekscan.com/products-solutions/force-sensors/a201

Texas Instruments. (1999). LMC660 CMOS Quad Operational Amplifier. Retrieved from http://www.ti.com/lit/ds/symlink/lmc660.pdf

Thiele, F., & Senden, K. (1986). Relationship between skin temperature and the insensible perspiration of the human skin. *The Journal Of Investigative Dermatology*, *47*(4), 307–312.

Tsiokos, D., Kanellos, G., Papaioannou, G., & Pissadakis, S. (2012). Fiber Optic-Based Pressure Sensing Surface for Skin Health Management in Prosthetic and Rehabilitation Interventions. *Biomedical Engineering - Technical Applications in Medicine*. https://doi.org/10.5772/50574

Vecchi, F., Freschi, C., Micera, S., Sabatini, A., Dario, P., & Sacchetti, R. (2000). Experimental evaluation of two commercial force sensors for applications in biomechanics and motor control. *Proceedings of the 5th Annual Conference of the International Functional Electrical Stimulation Society, Aalborg, Denmark*, *June*(May 2016), 44–54. Retrieved from http://www.researchgate.net/profile/Silvestro_Micera/publication/228790680_Experimental_evaluation_of_two_commercial_force_sensors_for_applications_in_biomechanics_and_motor_control/links/0fcfd50c058ed8272c000000.pdf

Vista Medical. (2017). FSA In-Socket System. Retrieved from http://www.vista-medical.com

Wallis, D., Broderick, T., Paul, O., Reed, L., Pettit, T., Pizatella, T., & Linn, H. (1998). Worker deaths by electrocution (a summary of NIOSH Surveillance and investigative findings), (May 1998), 43.

Welltech Instrument Company. (2016). FBG Sensor Catalog. Retrieved from http://www.fbg.com.cn/catalogs/FBG-Sensor.pdf

Wong, V., Stotts, N., Hopf, H., Dowling, G., & Froelicher, E. (2010). Changes in Heel Skin Temperature Under Pressure in Hip Surgery Patients. *Advances in Skin & Wound Care*, *24*(12), 562–570.

World Health Organisation. (2005). Guidelines for training Personnel in Developing countries for Prosthetics and Orthotics Services. *WHO Library Cataloguing-in-Publication Data*.

Zachariah, S., & Sanders, J. (2001). Standing interface stresses as a predictor of walking interface stresses in the trans-tibial prosthesis. *Prosthetics and Orthotics International*, *25*(1), 34–40. https://doi.org/10.1080/03093640108726566

Zhang, M., Turner-Smith, A., Roberts, V., & Tanner, A. (1996). Frictional action at lower limb/prosthetic socket interface. *Medical Engineering and Physics*, *18*(3), 207–214. https://doi.org/10.1016/1350-4533(95)00038-0

Zhang, M., Turner-Smith, R., Tanner, A., & Roberts, V. (1998). Clinical investigation of the pressure and shear stress on the trans-tibial stump with a prosthesis. *Medical Engineering & Physics*, *20*(3), 188–198. https://doi.org/10.1016/S1350-4533(98)00013-7

Ziegler-Graham, K., MacKenzie, E., Ephraim, P., Travison, T., & Brookmeyer, R. (2008). Estimating the Prevalence of Limb Loss in the United States: 2005 to 2050. *Archives of Physical Medicine and Rehabilitation*, *89*(3), 422–429. https://doi.org/10.1016/j.apmr.2007.11.005

11 Appendix A

This appendix provides the datasheet of all electrical components used within the study.

11.1 Tekscan® FlexiForce™ Standard Model A201 Datasheet

The Tekscan® FlexiForce™ A201 was used for the pressure transducers and gait load sensors within the study. The datasheet is show in Figure 11.1.

Tekscan

FlexiForce™
Standard Model A201

The FlexiForce A201 is our standard sensor and meets the requirements of most customers. The A201 is a thin and flexible piezoresistive force sensor that is available off-the-shelf in a variety of lengths for easy proof of concept. These ultra-thin sensors are ideal for non-intrusive force and pressure measurement in a variety of applications. The A201 can be used with our test & measurement, prototyping, and embedding electronics, including the OEM Development Kit, FlexiForce Quickstart Board, and the ELF™ System*. You can also use your own electronics, or multimeter.

BENEFITS

- Thin and flexible
- Easy to use
- Convenient and affordable

PHYSICAL PROPERTIES

Thickness	0.203 mm (0.008 in.)
Length	191 mm (7.5 in.)** (optional trimmed lengths: 152 mm (6 in.), 102 mm (4 in.), 51 mm (2 in.))
Width	14 mm (0.55 in.)
Sensing Area	9.53 mm (0.375 in.) diameter
Connector	3-pin Male Square Pin (center pin is inactive)
Substrate	Polyester
Pin Spacing	2.54 mm (0.1 in.)

✓ROHS COMPLIANT

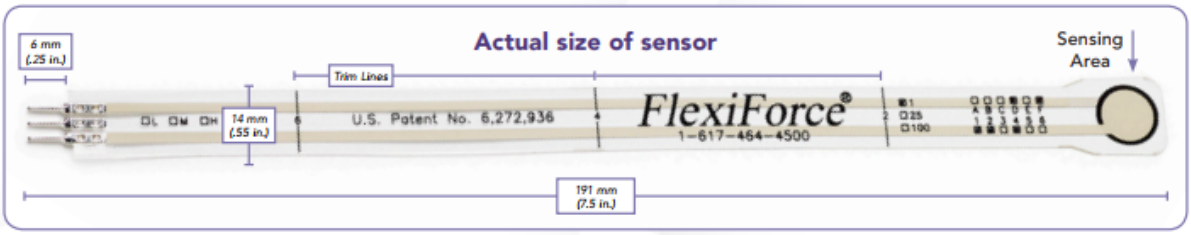

STANDARD FORCE RANGES
(as tested with circuit shown)

4.4 N (0 - 1 lb)
111 N (0 - 25 lb)
445 N (0 - 100 lb)

In order to measure forces above 445 N (100 lb) and up to 4,448 N (1,000 lb), apply a lower drive voltage (-0.5 V, -0.25 V, etc.) and reduce the resistance of the feedback resistor (1kΩ min.) Conversely, the sensitivity can be increased for measurement of lower forces by increasing the drive voltage or resistance of the feedback resistor.

Recommended Circuit

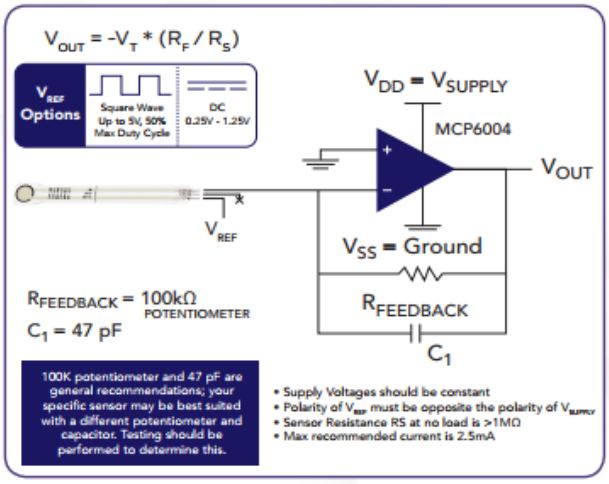

	Typical Performance	Evaluation Conditions
Linearity (Error)	< ±3% of full scale	Line drawn from 0 to 50% load
Repeatability (CoV)	< ±2.5%	Conditioned sensor, 80% of full force applied
Hysteresis	< 4.5 % of full scale	Conditioned sensor, 80% of full force applied
Drift	< 5% per logarithmic time scale	Constant load of 111 N (25 lb)
Response Time	< 5µsec	Impact load, output recorded on oscilloscope
Operating Temperature	-40°C - 60°C (-40°F - 140°F)	Time required for the sensor to respond to an input force

• Force reading change per degree of temperature change ▪ 0.36%/°C (±0.2%/°F)

Figure 11.1: Tekscan® FlexiForce™ A201 datasheet (Tekscan®, 2016)

11.2 103 JT-025 thermistor datasheet

The 103 JT-025 thermistor was used as the skin temperature sensor within the study. The data sheet is shown in Figure 11.2.

JT THERMISTOR

JT thermistors feature ultra thinness of 500μm and superior electrical insulation.
It is possible to use with safety in ambience that might contact with electrodes.

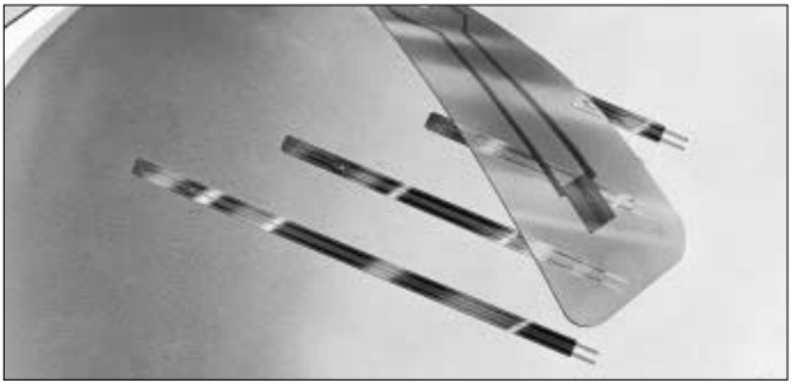

Part number

103 JT-025

- Shape
- JT thermistor
- Rated zero-power resistance at 25℃ 103 : 10kΩ

Dimensions

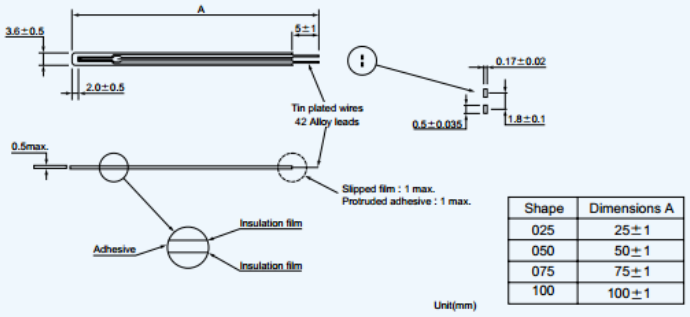

Shape	Dimensions A
025	25±1
050	50±1
075	75±1
100	100±1

Resistance-Temperature

Temperature (℃)	Type	
	103JT	104JT
−50	367.7	9584
−40	204.7	4572
−30	118.5	2282
−20	71.02	1191
−10	43.67	647.2
0	27.70	365.0
10	18.07	212.5
20	12.11	127.7
30	8.301	78.88
40	5.811	50.03
50	4.147	32.51
60	3.011	21.61
70	2.224	14.66
80	1.668	10.13
90	1.267	7.135
100		5.111
110		3.720
120		2.746
125		2.371

Unit(kΩ)

Specifications

Part No.	R_{25}*1	B value*2	Dissipation factor (mW/℃)	Thermal time constant(s)*3	Rated power at 25℃(mW)	Operating temp. range(℃)
103JT-□□□	10kΩ±1%	3435K±1%	0.7	5	3.5	−50~90
104JT-□□□	100kΩ±1%	4390K±1%	0.7	5	3.5	−50~125

*1 R_{25} : Rated zero-power resistance value at 25℃, ±2% and 3% are also available.
*2 B value : determined by rated zero-power resistance at 25℃ and 85℃.
*3 Time when thermistor temperature reaches 63.2% of the temperature difference. The value is measured in the air.

Figure 11.2: 103 JT-025 Thermistor Datasheet (Semitec, 2017)

12 Appendix B: Ethical Approval

UNIVERSITY OF CAPE TOWN
Faculty of Health Sciences
Human Research Ethics Committee

Room E53-46 Old Main Building
Groote Schuur Hospital
Observatory 7925
Telephone [021] 406 6492
Email: sumayah.ariefdien@uct.ac.za
Website: www.health.uct.ac.za/fhs/research/humanethics/forms

15 May 2017

HREC REF: 019/2017

A/Prof G Vicatos
Department of Mechanical Engineering
Electrical & Mechanical Engineering Building
Upper Campus-UCT

Dear A/Prof Vicatos

PROJECT TITLE: THE DESIGN, DEVELOPMENT AND VALIDATION OF A TACTILE MULTI-MEASUREMENT TOOL FOR THE REAL TIME DATA-MAPPING OF THE TRANS-TIBIAL AMPUTEE SOCKET-LIMB INTERFACE (MSc candidate- Mr S Bruton)

Thank you for your response letter, addressing the issues raised by the Human Research Ethics Committee (HREC).

It is a pleasure to inform you that the HREC has **formally approved** the above-mentioned study.

Approval is granted for one year until the 30 May 2018.

Please submit a progress form, using the standardised Annual Report Form if the study continues beyond the approval period. Please submit a Standard Closure form if the study is completed within the approval period.
(Forms can be found on our website: www.health.uct.ac.za/fhs/research/humanethics/forms)

We acknowledge that the student, S Bruton will also be involved in this study.

Please quote the HREC REF in all your correspondence.

Please note that the ongoing ethical conduct of the study remains the responsibility of the principal investigator.

Please note that for all studies approved by the HREC, the principal investigator **must** obtain appropriate institutional approval before the research may occur.

Yours sincerely

PROFESSOR M BLOCKMAN
CHAIRPERSON, FHS HUMAN RESEARCH ETHICS COMMITTEE

Federal Wide Assurance Number: FWA00001637.
Institutional Review Board (IRB) number: IRB00001938

HREC 019/2017

Figure 12.1: Ethics Approval Letter

13 Appendix C: Subject Information

13.1 Subject Details

Table 13.1: Interface Details

SUBJECT DETAILS

ID	Gender (M/F)	Amp Type	Age	Weight (kg)	Height (m)	Side	Socket/Liner	Interface Number	Skin Problem Present?
1	M	Bilateral Amputee	60	85	1.65	R	Hydrostatic Socket (TSB) / Ossur Iceross Dermo Locking Liner	1R1	No
						L	Hydrostatic Socket (TSB) / Locking Liner	1L1	
2	M	Bilateral Amputee	64	73	1.7	R	Hydrostatic Socket (TSB)/Ossur Iceross Dermo Cushion Liner (Silicone) & Otto Bock Derma Pro-Flex Sleeve	2R1	No
						L	Hydrostatic Socket (TSB)/ Ossur Iceross Dermo Cushion Liner & Otto Bock Derma Pro-Flex Sleeve (Silicone)	2L1	
						R	Hydrostatic Socket (TSB)/ Ossur Iceross Dermo Cushion Liner	2R2	
						L	Hydrostatic Socket (TSB)/ Ossur Iceross Dermo Cushion Liner	2L2	
3	M	Unilateral Amputee	42	83	1.86	R	TSB and PTB hybrid, Vacuum system with expulsion valve (hand casted) / Ossur XTT Liner with Seal-in ring	3R1*	Yes PS (ProxTib)
							TSB and PTB hybrid, Vacuum system with expulsion valve (hand casted) / Ossur XTT Liner with Seal-in ring + Ottobock Proflex Knee Sleeve	3R2	No
4	M	Unilateral Amputee	32	82	1.75	L	PTB socket with unity elevated vacuum syspension (hand casted) / Ossur XYY with Seal-in ring + ottobock proflex knee sleeve	4L1*	Yes PS (DT)
5	M	Unilateral Amputee	29	70	1.78	R	PTB socket with locking pin liner (hand casted) / Ossur Synergy Locking Liner	5R1	No

*M – Male, F – Female, R – Right, L – Left, * - Indicates pressure sore visibly present in interface, ProxTib – Proximal Tibia, DT – Distal Tibia, Amp – Amputation, PS – Pressure Sore*

13.2 Subject Sockets

13.2.1 TSB Sockets

Subject 1: Left and Right Sockets

Figure 13.1: Interface 1L1 and 1R1 sockets

Subject 2: Left and Right (1st Testing Session Socket)

Figure 13.2: Interface 2L1 and 2R1 sockets

Subject 2: Left and Right (2nd Testing Session Socket)

Figure 13.3: Interface 2L2 and 2R2 sockets

13.2.2 PTB Sockets

Subject 3 Right Leg

Figure 13.4: Interface 3R1 socket

Subject 4 Left Leg

Figure 13.5: Interface 4L1 socket

Subject 5 Right Leg

Figure 13.6: Interface 5R1 socket

13.3 Interface 4L1: Distal Tibia (DT) Pressure Sore Area

Figure 13.7: Distal Tibia (DT) area of interface 4L1 presenting a pressure sore with surrounding inflamation

13.4 Interface 3R1: Proximal Tibia (ProxTib) Pressure Sore Area

Figure 13.8: Proximal Tibia (ProxTib) area of interface 3R1 presenting a pressure sore with no surrounding inflammation

14 Appendix D: Study Procedure Results

14.1 Straight Line Walking Peak Pressure Results

This section illustrates the peak pressures from all strides over the SLW procedure.

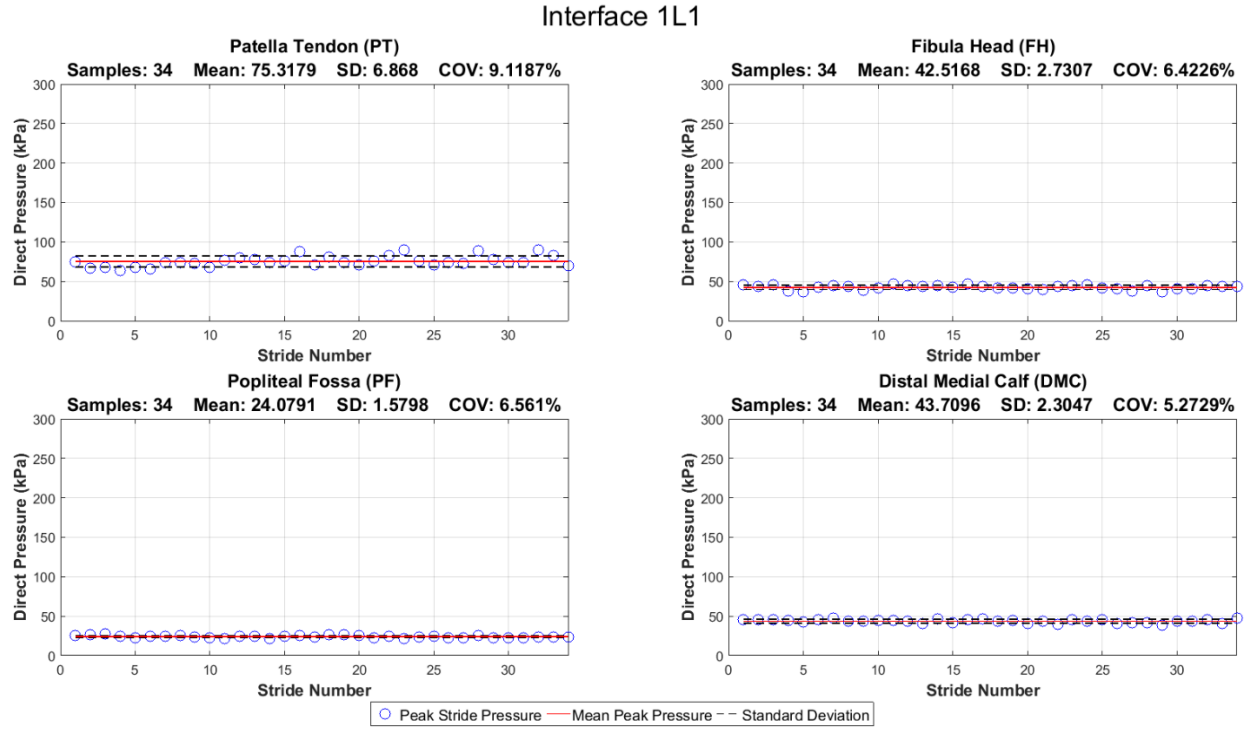

Figure 14.1: SLW peak pressures - Interface 1L1

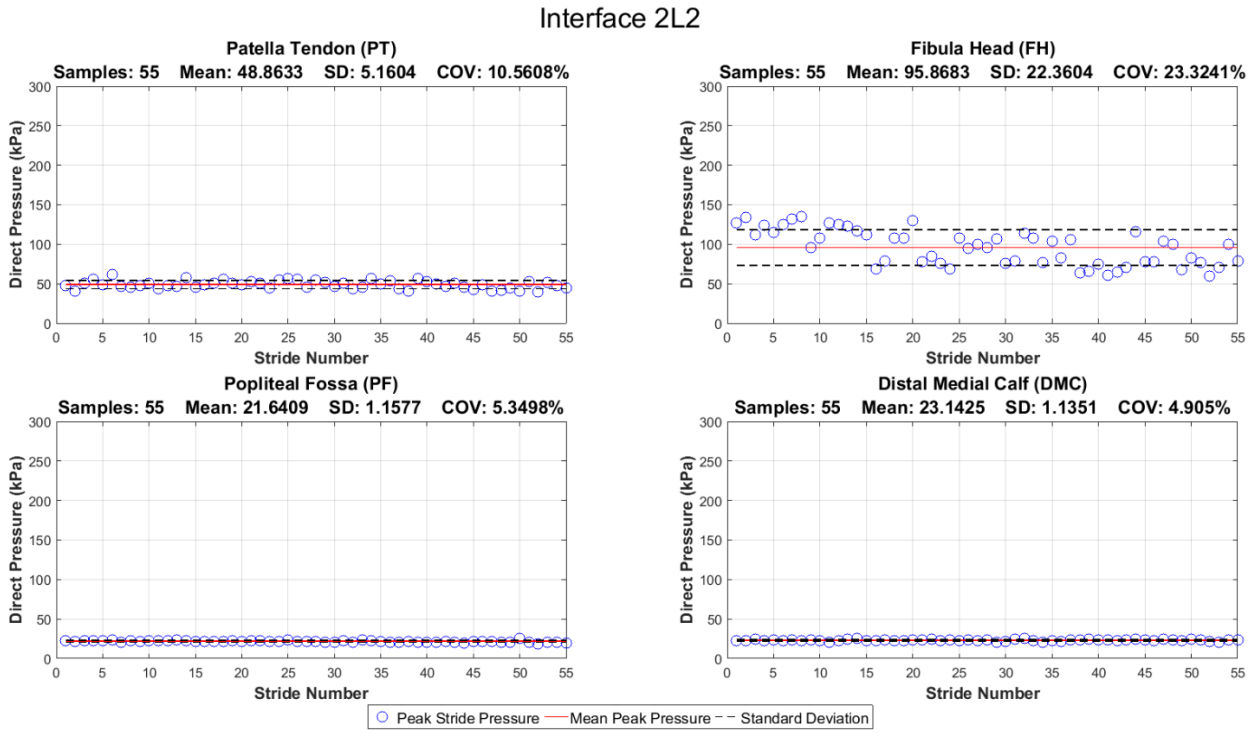

Figure 14.2: SLW peak pressures - Interface 2L2

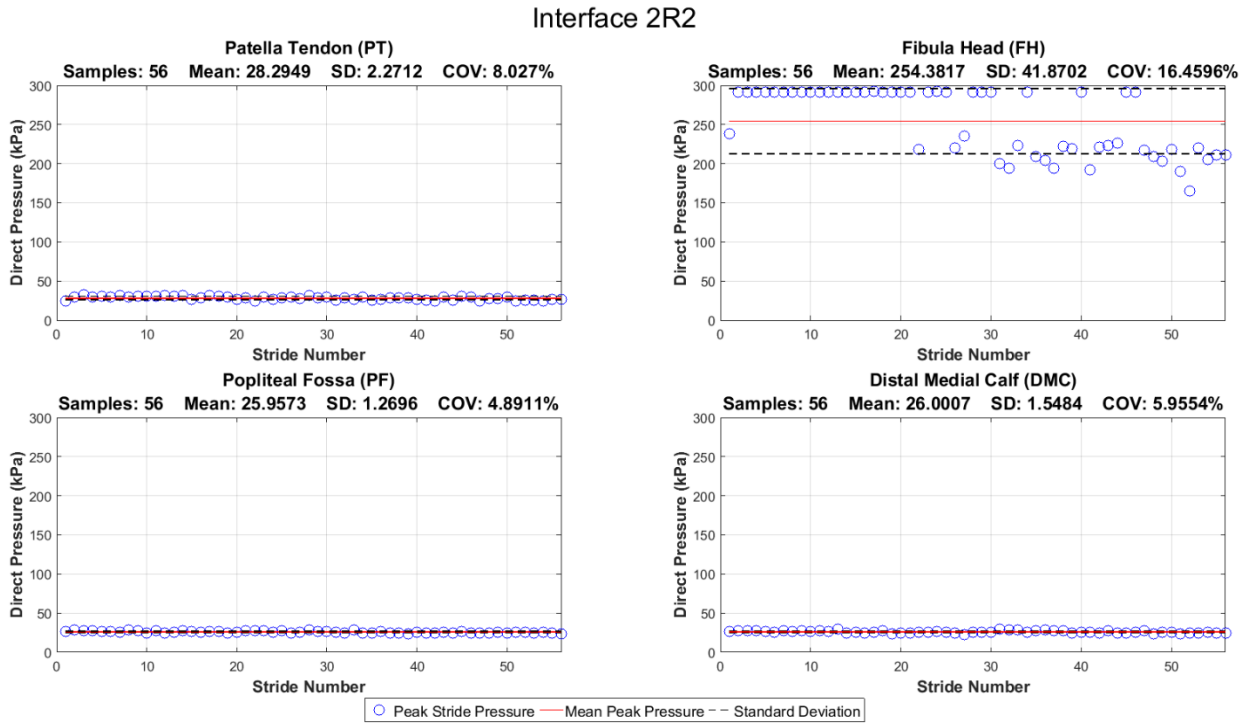

Figure 14.3: SLW peak pressures - Interface 2R2

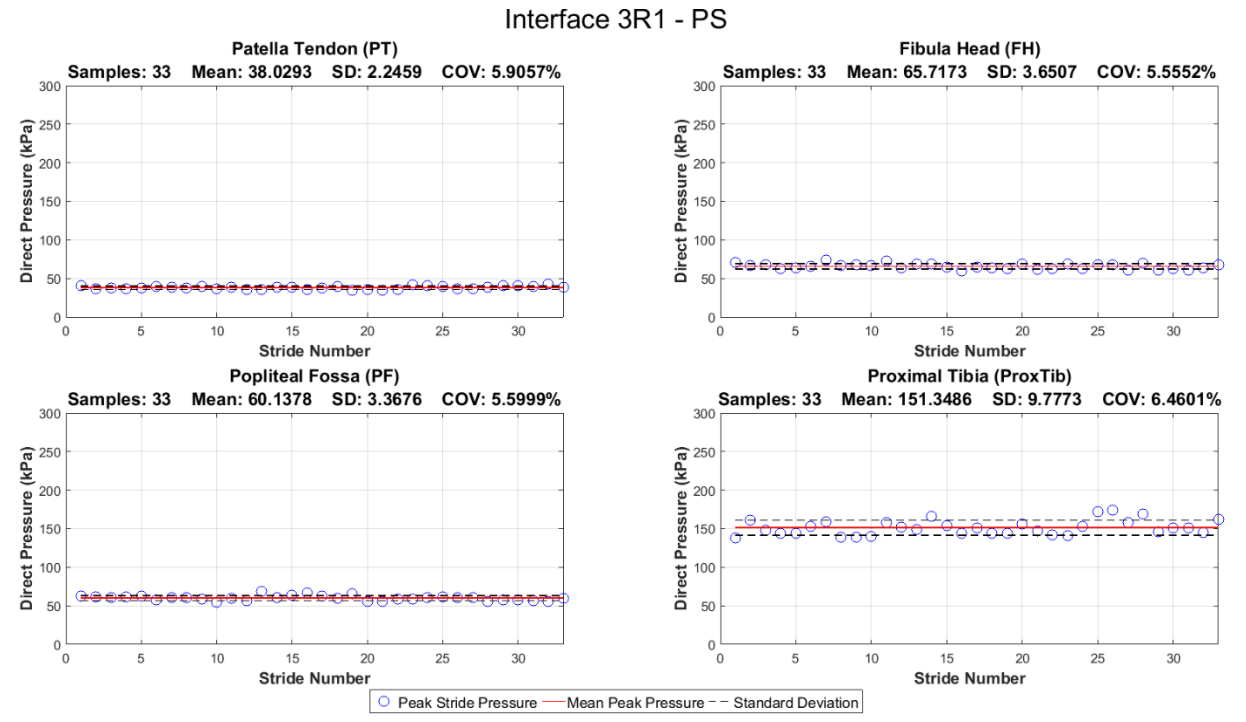

Figure 14.4: SLW peak pressures - Interface 3R1 – Pressure Sore present on ProxTib

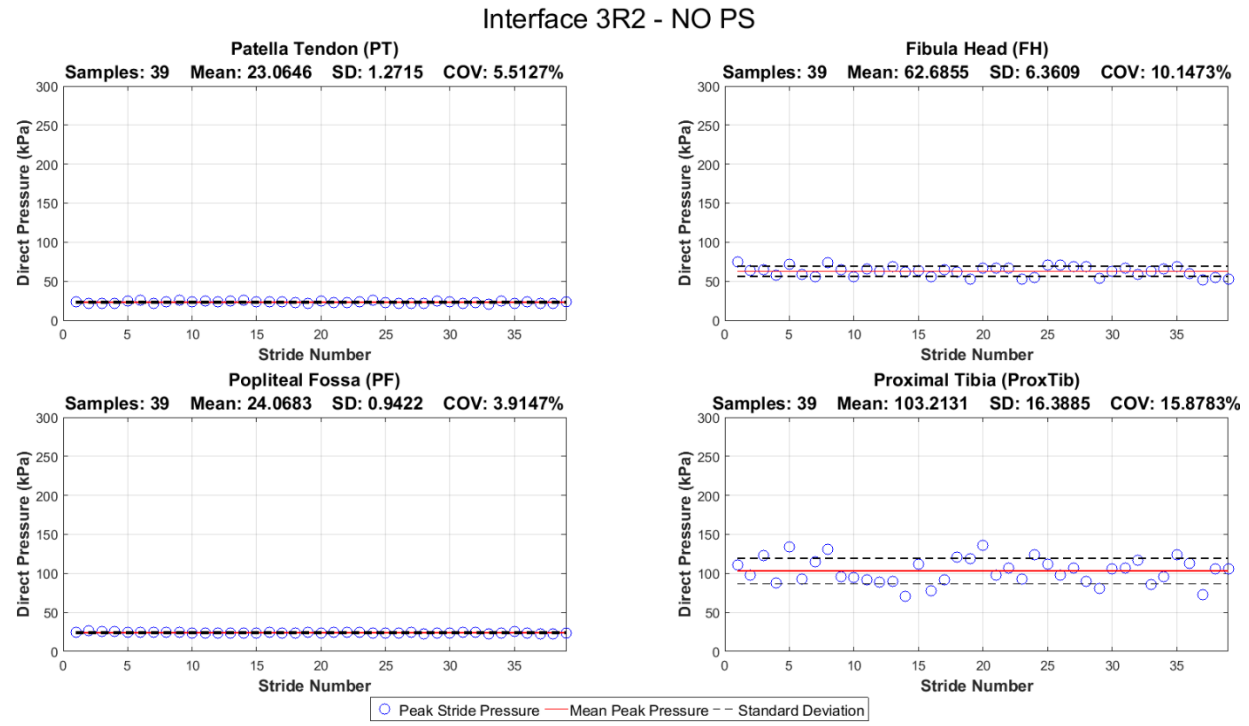

Figure 14.5: SLW peak pressures - Interface 3R2 - No Pressure Sore Present

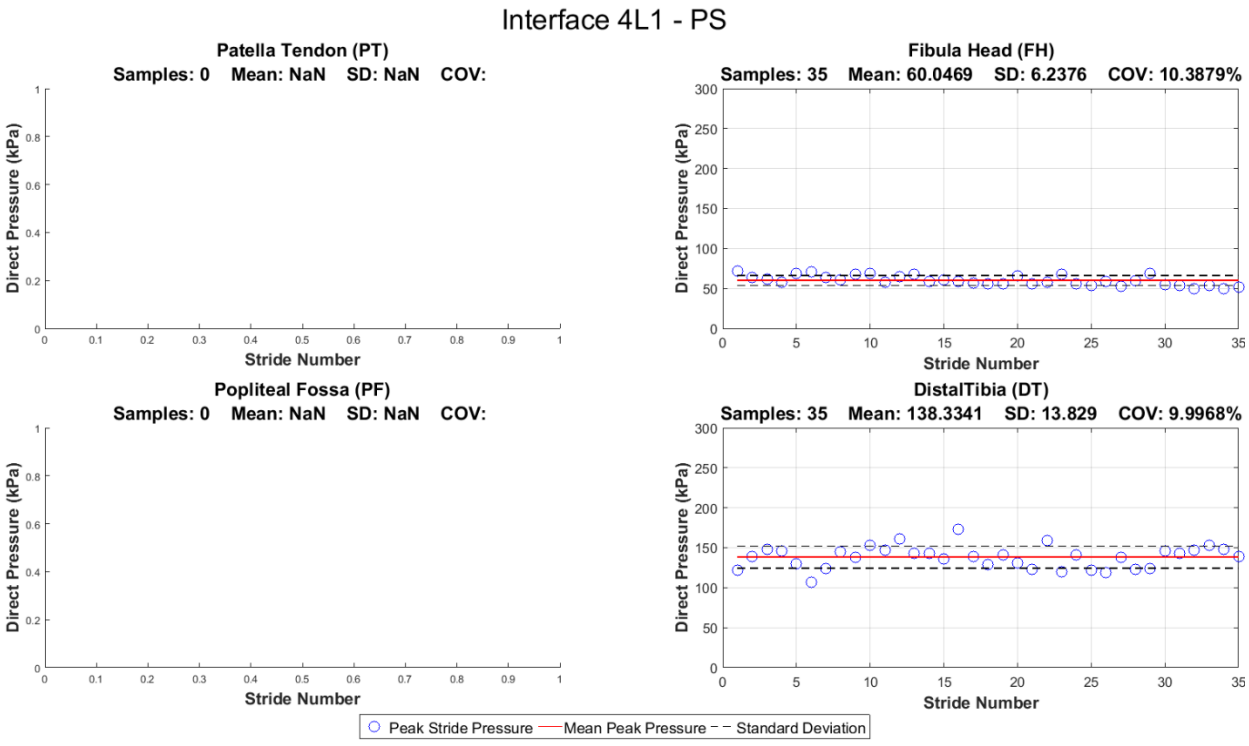

Figure 14.6: SLW peak pressures - Interface 4L1 - Pressure Sore Present at DT, Signal lost at PT and PF areas.

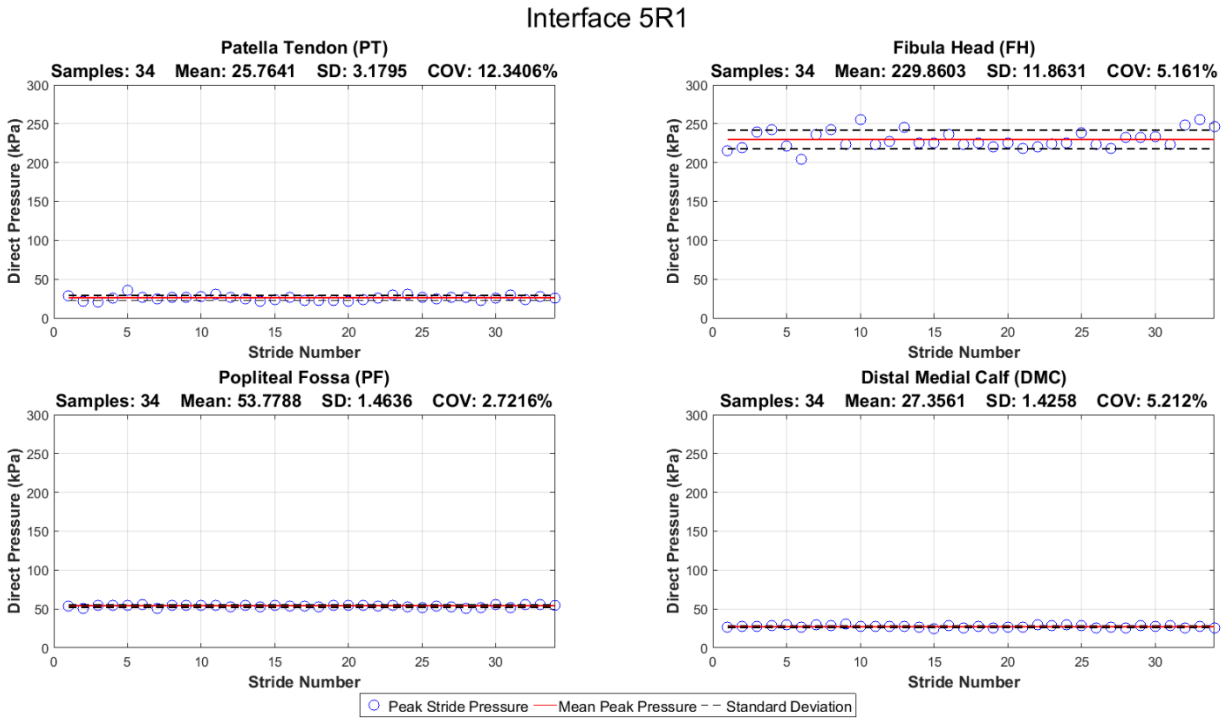

Figure 14.7: SLW peak pressures - Interface 5R1

14.2 Figure-of-8 Peak Pressures

This section illustrates all peak pressures from the F8W procedure

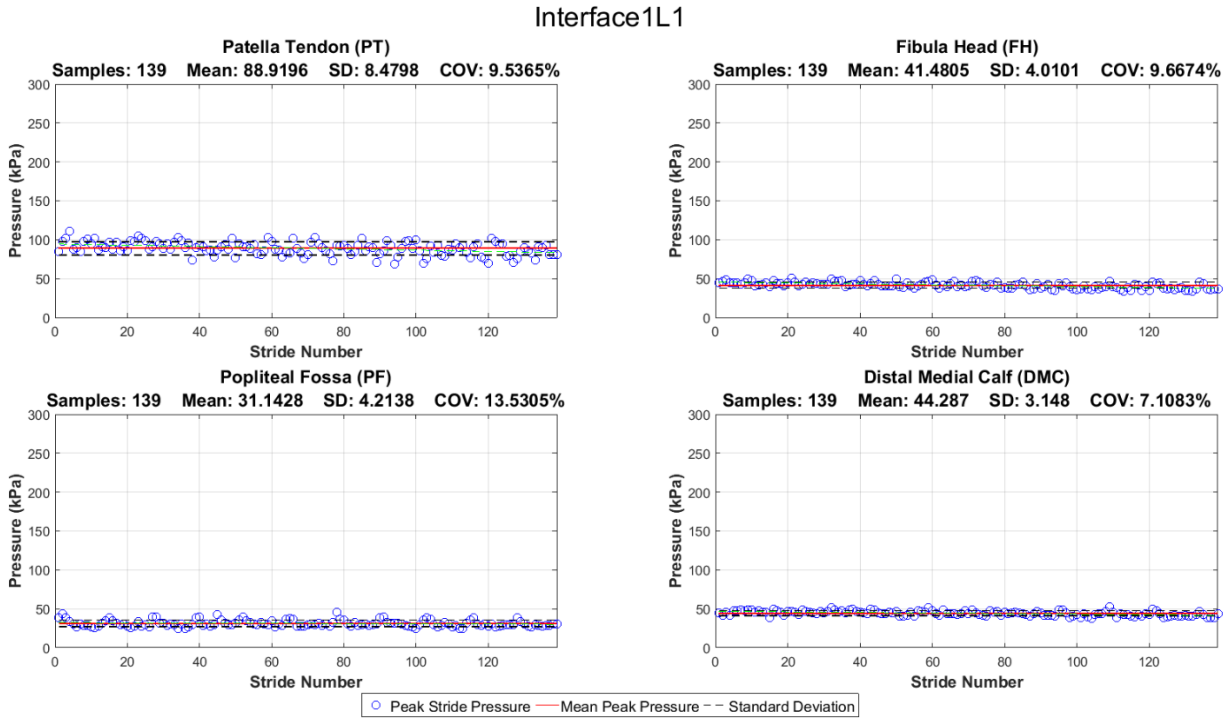

Figure 14.8: F8W peak pressures - Interface 1L1

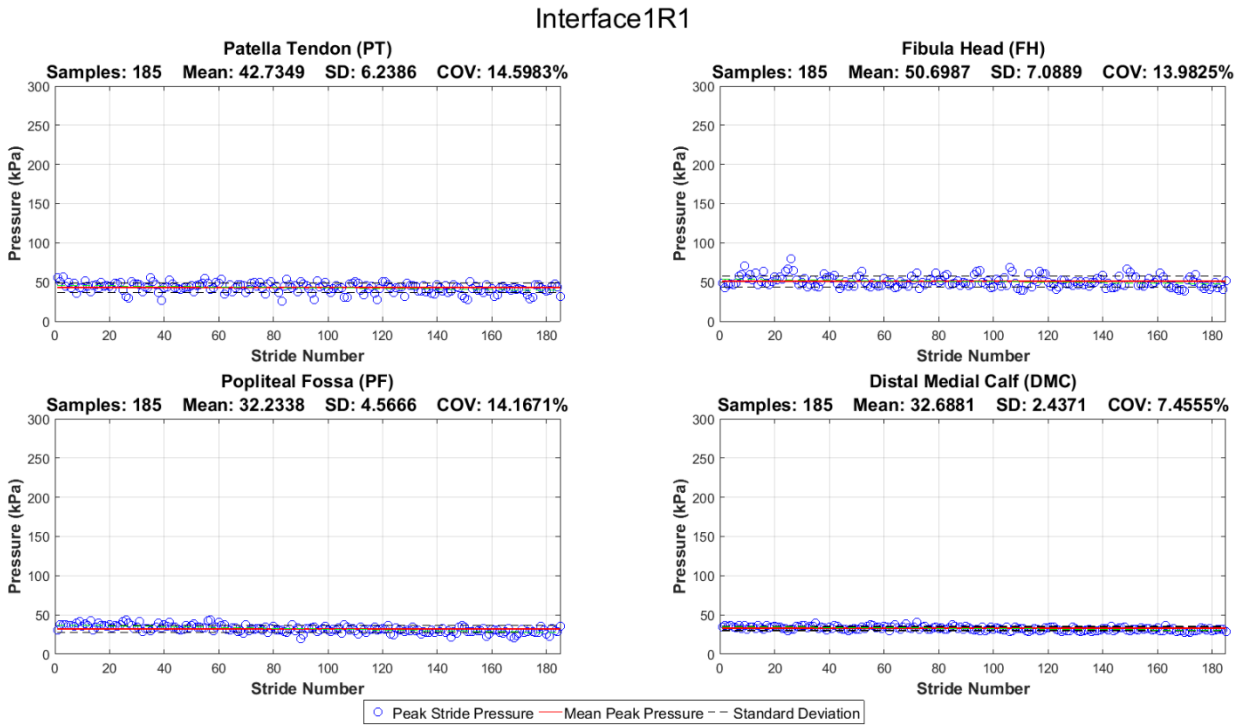

Figure 14.9: F8W peak pressures - Interface 1R1

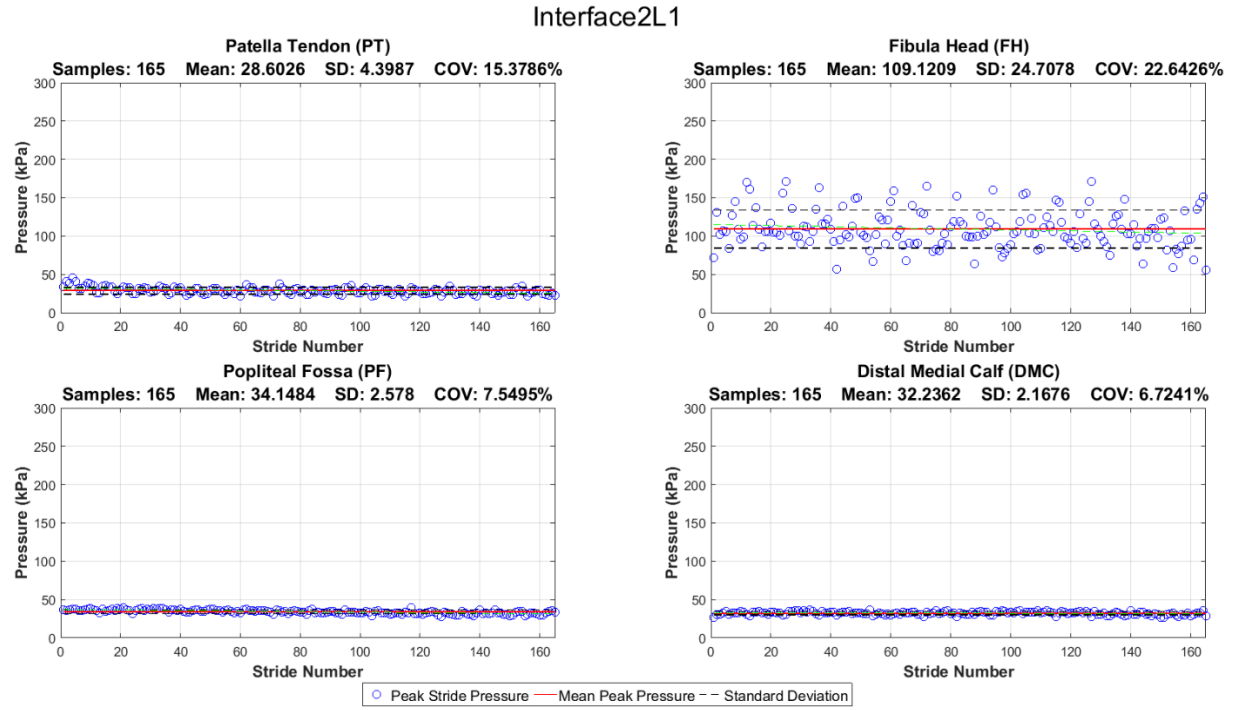

Figure 14.10: F8W peak pressures - Interface 2L1

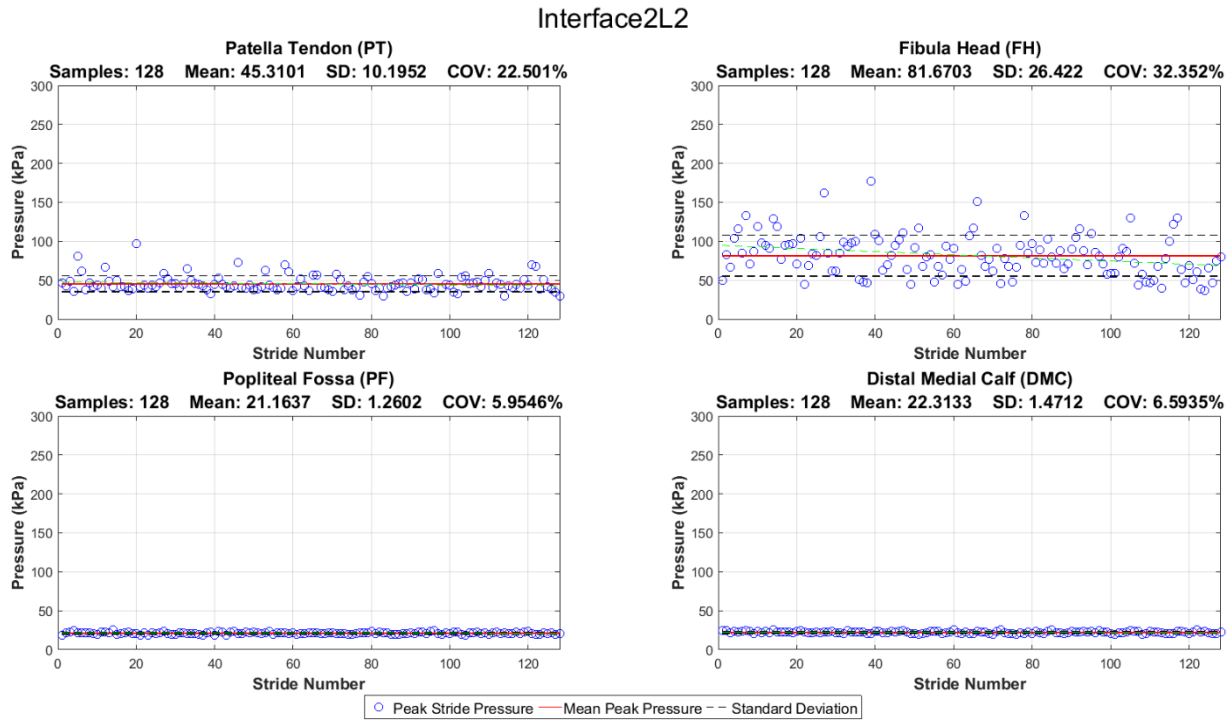

Figure 14.11: F8W peak pressures - Interface 2L2

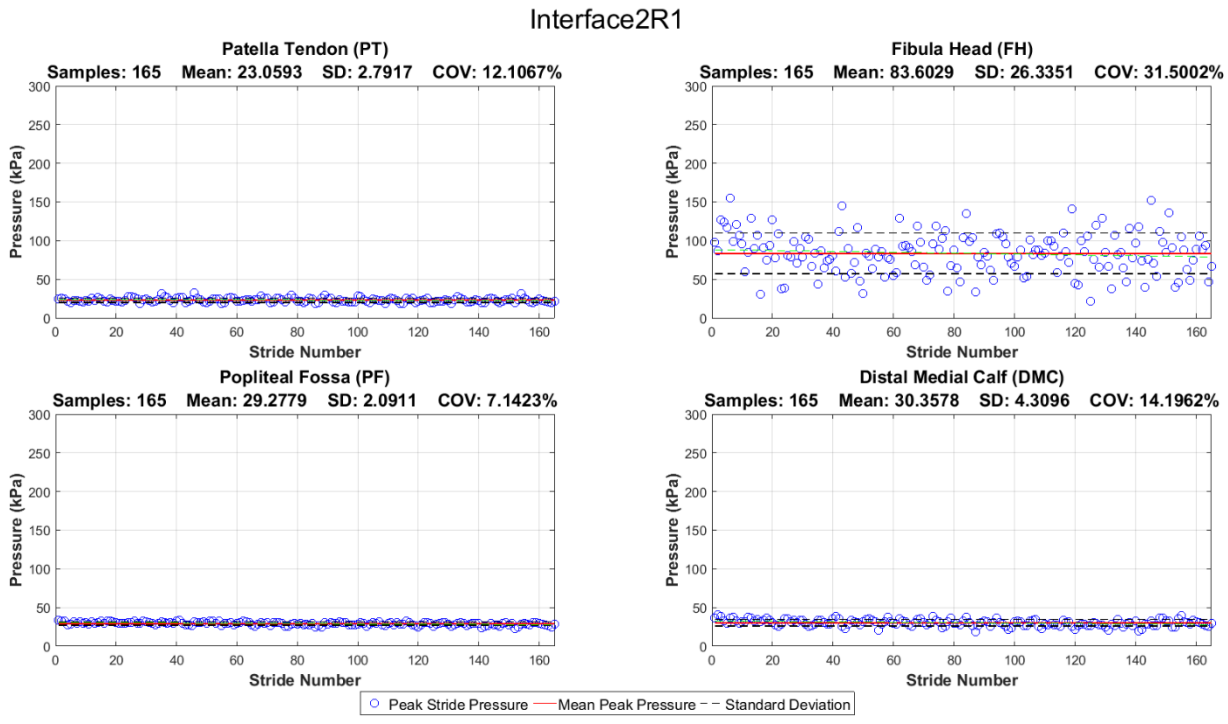

Figure 14.12: F8W peak pressures - Interface 2R1

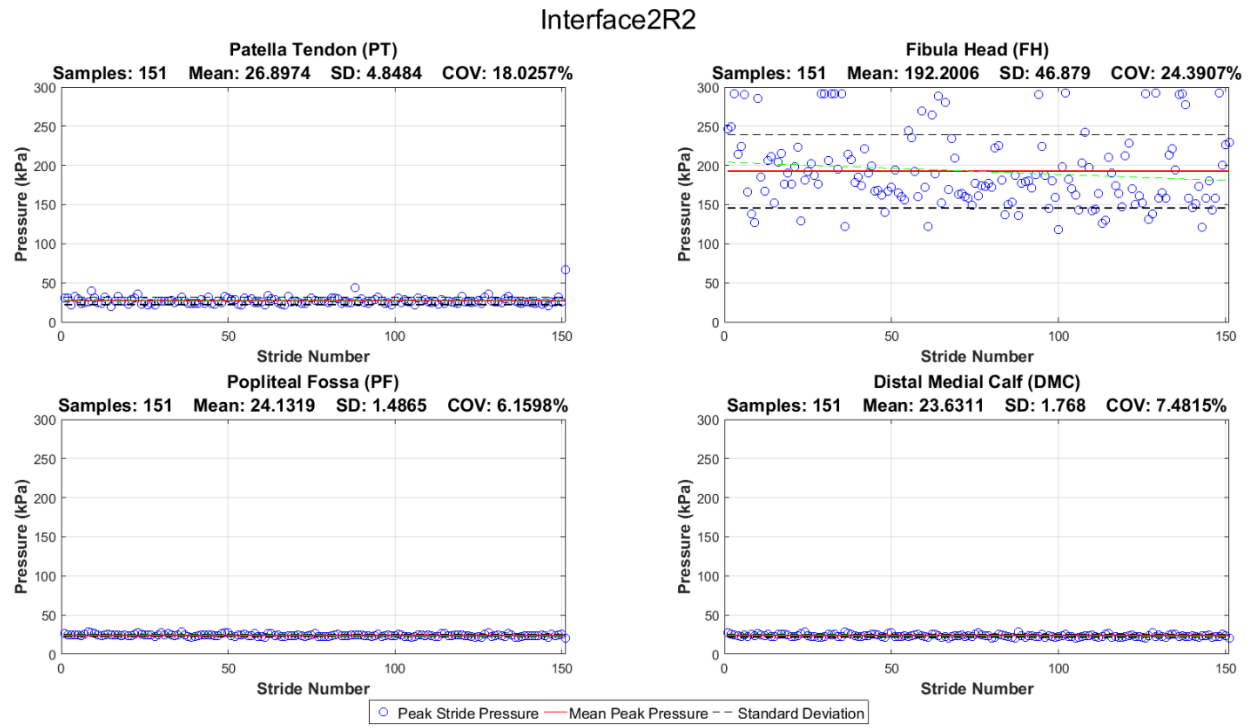

Figure 14.13: F8W peak pressures - Interface 2R2

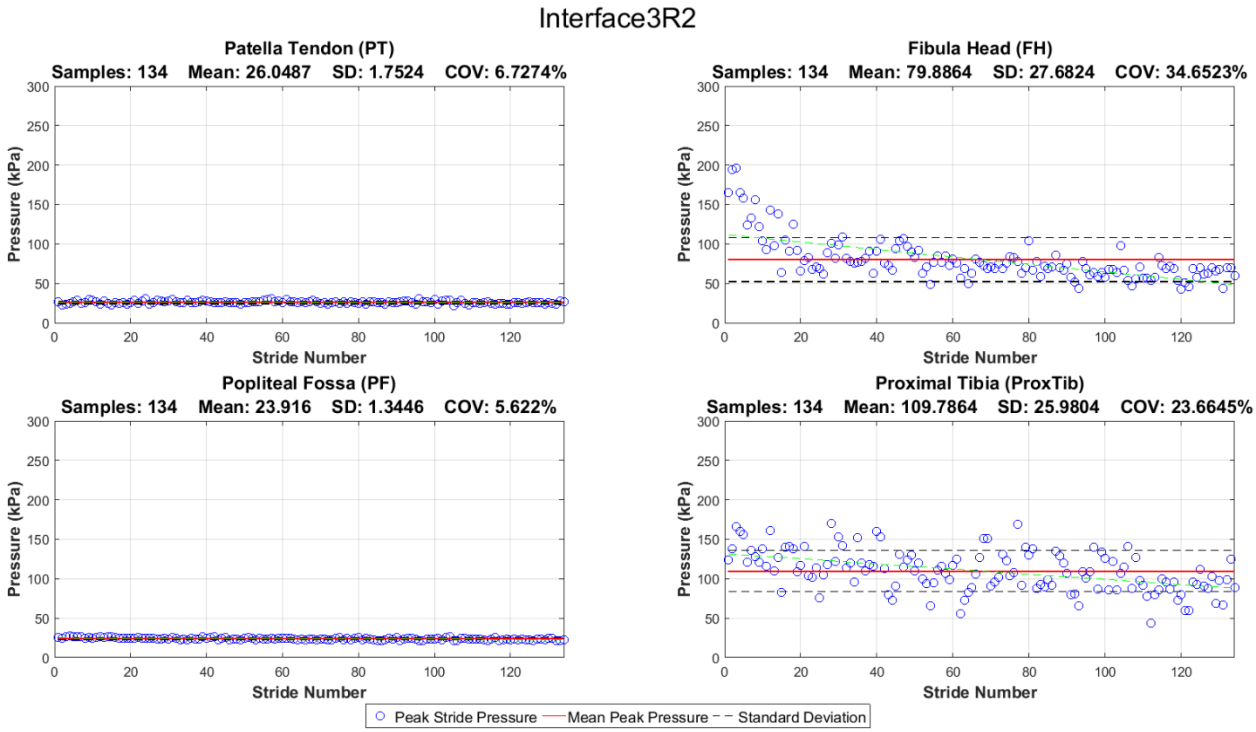

Figure 14.14: F8W peak pressures - Interface 3R2

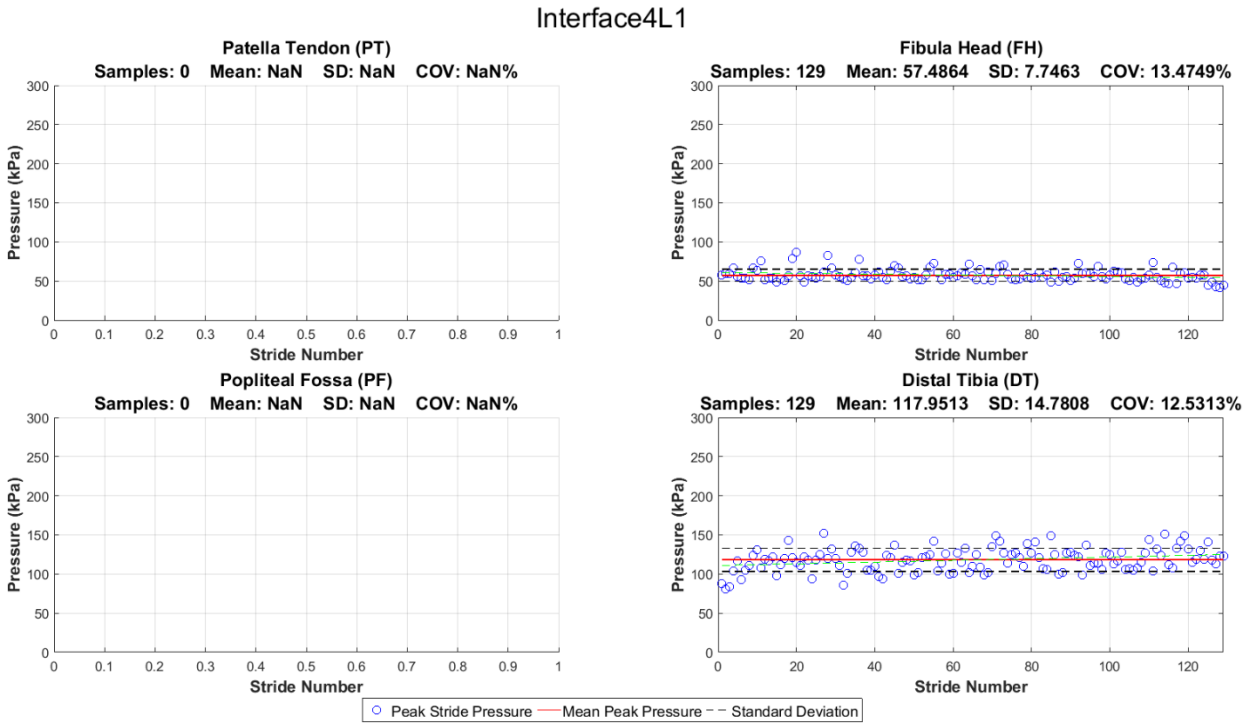

Figure 14.15: F8W peak pressures - Interface 4L1 - Pressure Sore Present on DT, Signal lost at PT and PF areas

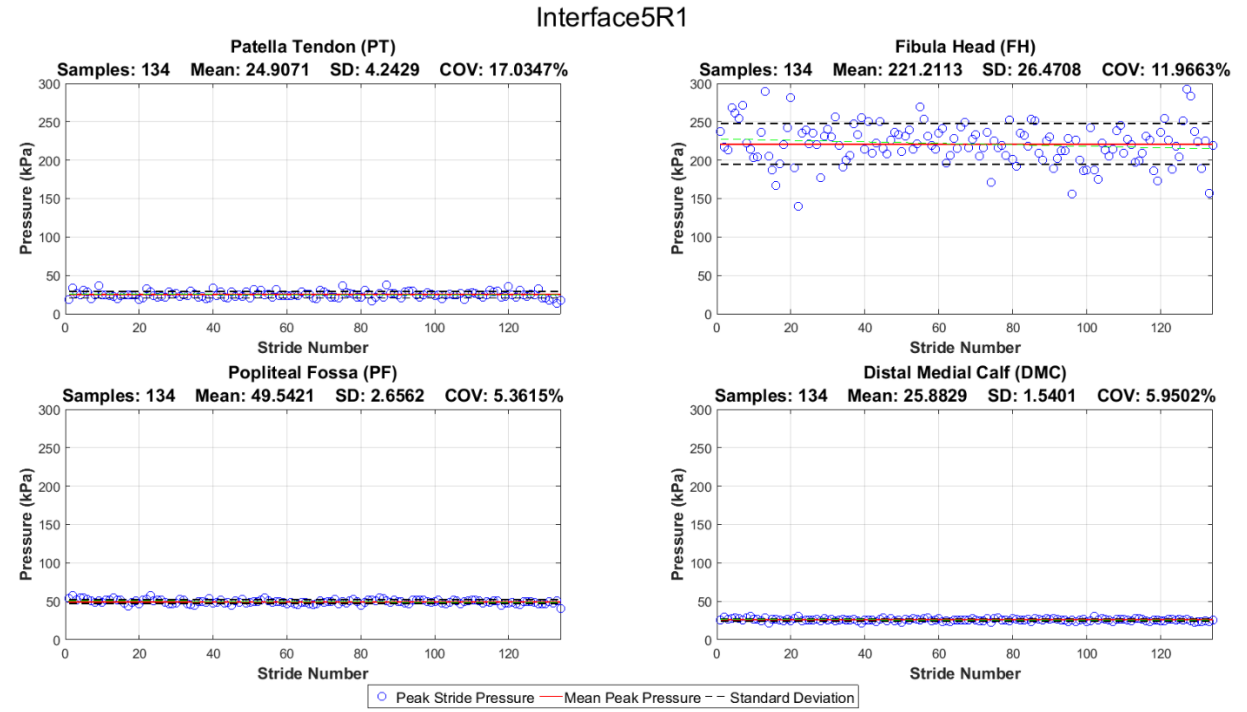

Figure 14.16: F8W peak pressures - Interface 5R1

14.3 SLW and F8W data table

Table 14.1 presents the maximum pressure, average peak pressure and the standard deviation between peak pressures for the SLW and F8W procedures.

Table 14.1: Pressure data found in SLW and F8W tests

		TEST	MAXIMUM PRESSURE (KPA)	AVERAGE PEAK PRESSURE (KPA)	SD (KPA)
PT	1L1	SLW	90.0	75.3	6.9
		F8W	110.4	88.9	8.5
	2L2	SLW	61.8	48.9	5.2
		F8W	96.5	45.3	10.2
	2R2	SLW	33.0	28.3	2.3
		F8W	66.4	26.9	4.8
	3R2	SLW	25.9	23.1	1.3
		F8W	30.8	26.0	1.8
	5R1	SLW	35.7	25.8	3.2
		F8W	37.8	24.9	4.2
FH	1L1	SLW	46.8	42.5	2.7
		F8W	50.3	41.5	4.0
	3R2	SLW	74.6	62.7	6.4
		F8W	196.4	79.9	27.7
	4L1	SLW	71.5	60.0	6.2
		F8W	87.1	57.5	7.7
	5R1	SLW	255.4	229.9	11.9
		F8W	292.2	221.2	26.5
PF	1L1	SLW	27.1	24.1	1.6
		F8W	45.3	31.1	4.2
	2L2	SLW	25.3	21.6	1.2
		F8W	25.3	21.2	1.3
	2R2	SLW	28.6	26.0	1.3
		F8W	28.9	24.1	1.5
	3R2	SLW	26.8	24.1	0.9
		F8W	27.4	23.9	1.3
	5R1	SLW	56.0	53.8	1.5
		F8W	58.1	49.5	2.7
DMC	1L1	SLW	47.8	43.7	2.3
		F8W	52.4	44.3	3.1
	2L2	SLW	26.0	23.1	1.1
		F8W	26.0	22.3	1.5
	2R2	SLW	29.8	26.0	1.5
		F8W	29.0	23.6	1.8
	5R1	SLW	30.2	27.4	1.4
		F8W	30.6	25.9	1.5
ProxTib	3R2	SLW	136.4	103.2	16.4
		F8W	170.5	109.8	26.0
DT	4L1	SLW	173.2	138.3	13.8
		F8W	152.1	118.0	14.8

14.4 Skin Temperature Change Results

This section presents figures and tables from which the skin temperature change due to the SLW and F8W procedures is portrayed.

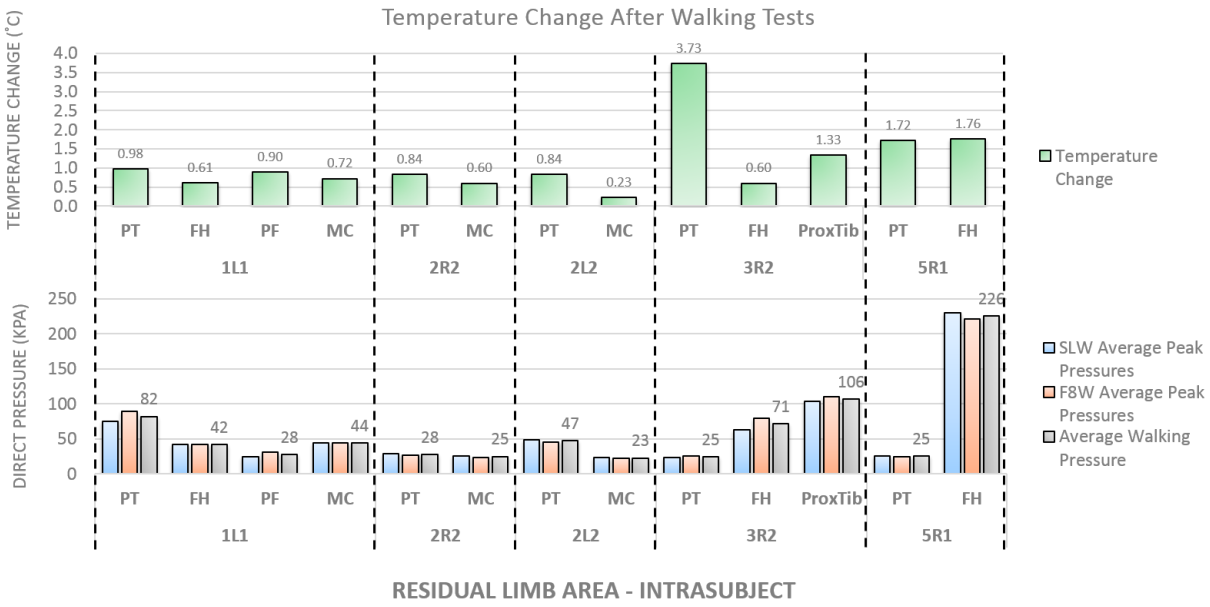

Figure 14.17: Skin temperature change after SLW and F8W procedures.

Table 14.2: Total Temperature Change During Walking Procedures (SLW + F8W)

INTERFACE	1L1				2R2		2L2		3R2			5R1		AVERAGE
Total Walking Time (minutes)	6.5				5.2		4.7		5.2			5.3		5.4
Ambient Temperature (°C)	22				19.2		19.2		19.5			19.4		19.9
RL Area	PT	FH	PF	MC	PT	MC	PT	MC	PT	FH	ProxTib	PT	FH	-
Average Walking Pressure (kPa)	82.11	42.01	27.61	44.00	27.60	24.80	47.08	22.72	24.53	71.29	106.50	25.34	225.54	82.11
Temperature Change (°C)	0.98	0.61	0.90	0.72	0.84	0.60	0.84	0.23	3.73	0.60	1.33	1.72	1.76	1.14

15 Appendix E: Statistical Information

15.1 Coefficient of Variance (COV)

The COV is the ratio between the standard deviation and the mean of a population and is calculated using the following equation:

$$\%COV = \left(\frac{Standard\ Deviation}{Mean}\right) \times 100 \quad [10]$$

This is used so that the ratio between the standard deviation and mean can be compared between different populations.

15.2 Outlier Removal

Table 15.1 presents the outliers found within the Interface datasets. These were removed from the datasets.

Table 15.1: Samples which were identified as outliers and removed

INTERFACE	AREA	OUTLIER	VALUE
3R1	Patella Tendon	Sample 4	79.6
5R1	Fibula Head	Sample 10	267.6
5R1	Popliteal Fossa	Sample 33	48.87